Extreme25 Expedition Report

Leg 1: 11th-19th November 2025 (Longyearbyen-Longyearbyen)
Leg 2: 19th-26th November 2025 (Longyearbyen-Tromsø)

Chief scientist: Giuliana Panieri
Co-chief scientist: Claudio Argentino

Capt. R/V:
Leg 1: Hallgeir M. Johansen
Leg 2: Karl Robert Røttingen

Report prepared by: Panieri, G., Argentino, C., Amaglio, G., Bagøien, G., Barrenechea Angeles, I., Basili, M., Burkitt-Gray, M., Cicerôn, B., Cuffaro, M., Dögg, H., Eilertsen, M. H., Faizeva, K., Fallati, L., Gentilucci, M., Grzinich J., Heinz, P., Hemmateenejad, F., Kjær, M., Lanci, V., Lennert, A. E., Lofqvist, B., Longo, A., Loven, K. R., Mattingsdal, R., Moles, A., Nilsson, C. L., Olafsdottir, T., Radovich, V., Redaelli, C., Savini, A., Selci, M., Skold, J., Smedile, F., Tesi, T., Thiessen, O., Youngs, S., Zimmerman, J.

Keywords: Cold seeps, Gas, Hydrothermal vent, Methane, Fram Strait, Barents Sea, Gas hydrate, Mud volcano, Carbonate, Craters, Biogeochemical processes, Deep-Sea Biology, DNA, Seafloor imaging, Education, Outreach, co-creation and participation, Microbiology, Meiofauna, Macrofauna, Biomarkers

DOI https://doi.org/10.7557/7.8619

Recommended citation: Panieri, G., Argentino, C., Amaglio, G., Bagøien, G., Barrenechea Angeles, I., Basili, M., … Zimmerman, J. Extreme25 Expedition Report. *Septentrio Reports*, (1) 2026. https://doi.org/10.7557/7.8619

Table of Contents

Participant list

	Name	Affiliation	Role	Discipline
1	Giuliana Panieri	UiT	Cruise leader	Chief Scientist, PI EXTREME25, micropaleontology, biogeochemistry
2	Claudio Argentino	UiT	Researcher	Co-chief scientist, Biogeochemistry, carbonates
3	Alessandra Savini	Unimib	Scientist	Seafloor imaging and mapping
4	Ann Eileen Lennert	UiT	Researcher	Anthropology
5	Anna Moles	CNR	Researcher	Biology
6	Antonio Longo	Unina	PhD student	Microbiology
7	Bjørn Cicerôn	UiT	Student	Chemistry
8	Carlotta Redaelli	UiT	Research assistant	Marine sciences and geochemistry
9	Christian Ludvig Nilsson	UiB	PhD student	Marine biology
10	Fereshteh Hemmateenejad	Unimib	PhD student	Seafloor imaging and habitat characterization
11	Francesco Smedile	CNR	Researcher	Microbiology
12	Giulia Amaglio	CNR	Post-doc	Biomarkers
13	Gry Bagøien	Freelance	Artist	
14	Hekla Dögg	Freelance	Artist	
15	Ines Barrenechea Angeles	UiT	Researcher	Micropaleontology and genetics
16	Jane Zimmerman	Freelance	Artist/illustrator	
17	John Grzinich	MoKS	Artist	
18	Kamila Faizeva	University of Vienna	PhD student	Micropaleontology
19	Luca Fallati	Unimib	Researcher	Seafloor imaging and mapping
20	Marco Basili	CNR	Post-doc	Microbiology
21	Marco Cuffaro	CNR	Researcher	Geodynamics and geophysics
22	Mari Heggernes Eilertsen	UiB	Researcher	Marine biology
23	Marta Gentilucci	UiB	Post-doc	Anthropology
24	Mary Burkitt-Gray	WHOI	Researcher	Ocean physics and engineering
25	Matteo Selci	Unina	Post-doc	Microbiology
26	Michale Kjær	University of Copenhagen	Researcher	Art history
27	Olaf Thiessen	Equinor	Researcher	Geology
28	Petra Heinz	University Vienna	Scientist	Micropaleontology
29	Rune Mattingsdal	NPD	Scientist	Geology
30	Sarah Youngs	WHOI	Researcher	Ocean physics and engineering
31	Thorgerdur Olafsdottir	Freelance	Artist	
32	Tommaso Tesi	CNR	Researcher	Biomarkers
33	Valentina Lanci	UiT	Advisor	Media
34	Violeta Radovich	UPV, CONICET	Researcher	Law of the Sea
35	Bjørn Lofqvist	UiB, NORMAR	ROV Engineer	
36	John Skold	UiB, NORMAR	ROV Engineer	
37	Kai Roger Loven	UiB, NORMAR	ROV Engineer	
38	Trym Rorstrand	IMR	ROV Student	
39	Alexander Finnvik	IMR	ROV Student	

Participants' Institutions:
UiT The Arctic University of Norway (https://uit.no)
Centre for Deep Sea Research, UiB, University of Bergen, Norway (https://www.uib.no/en/deepsea)
CNR, National Research Council, Italy (https://www.cnr.it)
CONICET, Argentine Council on Scientific and Technical Research (https://www.conicet.gov.ar)
Equinor, Norway (https://www.equinor.com/)
IMR Institute of Marine Research, Norway (https://www.hi.no)
NORMAR, The Norwegian Marine Robotics Facility (https://www.normardeepsea.com)
MoSK, MTÜ Mooste KülalisStuudio, Estonia (https://moks.ee)
NOD, Norwegian Offshore Directorate (https://www.sodir.no)
Unimib, Università degli Studi di Milano-Bicocca, Italy (https://www.unimib.it)
Unina, University of Naples Federico II (https://www.unina.it)
University of Copenhagen (https://www.ku.dk)
University of Vienna (https://www.univie.ac.at)
UPV, Valencia Polytechnic University (https://www.upv.es)
WHOI, Woods Hole Oceanographic Institution, USA (https://www.whoi.edu)

Figure 1. EXTREME25 cruise participants.

1 Introduction and objectives

The Extreme25 expedition is conducted as a continuation of Extreme24 and within the umbrella of EXTREMES UArctic project (UA 06/2024), a collaboration between UiT-The Arctic University of Norway (Department of Geosciences), the University of Copenhagen (Department of Arts and Cultural Studies), and the University of Iceland Research Centre in Þingeyjarsveit. The Extreme25 expedition brought together scientists, students, media experts, and artists from around the world to explore extreme environments. The international team included geologists, geophysicists, geochemists, methane specialists, and marine ecologists, and for the first time, the EXTREME expedition also hosted an active delegation from the National Research Council of Italy (CNR), representing multiple institutes and disciplines. The various groups included a team of chemists and engineers from Woods Hole Oceanographic Institution; researchers from EXTREMES, scientists from the University of Bergen contributing expertise in deep-sea chemosynthesis-based ecosystems; scientists from University Milano Bicocca supporting the high-resolution mapping effort; microbiologists from University of Naples Federico II; micropalaeontologists from University of Vienna; anthropologists and artists studying human–polar interactions and new modes of science communication.

The overarching goal of the expedition was to explore deep-sea habitats of cold seeps and hydrothermal vents within Norwegian waters, from the Fram Strait to the Barents Sea, and collect samples that can tell us about the geodynamics and biology of these extreme environments. The expedition has been developed by leveraging the extensive knowledge gained from two significant projects funded by the Norwegian Research Council: CAGE (Centre for Arctic Gas Hydrate, Environment and Climate) and AKMA (Advancing Knowledge of Methane in the Arctic), hosted at the Department of Geosciences at UiT.

2 Geological setting of the working areas

2.1 Leg 1 (Molloy ridge-transform system)

The Arctic Mid-Atlantic Ridge at the Molloy ridge-transform system represents the plate boundary between Eurasia (EU) and North America (NA) plates, and this region is located at the Fram between the Norwegian-Greenland Sea and the Arctic Ocean (Figure 2). The Molloy Ridge and the Transform Fault system began to form after the opening of the Norwegian-Greenland Sea ~56 Ma ago (Talwani & Eldholm, 1977; Chand et al., 2024), and seafloor spreading started in this area at 20 Ma, following the recent plate reconstruction proposed by Dumais et al. (2021). In this region, Moho is described at a depth of 5 km (Czuba et al., 2005; Chand et al., 2024), suggesting a very thin crust. The nodal basin at the intersection of the Molloy Transform Fault and the Molloy Ridge is detected at the Molloy Hole, a huge depression of 5500 m (Klenke & Schenke, 2002). Northward, the Spitsbergen Transform Fault connects the oceanic spreading system with a large portion of continental lithosphere, which continues northward toward the Gakkel Ridge.

At the intersection between the Molloy transform and the Molloy Ridge, a large detachment is detected in the bathymetry maps, suggesting the presence of an Oceanic Core Complex (OCC) (Chand et al., 2024), and some gas flares are described in the northern intersection between the Molloy Ridge and the Spitsbergen Transform Fault (Chand et al., 2024).

2.2 Leg 2 (Barents Sea)

The Norwegian sector of the Barents Sea is known to host topographic features on the seafloor that are related to active or extinct hydrocarbon emissions (cold seeps). These structures often correspond to seafloor depressions, such as pockmarks (Chand et al., 2012; Panieri et al., 2017) and larger craters (Andreassen et al., 2017). However, mounds hosting gas hydrates have also been reported (Serov et al., 2017).

The Barents Sea is characterized by a widespread petroleum system (Vadakkepuliyambatta et al., 2013) and has favorable geological conditions (plastic shale intervals, fluid plumbing systems) for mud volcanism. Still, only a few mud volcanoes have been confirmed, specifically the Håkon Møsby Mud Volcano (1995) (Vogt et al., 1997), Borealis (2023) (Panieri et al., 2025), and the Polaris Mud Volcano Complex (2024) (Argentino et al., 2025). These recent discoveries suggest that mud volcanoes have been largely overlooked so far, likely due to challenges in their univocal interpretation. During previous UiT expeditions crossing several abandoned exploration wells left behind from industry activities since the 1980s, gas-related water column anomalies were observed, implying ongoing leakage from these infrastructures at the seafloor. During this cruise, particularly during Leg 2, we investigated both naturally occurring gas seeps (NAGS), oil seeps, and well-associated gas seeps (WAGS). Additionally, we revisited Borealis and explored a nearby site with indications of potential mud volcanism.

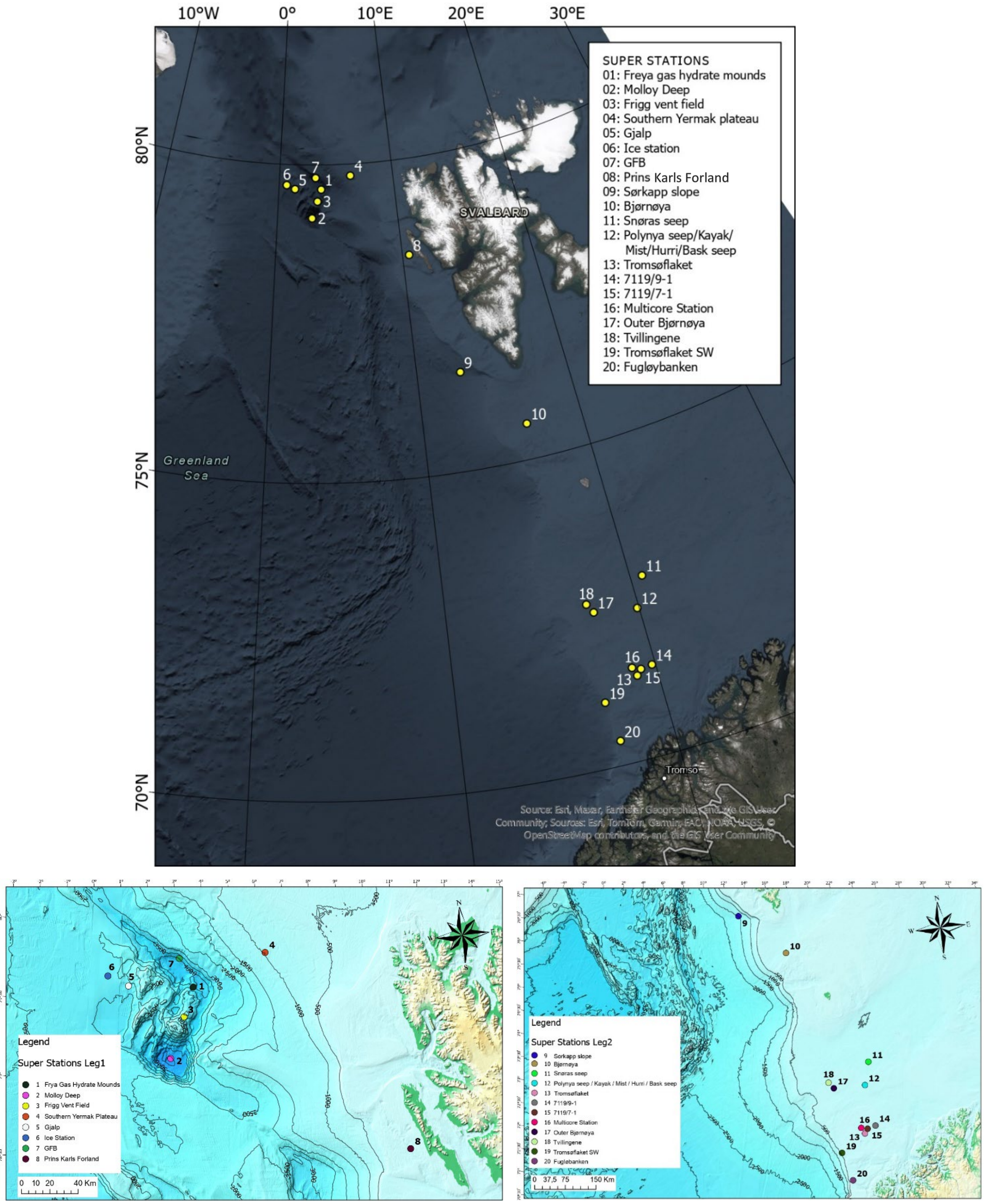

Figure 2. Study sites visited during the legs 1 and 2 of the Extreme25 Expedition. Bottom left: Leg 1; Bottom right: Leg 2.

3 Scientific Narrative of the Expedition

3.1 Leg 1

Tuesday 11th November DAY 1

Between 09:00 and 10:00, all participants boarded the vessel and completed the initial check-in procedures. At 14:00, the mandatory safety briefing was conducted, covering emergency protocols, muster points, and onboard operational guidelines.

A cruise meeting followed at 18:00 to review the scientific objectives, planned stations, and daily work structure for Leg 1.

At 20:00, the vessel departed and began steaming toward the Molloy region, marking the official start of the first leg of the expedition.

Wednesday 12th November DAY 2

Superstation 1: Freya Gas Hydrate Mounds

15:50 started ROV dive to the Freya mounds (Superstation 1) and reached the seafloor at 17:19. We found a gas hydrate mound and attempted push coring, but the material was lost during transfer to the TMS push core holder. We collected a blade core from the side of the gas hydrate mound and pointed the SAGE into the hydrate mound for methane measurements. The ROV came up at 20:00, and we started an MB line across the mound to track the location of the gas flare reported in previous studies (named GFA in Chand et al., 2024; Panieri et al., 2025, in press). The MB system failed during the line, so we just decided to do the CTD at the same spot as seen in previous expeditions. We started the CTD 564 at 22:25 and sampled for microbiology and gas at 6 depths. Then we started transiting to the northern flare named GFB (Chand et al., 2024) for an MB grid. MB surveys all night at the northern site.

Thursday 13th November DAY 3

Superstation 1: Freya Gas Hydrate Mounds

During the night, a CTD cast was carried out on top of Freya (Superstation 1). Locating the gas flare observed last year during the Ocean Census cruise proved challenging, despite operating at the same coordinates. Although an additional CTD was initially planned as part of the oceanographic transect, it had to be cancelled due to the extended duration of the sampling operations from the previous cast.

At 7:50, we started diving ROV 1061 and reached the seafloor at 9:37. This marked the second dive of the cruise on the Freya gas hydrate mounds. Weather conditions had improved significantly compared to yesterday, and the atmosphere on board was calm and focused.

During the descent to 450 m water depth, the SAGE system experienced some technical issues; the inlet pressure, which measures the amount of gas being extracted from the water into the instrument headspace, was measuring a significantly lower value than would be expected from previous instrument performance. While on previous dives, this problem had originated due to restricted water flow, the ROV camera had a view of the spinner, which confirmed that the pump was flowing extremely well. While the data continued to collect throughout the dive, the response time and sensitivity of SAGE are likely both significantly reduced. Further tests when the vehicle is on deck to identify whether this dataset can still be useful for scientific analysis.

However, the team decided to continue the dive. Upon reaching the seafloor, we conducted three detailed photo-mosaics over three distinct mounds within the Freya gas hydrate mounds field. The area is characterized by a series of ridges and mounds of varying size and morphology. The mosaic was done on three mounds located at the following positions: Area1: 79°36.8474'N 003°39.4612'E; Area2: 79°36.8467'N 003°39.6309'E; Area3: 79°36.7796'N 003°39.6969'E

We then began sampling on one mound in Area 2. The site is characterized by a distinct layer of rock concretions, likely composed of carbonate or barite, and scattered pebbles of various shapes—some rounded, others with sharp edges—probably originating from ice-rafted debris. Several of the concretions contained bivalve shells and were covered by a reddish patina, possibly iron oxides, which also coated other pebbles and small blocks regardless of their lithological composition. High-resolution video and still images were collected to document the lithological features and the associated fauna, mainly tubeworms and shrimps. Two push cores were taken, together with samples of carbonate crusts and scoops of surface sediment for surficial fauna collection.

We then decided to move to Area 3 to perform a photomosaic; however, the site did not present any particularly interesting morphological or biological features. At the end of the mosaic, we proceeded north toward Area 1. During transit, we noticed a very interesting mound and decided to stop the ROV to conduct additional sampling using pushcorer and bladecorer. We left the seafloor at 16:39.

Once all samples were brought on board, each group received its material and began processing immediately. Both the blade corers and the push cores were highly gas-charged, containing substantial amounts of methane and oil. The vessel's alarm system was triggered due to the elevated concentration of hydrocarbons in the air, and the laboratory doors were opened to ensure proper ventilation. However, with outside temperatures at –20 °C, the doors were closed again as soon as the air inside had cleared sufficiently.

Once the ROV was back on board, we immediately started steaming toward the Molloy Deep (Superstation 2) with the objective of collecting a gravity core.

Friday 14th November DAY 4

Superstation 2: Molloy Deep

Superstation 3: Frigg Vent Field

During the night, after a multibeam survey in Molloy Deep (Superstation 2), we ran a chirp line to identify the most suitable coring location, keeping the vessel at 4 knots. The gravity corer was deployed successfully and recovered 2.95 m of sediment. Two CTD casts (565 and 566) were then conducted at the same location as the gravity core.

Afterwards, we began steaming toward the "Atla Seamount," nominally the highest bathymetric point in the area. However, our objective was to explore the adjacent region where oceanic core complex corrugations had been identified in the bathymetry from Chand et al. (2024). This area is characterized by two pronounced faults that were detected as the best location for the exposure of the upper mantle and lower crust at the seafloor.

We arrived at approximately 08:00. At this new site (Superstation 3), we conducted a ROV dive. The plan of the dive was to explore this area with a transect of ca 1.5 km in length connecting the two fault escarpments to find exposed upper mantle peridotite and lower crust gabbroic rocks. The first fault scarp and the surface connecting the two faults were covered by sediments, and only a few dropstone rocks were collected. At 11:51, we reached the base of the second fault scarp showing a rock outcrop, where we collected samples, which were promising peridotites and serpentinites. We also collected spongers, and at 12:42, during the observation activities, we found a small area covered by microbial mats with pronounced filaments and shimmering waters. We conducted SAGE and microbial mat sample activities, as well as two ROV video transects of the outcrop to obtain a photomosaic image of the entire area. We discovered Frigg Vent Field.

Saturday 15th November DAY 5

Superstation 4: Southern Yermak Plateau

Superstation 3: Frigg Vent Field

During the night, we steamed toward the southern Yermak area to collect multicore samples. Before approaching the station, we ran a quick chirp survey to identify the most suitable spot for sampling. Once we located a promising site, we deployed the multicorer (MC 1 and MC2). The first recovery yielded only one core out of six, so we carried out a second deployment, which successfully returned five cores. We did a CTD (567) on the same location.

By morning, we reached Frigg and began preparing the ROV. We installed the CO_2 SAGE system and repositioned the methane SAGE to accommodate both instruments on the vehicle. To support planned water sampling, we modified the 2 Niskin bottles by taping around the handles to secure them properly on the frame, and we connected the biosyringe to the manipulator. We also prepared the T-probe, and by around 11:00, everything was ready for Dive 4 (1063) on Frigg.

Our first operation was a mosaic survey to obtain an updated overview of the area. The mosaic from the previous dive had already provided useful context. The site consists of a massive, fractured rock outcrop with several shimmering points associated with microbial mats. Fluid discharge is visible along cracks and faults in the rock. At the base of the outcrop, the surrounding sediment contains small patches of tube worms. We also observed shell debris coated with iron oxides(?), giving a reddish appearance.

We then focused on a shimmering flow and collected two Niskin bottles. One Niskin lost its handle during the operation, leaving two openings, but it was still used to collect shimmering fluids for filtration.

At 13:50, the vessel had to reposition due to drifting ice. The wind increased, and the manoeuvre took almost 45 minutes. Despite these constraints, the subsequent sampling operations were completed successfully. Deploying multiple tools inside the same opening—including the SAGE system, the T-probe, and later the biosyringe—was extremely challenging, but the skill of the ROV pilots and the strong, coordinated teamwork between operators and scientists ensured a smooth and efficient workflow.

We deployed the SAGE system in the same opening from which the Niskin samples had been taken and subsequently inserted the T-probe. Using the biosyringe, we collected several microbial mat samples emerging from a fracture colonised by at least three distinct types of biofilms—pink, green, and white. Some filaments covered dense patches of tube worms, while other biofilms displayed a reticulated texture or formed more compact pink layers.

We also retrieved a green-coloured rock. In addition, we collected two push cores from a nearby sedimented area and two blade cores from two different patches of tube worms, which we documented carefully with the ROV camera. Shell debris and a fragment of cemented pavement observed around the massive, fractured outcrop were also sampled.

We ended the dive at 17:45. By then, the waves had increased significantly, and the weather was deteriorating rapidly, with winds reaching 40 knots. The captain did not allow us to deploy a CTD, as conditions were too dangerous for both the crew and the scientific team.

Throughout the evening, all groups continued processing the collected samples while the weather worsened further. Wind speeds reached 61 knots, just below hurricane force (63 knots).

Sunday 16th November DAY 6

Superstation 5: Gjalp

Superstation 6: Ice station

In the early morning, there was an empty spot in the ice, and we conducted a CTD (568) cast to 200 m, with additional stops at 15 m, and collected three Niskin bottles.

Before beginning the ROV operations, and due to strong winds and increased ice drifting southward, the vehicle had to be re-ballasted to ensure safe manoeuvring at depth.

At 10:00, we launched ROV Dive 5 (1064). While surveying the seafloor, the SAGE sensors detected a slight increase in methane concentration. Based on this signal, we mounted SAGE on the manipulator arm to perform targeted measurement tests. The landing area was characterized by a sandy seabed with scattered rocky patches colonised by sponges. We collected several sponge samples as well as a few pieces of wood, and we also recovered a fragment of seaweed.

Two sediment cores were taken for the sponge-related project, and an additional two cores were collected for palaeoclimate reconstruction. One core was designated as the reference sample for this site.

Maintaining position was extremely challenging due to the persistent wind and drift. After completing the sampling programme, we decided to end the dive and recovered the ROV at 15:00.

In the evening, the vessel stopped for a brief ice station. Two microbiologists collected snow samples via crane. Limited ice samples were obtained using a steel stick. All crew and scientists were allowed a short time on the ice, boosting morale. Later, the team watched the football game Italy vs. Norway (Norway 4–1).

After the ice station, the vessel steamed back to the Freya gas hydrate mounds to conduct multibeam surveys and locate station GFB according to Chand et al (2024). The site was reached around 04:00, with challenging but manageable conditions due to ice sheltering.

Monday 17th November DAY 7

Superstation 7: GFB

We acquired more multibeam lines overnight to better locate the flare location. We mounted the multibeam on the ROV, and at around 9, we lowered the ROV into the water. We explore the area to find evidence of seepage (i.e., bubbles, chemosynthetic ecosystems). During Dive 6 (1065), we observed several sponges and collected a few of them, as well as some flat rock, which could be methane-derived carbonate. We spotted a small white microbial mat and measured methane with SAGE before collecting a pushcore. A second pushcore was collected from tubeworms nearby. When the ROV came up, we conducted a CTD (200 m, 569), but no samplings because some bottles were empty, and we preferred to move to a better location with shallow flare. We conducted a second CTD (400 m, 570, and 571) and sampled at various depths for microbiology and gas headspace to compare with SAGE measurements. During the night, we moved to NE on the shelf with the CHIRP to find a spot for multicoring and CTD. When we arrived at the end of the CHIRP line, we noticed that the sedimentary layer was discontinuous and not good for multicoring. We opened the CTD room side door, but the waves were reaching the working deck, so the crew decided that it was unsafe. Therefore, we continued our transit to the SE.

Tuesday 18th November DAY 8

Superstation 8: Prins Karls Forland

During the night, we attempted to deploy the multicorer, but the hard seafloor prevented a successful recovery. The planned CTD cast was also cancelled due to strong winds. We then decided to stop at Prins Karls Forland and deployed the ROV Dive 7 (1066). This site was found during the AKMA1 expedition, and the data were published in Panieri et al. 2023. A mosaic survey was conducted along the same line used during the AKMA1 expedition to observe changes in bacterial mat distribution. Several bacterial mats were observed, characterized by biofilms and filamentous microbes. Notably, emissions of methane and dark oil bubbles were observed rising from the seabed. SAGE measured elevated methane in all areas, but there was an increase in the patches. One push core was collected outside a bacterial mat, and a 2 blade corer were collected within the mats, and scoops and nests were taken in the same bacterial mat that was ca 1 m in diameter and had an elongated shape. At the end of the dive, a SAGE system was deployed to measure methane in the water column, followed by a CTD (572) cast at the same location. After the operations, a science meeting was held to conclude the first leg of the cruise. There was also an exchange of crests between the Kronprins Haakon and the Italian research vessel Gaia Blu from CNR. The day ended with everyone gathering around the moon pool to sing a song composed by Gry Bagøien.

3.2 Leg 2

Wednesday 19th November DAY 9

We arrived in Longyearbyen at 06:00 in the morning, marking the transition between the first and second legs of the expedition. The crew change took place throughout the morning, with people moving efficiently.

At 15:30, we held the safety briefing for the participants joining the second leg. The atmosphere was focused but upbeat, with everyone eager to get started and fully aligned on procedures and expectations for the days ahead.

At 17:00, with the new team on board and operations fully reset, we set sail once again, heading out into improved weather and preparing for the next phase of scientific work.

At 18:00, as soon as we cleared the 12-nautical-mile limit, we activated the multibeam system and began continuous seafloor mapping.

Thursday 20th November DAY 10

Superstation 9: Sørkapp Slope

(Superstation 9-1: Multicoring; Superstation 9-2: Mooring S1; Superstation 9-3: cold seep dive)

We reached a multicoring station (MC-07) at 3:20 and successfully retrieved 6 cores. Then we transited for ~1.5 h toward a mooring station, which failed to release, so we need to collect underwater imagery of the system. We identified the mooring on the singlebeam and started ROV Dive 1067 at 7:05. We followed the mooring until the seabed and had a closer look at the releasing mechanism. We moved to the next nearby station, which is a cold seep reported in Bellec et al. (2024). At 9:00, we start ROV Dive 1068 at the cold seep site (SS9-3). We landed near a microbial mat and started SAGE measurement on top of it.

We take a CTD (CTD-573; 200 m, samplings at 15 m) in parallel to the ROV Dive. We observed a clear spatial zonation of tubeworm forests and microbial mats, and seep carbonates scattered all around. We also noticed trawl marks, which might explain the broken carbonates. At 9:48, we ran an east–west multibeam line of approximately 150 m to map the spatial extent of the active seepage zone. Only one distinct flare was detected in the water-column data. Following this, the ROV conducted a high-resolution mosaic survey flown at an altitude of 2.5 m above the seabed. Sea and current conditions remained calm, enabling steady operations throughout the dive.

The seafloor is defined by microbial mats, dense tube-worm assemblages, carbonate concretions, and scattered carbonate blocks. Several of these blocks appear fragmented and reworked by previous fishing activity. We also documented fishing nets entangled in carbonate debris, now colonised by anemones, indicating long-term deposition on the seabed.

Friday 21st November DAY 11

Superstation 11: Snøras seep

During the morning, we continued steaming toward the Carlberg Field while acquiring multibeam data along the transit. At 15:30, we reached the station named Smørås Seep and deployed ROV 1069. Upon arrival at the seafloor, we immediately observed bacterial mats. A short ROV multibeam survey was conducted to map local morphological features; the seabed in this sector is relatively flat. In parallel, favorable sea conditions allowed us to perform a CTD cast to 200 m, collecting water samples at 15 m. We collected one push core from a bacterial mat and one reference push core from a nearby area without mats or tubeworms. During coring of the bacterial mat, the SAGE open-top sampler recorded high methane concentrations, confirming the presence of active gas-charged sediments.

We then proceeded to collect a gas sample. Since no bubble plumes were visible in the ROV video feed, we disturbed the sediment with a shovel to identify potential gas pockets. The sediment was strongly methane-charged, and disturbance immediately released gas bubbles, enabling us to successfully fill one gas bottle (Bottle No. 5). A blade corer was also taken within a patch of tubeworms before ending the dive. Once the dive was completed and the ROV was secured on deck, we transited southwest toward an exploration well (7220/2-2) and a pilot hole (7220/2-U-1) to assess potential methane emissions. These wells were drilled recently (2024), and seismic data had suggested the possibility of gas release. However, no methane flares or anomalous acoustic signals were detected in the multibeam water-column data.

We then returned to the previous site, Snøras, to attempt an additional blade core, despite the limited time available before the end of the ROV shift at 20:00. The operation was successful, and one blade core was recovered. The core showed vigorous degassing during ascent, and the sediment continued to release methane once on deck.

After recovering the ROV, we deployed a gravity corer at the same location where the blade core had been collected, with the objective of retrieving deeper sediments potentially containing gas hydrate.

Saturday 22nd November DAY 12

Superstations 12-1: Polinya Seep

Superstations 12-2: Kayak well

Superstations 12-13: Mist well

Superstations 12-4: Hurri Seep

Superstations 12-5: Bask Seep

We started ROV dive 1071 at 7:00 at the Polinya seep. During the dive, we observed several red fishes and wolf fishes. We collected carbonate crusts and gas from a bubbling spot. An attempt was made to perform blade coring, but it failed due to the hard sediment. The dive concluded with a vertical SAGE profile conducted on the way up to the ship.

We started ROV dive 1072 at 10:45 and observed a muddy seafloor with some sponges and small holes. During the dive, we located the Pilot well and noticed a wolf fish inside it. Five minutes later, we discovered the exploration well, which was emitting bubbles. These bubbles were sampled from both around the well and inside it. We attempted to collect potential authigenic carbonates, but the sample was too friable, and the collection failed. In parallel with this dive, we conducted a CTD cast (CTD-576) at a depth of 200 m, with samplings taken at 15 m.

We started ROV dive 1073 at 13:00 at the Mist wellbore. During the dive, we crossed two holes that resembled pilot wells or at least signs of non-biological activity. Shortly after, we located the exploration well, which was surrounded by a ring of microbial mats (~1–2 m from the well hole). We sampled the gas coming from inside the well hole. Additionally, we investigated a couple of flares seen nearby in the MB data. However, it turned out to be a mismatch in coordinate conversion, and the flares were likely the same ones we observed with the ROV over the well.

During ROV dive 1074, which started at 15:10, we located the wellbore associated with shallow gas anomalies beneath URU. The site showed intense flares in the MB data. We quickly found the wellbore and observed strong bubbling activity. Two gas samples were successfully collected during this dive (1 completely full, 1 half full, for comparison of gas geochemistry). A Niskin bottle was opened to collect the water for multiparametric analyses onboard. At 16:00, we noticed a crab inside the well hole and a fish biting the bubbles (multiple times). We come up and notice gas bottle 10 leaking from a valve connector. We started Dive 1075 on a natural seep at 16:45. The site shows widespread carbonate deposits, some sparse mats, and lots of red fish. We conducted an ROV multibeam survey and collected a carbonate crust beside a mat with bubbles. At 16:30, we picked up a sponge near a mat and plastic trash. Sample a scoop of microbial mat. We measured with SAGE the seafloor and collected gas bubbles coming from a mat. At 19:00, we played bingo in the mess room. After ROV dives, we started transiting and a MB survey for the next site.

Sunday 23rd November DAY 13

Superstation 13: Tromsøflaket
Superstation 14: 7119/9-1
Superstation 15: 7119/7-1
Superstation 16: Multicore Station

At 6:40, we collected CTD 577 with water samplings at 220 m and at 15 m. We started the dive at 7:00 on a natural seep and placed the fish trap at the seafloor, then we started a ROV multibeam survey and photomosaiking. The fish trap was empty, although several fishes were close to it, so we think that the trap was not completely floating. We decide to end the dive and come up to take the bladecorers, two Niskin, and the bubble sampler. During dive 1077, we placed the bubble sampler on a bubbling spot and then explored the area. The seafloor is very coarse-grained with several cobbles (6-25 cm) and boulders (>25 cm). There are seep carbonates and microbial mats in this area. We sampled the water with two Niskin bottles. At 10:19, we collected snails on a mat using the large scoop. We sampled a carbonate and a rock with a mat on top.
We transited 2h away to the next Superstation 14 and started Dive 1078 at 13:15. We sampled a mat with tubeworms using a scoop-net with the ROV arm at 13:41. We observed several crustaceans, and the ROV zoomed camera clearly showed that they are eating the microbial filaments. During the dive, we collected a bladecore from a mat and grabbed a potential seep carbonate slab next to it, having a white fringe of filaments and bubbles sporadically flowing from underneath. Another bladecore was taken as a reference nearby on a sandy seabed. We travel an hour west to visit an exploration well. During Dive 1079 at the wellbore 7119/7-1, we sampled a flare with a Niskin, gas bubbles, and came up. After the dive, we conduct a chirp line to find a sedimented area for multicoring, which we conduct at 10:17.

Monday 24th November DAY 14

Superstation 17: Outer Bjørnøya
Superstation 18: Tvillingene

At 7:00, we start diving at Borealis (Dive 1080), and we land on the edge of the crater, in a microbial mat and carbonate area. 7:31, we spot a gryphon emitting fresh mud and bubbles, surrounded by white microbial mats. It seems to be composed of three small cones with orifices, of which only one is currently emitting mud. We cross a wide carbonate area and set the fishing trap at 7:39 before conducting the ROV multibeam survey. At 9:30, we stopped microbathymetry and went to check on the fish trap, which turned out to have trapped three fish. At 10:27, we are back to the seafloor for Dive 1081 with 4 bladecorers. We collected two cores on tubeworms and a mat near the gryphon.

We collected 3 carbonates from the same stratified outcrop from the topmost strata (CarC01), lowermost strata (CarC02), and the middle portion (CarC-03). We attempted blade coring in the gryphon but lost the material due to the sandy texture and small fissure between the blades at the bottom. A second attempt behaved similarly, but some sand remained inside (we collected it for biostratigraphy). We collected a dead fish located in the shimmering waters (gryphon crater). During dive 1082, we collected a Niskin from the gryphon, placed the temperature probe, and collected a carbonate crust next to it. We used the net to scoop some snails from the seafloor and ended with a CTD guided by the ROV coupled with SAGE in order to characterize the fluids emitted with shimmering waters. The ROV grabbed the CTD rosette for the first two samplings and then let it go so it could grab the tools and rise vertically along the same path as the CTD for a SAGE profile. We transited ~1 h to Tvillingene and started Dive 1083 at 15:30 by mapping the two craters with multibeam. The microbathymetry provided detail on seafloor structures, which we interpreted as craters with rocky cores at their centers. We explored the northern crater and observed several bubbling spots from the edges of a large carbonate crust and through it. We discovered an active gryphon. We collected a gas sample, but we had to hold the sampler due to the angle of the ground, which could make the sampler fall. We then collected the fluids emitted from the gryphon using a Niskin bottle. We tried to collect blade cores from microbial mats, but the seabed was too hard, so we believe that there is only a thin layer is sediment overlying a wide carbonate pavement. We managed to retrieve a small blade core on a mat with tubeworms. We then collected two carbonates from the southern crater and one from the northern crater. With a scoop net, we sampled some tubeworms and started a photomosaic to cover the northern crater. We ended the dive with a SAGE vertical profile on the way up, above the gryphon. In the evening and overnight, we acquired multibeam data toward the saltdomes and Tromsøflaket SW, the next planned diving site.

Tuesday 25th November DAY 15

Superstation 19: Tromsøflaket SW

Superstation 20: Fugløybanken

We conducted a CTD before the ROV dive to calibrate the acoustics. We started Dive 1084 at 7:00 and explored visually the seafloor to locate a gas flare that was visible in multibeam and also during AKMA3. We started the ROV multibeam and ran two transects crossing the coordinates of the flare and managed to localize the flare. We found three bubbling spots associated with a few small microbial mats (10-20 cm diameter), very localized in an area approximately 10 x 10 m. We collected a gas sample on the most stable and intense bubble stream (GasS-17). In the meantime, we attempted blade coring, but the seafloor is too hard. We went back to the gas sampler and sampled the gas. We filled an ROV Niskin bottle with water from the bubbling spot and then conducted a SAGE vertical profile on the way up, starting at 8.22. We move to the next location at Fugløybanken, where during

AKMA3 we couldn't sample with the bubble catcher due to logistical issues. At 13:30, we are starting ROV Dive at the new site on Fugløybanken, which hosts gas flares and oil slicks. We conducted MB and visual exploration at oil slicks but couldn't locate any seep or chemosynthetic ecosystem, so we moved to the area with gas flares and spotted some small microbial mats on rocky substrate. Bubbles were escaping intermittently, with a low flux. We managed to collect a blade core from a mat. We collected water over a seep with the Niskin and performed some SAGE measurements over mats. We ended the dive at 17:44.

Wednesday 26th November DAY 16

We arrived to Tromsø in the morning at around 8:00 and had police passport control at 9 am at the harbor.

4 Scientific Equipment

4.1 Hydroacoustic systems

The RV Kronprins Haakon is equipped with hydroacoustic systems that can be operated simultaneously. These systems are managed by dedicated software that intelligently coordinates transducer pings to prevent interference.

During the EXTREME24 cruise, the following hydroacoustic systems were extensively utilized:

- Simrad Kongsberg EA 600 – 12kHz single beam echosounder
- Kongsberg EM710 and EM 302 multibeam echosounder and SBP 300 Sub-Bottom Profiler

4.1.1 Kongsberg EA 600 –12kHz single beam echosounder

The single-beam echosounder EA 600 can simultaneously operate up to four high-power transceivers. Frequencies ranging from 12 to 710 kHz are available. A range of highly effective transducers is offered to meet all operational requirements from very shallow water to a depth of 11,000 meters. The primary purpose of this echosounder is to determine depth and locate highly reflective objects in the water column. During this expedition, we used the echosounder at 12 kHz as this frequency provided the best detection of the seafloor.

4.1.2 EM 710

The EM710 multibeam echosounder is a high to very high-resolution seabed mapping system that uses sonar frequencies in the 70-100 kHz range. It is installed on the port drop keel of the Kronprins Haakon and is well-suited for swath bathymetry surveys in water depths of up to 800 meters. The system emits 400 beams at angles of up to 70° on each side, with options to adjust the beam spacing to be equiangular or equidistant. It also has a high-density mode to achieve greater sounding density by reducing the acoustic footprint. During the EXTREME24 cruise, the system operated in high-density equidistant mode. Additionally, the EM710 can record water column backscatter data, which helps identify gas bubbles in the water column. This system was the primary multibeam system used during the expedition, and new CTD data were collected as needed to update the water velocity used by the EM710 system.

4.1.3 EM 302 and SBP 300

The multibeam echosounder EM 302 operates at a frequency of 30 kHz and is specifically designed for detailed and accurate seabed mapping at depths exceeding 7000 m. It utilizes beam focusing during both transmission and reception. Additionally, the EM 302 is equipped with a feature to minimize transmission power to avoid disturbing marine mammals nearby.

The system can produce up to 432 soundings per swath, with pointing angles automatically adjusted based on achievable coverage or user-defined limits. In dual swath mode, the system can generate up to 864 soundings, with the transmit fan duplicated and transmitted with a slight difference in a long-track tilt. The applied tilt is adjusted based on depth, coverage, and vessel speed to maintain a consistent sounding separation along the track. Furthermore, the transmit fan is divided into individual sectors with independent active steering to compensate for vessel movements such as yaw, pitch, and roll. Each transmit sector has its own beam focusing.

When combined with a separate low frequency transmit transducer, the EM 302 can potentially provide sub-bottom profiling capabilities with a narrow beam width, known as the SBP 300 sub-bottom profiler.

The EM 302 (including the SBP 300) is installed in the ice window in the vessel's bottom hull. However, during ice breaking, the movement of ice beneath and alongside the ice window significantly impacts data acquisition, resulting in elevated noise levels and inaccurate measurements.

4.2 Oceanographic systems

Physical and chemical measurements in the water column were measured from a CTD (conductivity, temperature, depth)/rosette. The CTD model is a Seabird 911 Plus mounted on a 12-bottle carousel of 10-litre Niskin bottles and was brought close to the seafloor. The CTD is coupled with different types of equipment such as oxygen sensors, transmissometers, and fluorimeters.

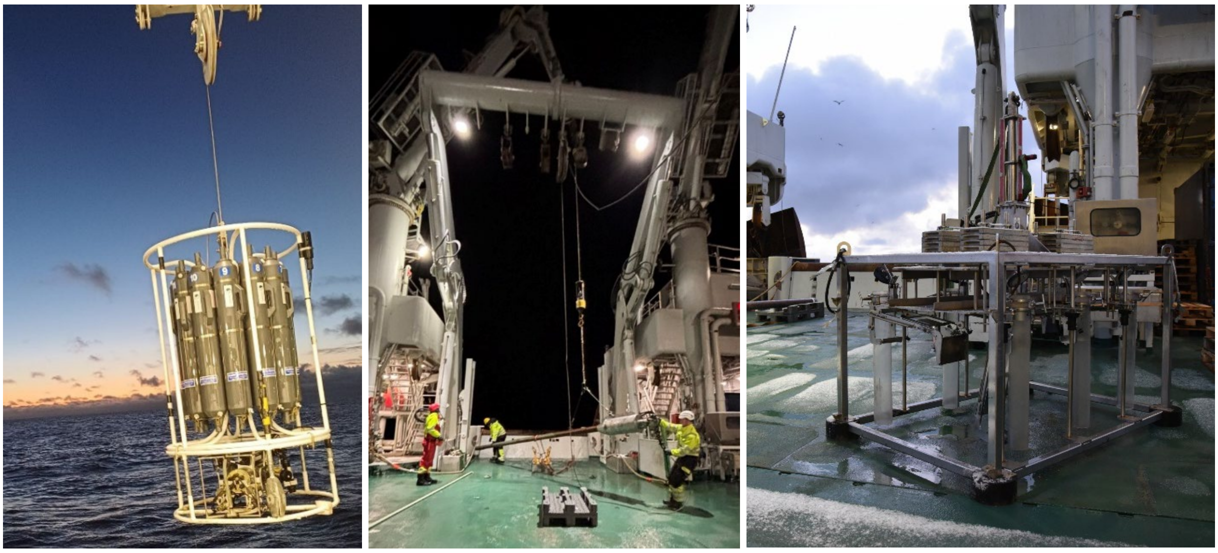

Figure 3. Left to right: CTD/rosette and gravity corer deploying from R/V Kronprins Haakon, and Multicorer on deck of the R/V Kronprins Haakon.

4.3 Attributed Sensors

4.3.1 GPS/Navigation, Motion Reference Unit

An integrated global navigation satellite system (GNSS) is utilized, which employs signals from GPS, GLONASS, Galileo, or Beidou, along with inertial measurements, to deliver high-quality outcomes for various applications such as hydrographic surveying, dredging, oceanographic research, and seismic work. This Seapath system is equipped with a 5th-generation MRU motion sensor package that offers a roll and pitch accuracy of up to 0.008° RMS. The precision of this accuracy is attained using precise linear accelerometers and unique MEMS-type angular rate gyros. The MRU's processing unit encountered some issues in providing precise pitch and roll information, which significantly impacted USBL positioning and EM302 multibeam acquisition.

4.3.2 USBL HiPaP

ROV NUI, OFOBS, CTD, and some coring equipment were equipped with a HiPaP beacon for precise positioning on the seafloor. The HiPaP 501 system uses a transducer mounted on the hull that can be lowered a few meters below the vessel's hull. A transceiver unit, which includes a transmitter, preamplifiers, and beam-forming electronics, is mounted near the hull unit. This system has a spherical transducer with hundreds of elements covering the entire sphere under the vessel. It dynamically controls the beam to always point toward the transponder, even if the transponder is moving and the vessel's roll, pitch, and yaw affect its position. Roll and pitch data from sensors are used to compensate for the vessel's position.

The Super Short Base Line (SSBL) principle has the advantage of requiring only one hull-mounted transducer and one subsea transponder to establish the transponder's threedimensional position. An SSBL system measures the horizontal and vertical angles along with the transponder's range. Any error in the angle measurement results in a position error that depends on the transponder's range. To achieve better position accuracy in deep water with an SSBL system, it is necessary to improve the angle measurement accuracy. The HiPaP 501 operates in the frequency band of 21 - 31 kHz with an operating range of 1 - 5000 m. The range detection accuracy is specified as 0.02 m under the assumption of unobstructed visibility between the transducer and transponder, minimal or no water column noise, and no errors from the heading/roll/pitch sensor. We observed interference between the HiPaP and multibeam EM 302 systems due to their use of similar frequency bands. During most seafloor operations, EM 302 acquisition was halted, resulting in a more stable positioning of the USBL transponder.

4.4 Sediment sampling

4.4.1 Gravity corer

The gravity core is a tool used in marine sediment sampling. It penetrates the seafloor under gravity. The gravity corer consists of a 6 m-long iron barrel with iron weights of 1035 kg attached on top of it. The whole apparatus weighs ~ 2 tons. A plastic liner with an outer diameter of 11 cm and an inner diameter of 10 cm is inserted into the steel barrel. Before the gravity corer deployment, a core catcher and a core cutter are attached to the lower end of the gravity corer. The core catcher prevents sediment from escaping from the core during operations, while the core cutter facilitates the core's penetration into the sediment bed.

4.4.2 Multi corer

The multicore is a KC Denmark DK8000 multicore simultaneously carrying six parallel tubes 80 cm long and 10 cm in diameter. At least one core tube was pre-drilled for pore water and headspace gas sampling. The core tubes are loaded with the top and bottom ends open. When the multicore is lowered to the seabed, the tubes are pushed into the soft sediment by lead weights and closed at both ends. It is possible to sample up to 60 cm of sediment, and the water overlying it.

4.5 ROV “Ægir6000”

The ROV ÆGIR6000 is a SUPPORTER 2-type ROV from Kystdesign in Aksdal, Norway (Figure 7). The ROV has a total combined power of 115 kW, a depth rating of 6000 m, and is maneuvered by 7 thrusters. Its dimensions are (LxBxH) 2,75 m x 1,7 m x 1,65 m, and it weighs 3600 kg in air. The ROV can carry a 400 kg payload and has two robust manipulator arms. 8 HD and composite video camera inputs provide full operational visibility and have limited zoom and focus capabilities. The video footage recorded by the ROV includes the overlay (date, time, depth, coordinates, cruise name) in UTC or ship time (local time), unless otherwise indicated. The lighting capacity includes ten dimmable lights and has a

maximum total load of 2300W. The SUPPORTER 2 can accommodate up to 24 additional hydraulic tooling functions, up to 21 additional survey sensors, and 8 camera connectors. All hydraulic functions are proportionally controlled, and all electrical power supplies are ground fault monitored. The ROV control system offers a variety of auto-functions like AutoPOS and AutoTRACK capabilities. The control pod and telemetry system for survey operations work via up to 6 fiber optic cables. The umbilical cable on RV Kronprins Haakon provides 4 fiber optic cables. In addition to the video feed, the system can support several additional communication channels, both serial and Ethernet. The ROV is equipped with an EM 2040 multibeam echosounder for deep water multibeam mapping of the near-bottom sounding environment in detail. The basic EM 2040 has a transmit transducer, a receive transducer, a processing unit, and a deck-side processing computer. The EM2040 operates at 200 - 400KHz, with 400 beams in single-swath mode offering 0.4 x 0.7-degree angular resolution. A swath angle of up to 140 degrees can be reached, providing a maximum coverage of 4 to 5 times the water depth.
The ROV is equipped with a large drawer to store sample material during dives. Aside from the manipulator arms that provide the opportunity to take direct carbonate or rock samples, the ROV ÆGIR6000 also offers several sampling tools, most prominently the push coring device, made of fiberglass, that can take up to 60 cm long sediment cores with a diameter of 8 cm (Figure 5). Another device is the blade corer; it is 32 cm long and can sample a volume of sediment with a larger rectangular area of approximately 25x10 cm (Figure 5). Push core and blade core liners are pre-drilled for pore water sampling with a resolution of 1-2 cm. The push cores are placed in the TMS frame of the ROV during the entire dive, while the blade core container is held by one of the ROV's arms during descent and ascent. When the ROV reaches the bottom, the blade cores container is placed on the seabed while the Dive is ongoing.

4.5.1 ROV exploration & sampling

During the EXTREME25 expedition, the ROV conducted 26 dives with various objectives. This included sampling sediment, meiofauna, macrofauna, fish, and gas. Additionally, the ROV used Sagasubsea AS to measure methane levels in seawater at different depths and near the seabed using the SAGE sensor developed at WHOI. The ROV also captured video footage with a downward facing 4k camera to visually represent different habitats and sedimentary facies at the explored sites. The precise locations for the ROV dives were chosen based on seafloor mapping and water column data analysis, as detailed in the Equipment section of this report.

4.5.2 Sampling equipment used by ROV Ægir6000

4.5.2.1 Gas sampling and flux measurements

Free gas (gas bubbles) was sampled by ROV and by using the KYSTDESIGN free standing gas sampler equipped with steel sampling bottles (Figure 4). Each sample bottle can be

operated separately by a valve using ROV manipulator. There is a clear cylinder in the middle on top of the funnel, with a total capacity of 500 ml and 25 ml subdivisions, enables precise volume measurements that can be converted into fluxes by timing the gas accumulation in the cylinder. Gas that gathers in the clear cylinder is drawn into a steel cylinder by opening a valve because of the pressure contrast between the steel cylinder (atmospheric pressure) and subsea pressure. Steel cylinders containing sampled gas were kept in the refrigeration room after retrieval. After the cruise, the samples will be examined for gas composition and isotopic signature.
Bubbles generally manifest as individual bubble streams emerging from small openings in the sandy and muddy sediments or through fissures in carbonate crusts. Bacterial mats often surround the source of the bubble stream. Seepage activity varied significantly across the study areas, as evidenced by the notably different numbers of total bubble streams and the visual intensity of the bubble stream.

Figure 4. The KYSTDESIGN standalone gas sampler was placed above the observed bubble stream, and the filling volume was documented at different time steps to calculate a bubble stream per minute.

4.5.2.2 Temperature probes

To measure temperatures in sediments at selected seep and vent sites, MISO High-Temperature, Full-Range (0°-450 °C) Self-Recording Loggers (MISO Facility, WHOI) were deployed. When possible, the temperature probes were left in the sediments for at least 30 minutes to allow for a stable temperature reading.

4.5.2.3 Scoop

A large scoop (~20 x 30 cm), informally called “Frankenstein” due to its composite structure, was used to collect biota.

4.5.2.4 Blade corer

Blade corers were used to sample sediment. Due to their closing mechanism, they provide the possibility of obtaining pristine sediment samples with preserved sediment surfaces. Their size is 320 x 100 x 250 mm. The blade corer frame has an automatic closing mechanism at the bottom to avoid sample loss. The blade cores are manually wound up beforehand, and when placed on the seafloor, the ROV will push them into the sediment and release a pin that makes the blades close. This traps the sediments in the core, and the whole core becomes sealed.

4.5.2.5 Push core

Push cores with an 8 cm diameter and 60 cm length were used. The tubes are transparent, made of fiberglass, and feature a holder for manipulation by the ROV arm.

4.5.2.6 Niskin Bottles

Niskin bottles, operated with Ægir6000's articulated arm, were used.

Figure 5. Sampling tools used by ROV ÆGIR6000 during EXTREME25. From left to right: blade corer, push core, Niskin.

4.6 SAGE Methane Instrument

SAGE, the Sensor for Aqueous Gases in the Environment (Figure 6A), is a deployable sensor that measures in situ dissolved methane or carbon dioxide in the deep sea. It was developed by a team of engineers and scientists at the Woods Hole Oceanographic Institution (WHOI), led by Jason Kapit and Anna Michel with support from Schmidt Marine Technology Partners (#G24-67175).

Carbon dioxide (CO_2) and methane (CH_4) have complex and often poorly characterized roles in the ocean and atmosphere. Methane is emitted from vents or seeps in the Greenland and Barents Seas, providing a rich energy source for chemosynthetic ecosystems, but is a potent greenhouse gas if it reaches the atmosphere. Carbon dioxide is both a component of some hydrothermal fluids, a product from the oxidation of methane, and drawn down into surface waters from atmospheric dissolution. Characterization of the distribution and fate of these dissolved gases and their relationships is essential for understanding their origins and their impacts.

The deployment of SAGE on EXTREME25 was intended to address the following research questions. 1) To identify sources of dissolved methane or carbon dioxide in deep sea vents or seeps and characterize the relationships between these dissolved gases and the surrounding ecosystems or geology. By providing real-time data, SAGE can both guide sampling and allow new sources of dissolved gases to be found. 2) To study the water column dynamics and potential expression in the surface seawater of methane emitted from seafloor sources, particularly from the shallow seep sites in the Barents Sea. These research activities were further supported by targeted CTD casts and discrete water sampling with post-cruise analysis for total methane and CO2 and their isotopic compositions. Research using SAGE on EXTREME25 was funded by a WHOI Access to the Sea Award.

SAGE provides the capability to measure the partial pressure of dissolved methane and carbon dioxide in real-time with advances in response time, detection limit, and versatility compared to existing commercial technologies. SAGE uses a membrane (Figure 6B) to extract dissolved gases from seawater into a hollow-core optic fiber inside the instrument (Figure 6C). The amount of extracted methane or carbon dioxide within this fiber is measured using tunable infrared laser absorption spectroscopy, with the wavelength chosen to target a specific absorption band for each gas. Using micron-scale fiber optics in place of traditional absorption cells means that the gas volume required for a measurement is extremely small, resulting in a fast response time (on the order of minutes), low detection limit (~1 µatm), and wide dynamic range (1 to ~30,000 µatm) — making the measurement of extremely small changes to surface dissolved gas concentrations possible.

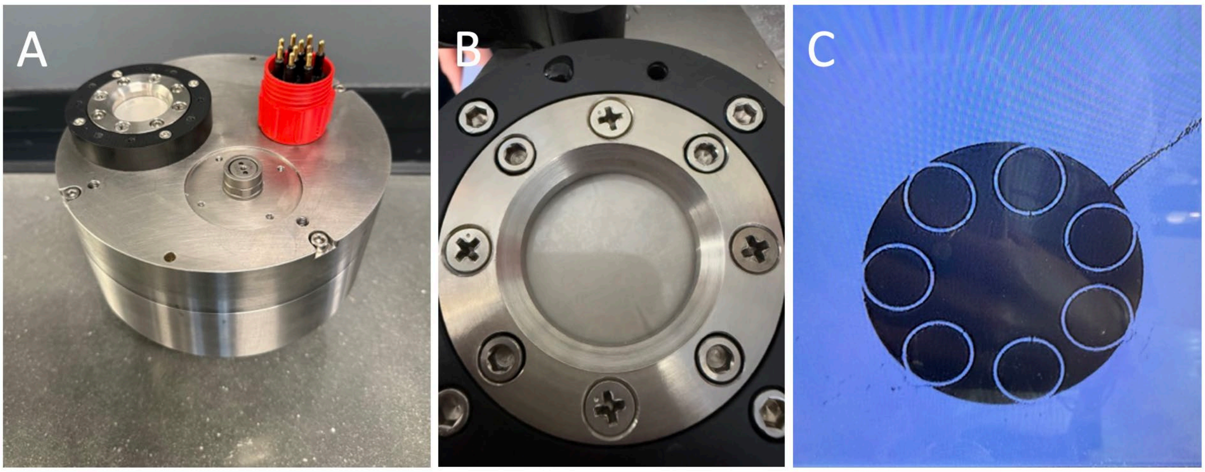

Figure 6. SAGE methane sensor (A). Internal structure of SAGE hollow core fiber (B). Gas permeable membrane which has a flow cap covering it when integrated onto an ROV (C).

SAGE operates on 24VDC power and uses RS232 communications to provide data and instrument control, including pump status and internal heater settings. A Seabird 5T pump, powered by SAGE, provides continuous water flow past the membrane.

5 Methods

5.1 Ship-based Multibeam Echosounder and Water Column Data (WCD)

The R/V Kronprins Haakon is equipped with two multibeam echosounder systems: a hull-mounted Kongsberg EM302 and a Kongsberg EM710 mounted on the drop keel. During the EXTRE25 cruise, only the EM302 system was used. The EM302 operates at a nominal frequency of 70 kHz and provides an angular coverage of up to 140°, with up to 400 beams per ping. During the cruise, the system was operated with an opening angle of 45°/45°. The ping rate varied with water depth and opening angle, typically ranging between 0.5 and 2 Hz. The EM302 is capable of acquiring high-resolution bathymetric data in water depths of up to approximately 7000 m, with the achievable swath width depending on both seafloor morphology and the selected angular coverage.

Throughout the cruise, the EM302 was used to collect continuous bathymetric data to provide a regional overview of seafloor morphology within the study area. Data acquisition was suspended during ROV operations to avoid acoustic interference with the vehicle's systems.

In addition to bathymetric mapping, the EM302 was used to acquire water-column data. These data were processed and analyzed using QPS FMMidwater software. Water-column analysis enables the detection of acoustic anomalies, such as gas flares, which may indicate active gas seepage from the seafloor into the water column. Detected flares were spatially correlated and visualized in relation to the underlying bathymetry.

The EM302 system also allows the simultaneous use of the SBP300 sub-bottom profiler, which operates at low frequencies with a very narrow beam width, enabling the imaging of shallow sub-seafloor structures. This capability provides complementary information on sedimentary layering and shallow geological features beneath the seafloor.

5.2 ROV-based Seafloor Mapping

5.2.1 ROV MBES Microbathymetry

The ROV Ægir 6000 was equipped with a high-frequency Kongsberg EM2040 multibeam echosounder for the acquisition of high-resolution morphobathymetric data (microbathymetry). The MBES mounted on the ROV enabled detailed mapping of localized seafloor features, with the vehicle typically flying at an average altitude of approximately 20 m above the seabed. MBES survey lines were acquired, maintaining approximately 50% overlap between adjacent lines to ensure adequate coverage and data quality. Under these operational conditions, digital elevation models (DEMs) with a spatial resolution of less than 0.50 m were achieved.

Similar to the ship-mounted system, the ROV-based EM2040 MBES enabled the acquisition and analysis of water-column data. These data were used to identify acoustic flares associated with potential gas seepage from the seafloor at a much finer spatial scale than that achievable with ship-based observations.

ROV positioning during dives was achieved using the HIPAP 501 Ultra Short Baseline (USBL) high-precision underwater positioning system. The integration of USBL navigation data with the EM2040 MBES measurements ensured accurate georeferencing of the microbathymetric datasets collected during ROV operations.

5.2.2 ROV Photogrammetry

ROV video acquisition was conducted using a downward-facing camera along planned, adjacent, and parallel transects spaced 2 m apart. During surveys, the ROV maintained a steady speed of 0.3/0.5 knots and an altitude of ~2–2.5 m above the seafloor, resulting in a field of view slightly greater than 2 m and ensuring sufficient image overlap for photogrammetric reconstruction (Figure 7). These acquisition parameters were validated during previous field campaigns. Operations were fully dedicated to collecting video footage suitable for seafloor photomosaic reconstruction in key areas. Accurate ROV positioning for both MBES and photogrammetric surveys was obtained using the HIPAP 501 Ultra Short Baseline (USBL) system, ensuring high-precision localisation. ROV videos were processed by extracting one frame per second, producing high-definition (1920 × 1080 px) PNG images sorted by survey area.

The extracted frames will be imported into Agisoft Metashape Professional 2.0 and processed following a standard Structure-from-Motion (SfM) workflow. After camera alignment, dense point clouds will be generated to produce ultra-high-resolution digital elevation models (DEMs) and orthomosaics. The spacing between the ROV laser pointers (9 cm) will be used as a ground-truth scale bar for each model. To accurately scale and georeferenced the products, USBL-derived coordinates and timestamps will be linked to selected video frames, primarily at the ends and centres of each transect, and cross-validated against geomorphic features visible in both the ROV-derived microbathymetry and the SfM-generated DEMs. The resulting orthomosaics will enable detailed reconstruction of representative seafloor features and assessment of the spatial distribution patterns of bacterial mats and associated macrofauna (e.g., tubeworms).

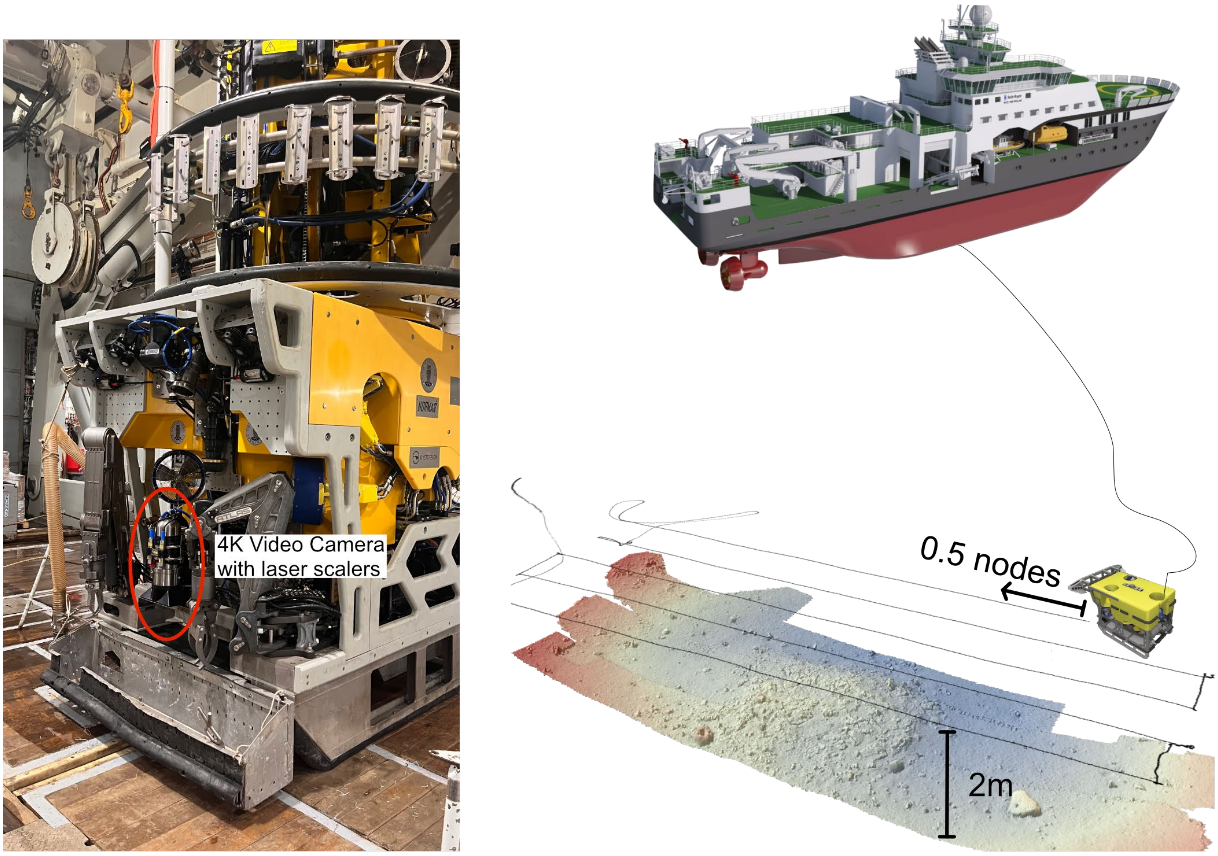

Figure 7. On the left, the ROV Ægir 6000 is used to collect video data; the red circle indicates the central video camera used for photogrammetric reconstruction. On the right, the graphic representation exemplifies the ROV's acquisition methodology (not to scale) along predefined paths.

5.3 Marine Geology

The Appendix contains a comprehensive list of all sediment samples gathered during the expedition. The "List of samples" table provides details about the sampling equipment used, including push cores and blade corers operated by the ROV Ægir6000, gravity-based methods, and multicorers. It also specifies the intended analyses for each sample.

5.3.1 Sedimentology

The seafloor sediment type was evaluated using high-resolution ROV images of the top layer and direct examination during push core and blade corer slicing. X-ray fluorescence (XRF) core-scanning, an efficient non-invasive method for quickly analysing elemental differences in grain size analyses, will be performed in the laboratory.

5.3.2 Rock sampling

Samples of rocks that caught the attention at the seafloor during the ROV Dives have been gathered using the manipulator arm of the ROV. The rocks were rinsed with freshwater to eliminate any salt deposits and then placed on the deck to air dry. At times, the biologist detached epiphytic organisms from the rocks.

5.3.2.1 *Exploring mantle-magma-seawater interaction processes at an Oceanic Core Complex at the Molloy Ridge*

Oceanic Core Complexes (OCCs) are geomorphological features with a domal mountain shape detected in bathymetric maps along Mid-Ocean Ridges or poorly magmatic continental rifts at extensional tectonic settings. OCCs are created by the activity of long-lived detachment faults that develop parallel to the ridge axis in regions of reduced magmatism. The continuous extension along the fault zone allows flexural rotations of large portions of oceanic basement, leading to the exposure of deep-seated rocks, i.e., lower oceanic crust and upper mantle, on the seafloor. At the same time, detachment faults act as migration pathways for seawater that interacts with the hot oceanic mantle, generating a widespread vent activity along the fault plane (Tucholke et al., 1998; Smith et al., 2008; MacLeod et al., 2011; Ligi et al., 2022, and references therein).

An archetypal oceanic core complex was recently described by Chand et al. (2024 - Figure 8) at the intersection between the Molloy fracture zone and the Molloy Ridge, along the Arctic plate boundary separating Eurasia (EU) and North America (NA) plates. A well-identified corrugated surface was identified along the Molloy ridge, representing the surface expression of a long-lived detachment located at a latitude of 79° 25.391′ N (Figure 8). Here, the corrugations are mostly oriented along a NW-SE direction, which represents the kinematic direction of flexural rotation. Two fault scarps crosscutting at high angle the corrugated surface can also be observed. These normal faults dissect the detachment surface and represent the best candidate locations to collect samples from the lower oceanic crust and upper mantle, with high potential to be associated with hydrothermal vents.

At this new site, we conducted an ROV dive exploring the corrugated area with an E-W transect along the direction of the corrugation. The ROV track extended for ca 1.5 km from the termination area, throughout the two fault escarpments. As expected, the detachment surface and the eastern fault scarp were covered by sediments, and only a few drop stones of likely continental origin were collected. The base of the second fault scarp is instead characterized by an outcrop, where we collected angular and fractured rock samples, potentially represented by serpentinized peridotites and minor gabbroic samples. The rocks were collected in proximity to a small area covered by microbial mats with pronounced filaments and shimmering waters, clear evidence of hydrothermal activity, and were thereby named as “Frigg Vent Field”.

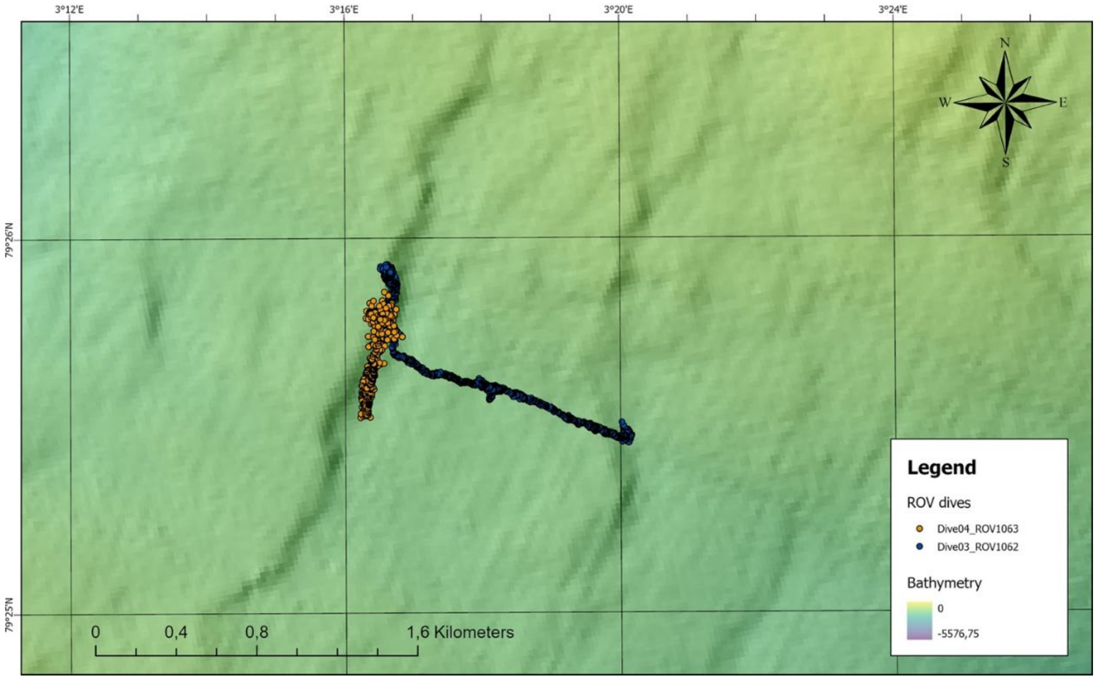

Figure 8. Multibeam bathymetry data from the [MAREANO repository](), showing the area of the detected Oceanic Core Complex. Corrugations are mostly oriented along a NW-SE direction, representing the kinematic direction of flexural rotation. Two fault scarps crosscutting at high angle the corrugated surface can also be observed. These normal faults dissect the detachment surface and represent the best candidate locations to collect samples from the lower oceanic crust and upper mantle, with high potential to be associated with hydrothermal vents. Black and orange dots are tracks of dives ROV1062 and ROV1063, respectively.

Our post-cruise research will consist of a twofold approach bridging petrological and geochemical studies with computational geodynamics, as recently developed by our research group (e.g., Sanfilippo et al., 2024). The activities will be developed on the following phases: (I) a detailed microtextural characterization by optical and electron microscopes, followed by a petrological study aimed at quantifying the mineral major and trace element compositions via electron microprobe and laser ablation ICP mass spectrometry; (II) the definition of the chemico-physical processes suffered by the peridotites, from melt extraction and melt percolation at high temperatures, to interaction with seawater at lower temperatures; these processes will be evaluated on the rock samples using high-resolution trace element geochemical mapping by laser ablation ICP time-of-flight mass spectrometry; (III) the definition of the nature of the upper mantle in this sector of Arctic ridge, and the signature of the percolating magma using radiogenic isotope determination (Nd-Hf-Sr-Pb) of mineral separates (pyroxene, amphibole, mica) by multicollector ICP mass spectrometry; (IV) the results of the petrological and geochemical study will be integrated in computational geodynamic numerical modelling activities. Using existing numerical solutions, we will quantify mantle thermal structure, mantle melting regime, and dynamic processes, reconstructing the oceanic lithosphere evolution of this sector of the Arctic Ocean and how this can be dependent on the heterogeneity of the mantle below the EU and NA plates.

5.3.3 Gas sampling

During former CAGE, AKMA, and EXTREME cruises led by UiT, acoustic observations of gas and fluid escape from the seafloor were documented in the Western Norwegian Barents Sea and west of Spitsbergen. These natural gas and oil emissions may be related to mud volcanoes, gas hydrate occurrences, and are often associated with patches of microbial mats and/or chemosynthetic communities on the seafloor. The seep intensities range from diffusive gas transfer with no acoustic anomalies to ebullition activity, i.e., bubbling. In addition to the naturally occurring gas seeps (NAGS), abandoned well locations from exploration drilling in the southern Barents Sea may show well-associated gas seeps (WAGS) as well.

Like the widespread occurrences of fluid escape from the seafloor are the hydrocarbon gas compositions and their generation pathways (Figure 9).

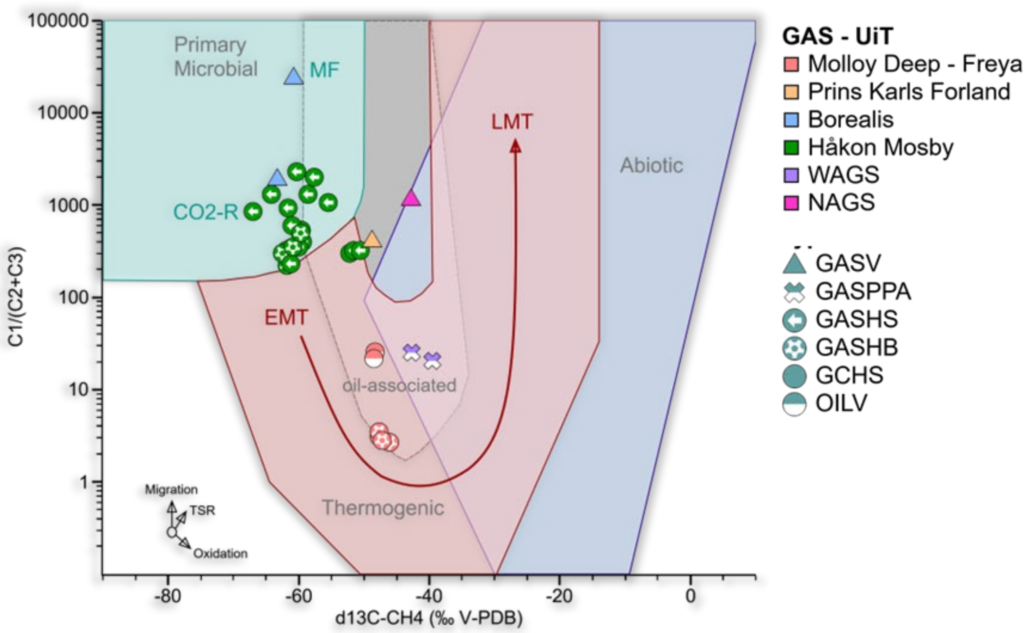

Figure 9. Gas interpretation diagram of δ13C methane versus the gas composition, given as the "Bernard" ratio (Bernard et al., 1979; Whiticar, 1999; Milkov and Etiope, 2018). GASV – Gas vent, GASPPA – gas from plugged and abandoned well, GASHS – head-space gas, GASHB – hydrate bound gas, GCHS – head-space gas from gravity core, OILV – oil vent site.

Typical microbial gas from CO2 reduction is reported from the Håkon Mosby (Lein et al., 1999) and Borealis (Panieri et al, 2025) mud volcanoes from both head-space gas from sediment samples, free gas bubbles, and as hydrate bound gas. Typical oil-associated thermogenic gas, on the contrary, is found in the Molloy Deep/Freya locations (Panieri et al., accepted manuscript), also as free and hydrate bound gas. The gas emanating from the oil-seep site to the west of Prins Karls Forland (Panieri et al., 2024a), however, is of

mixed microbial-thermogenic origin. WAGS from plugged and abandoned wells in the Snøhvit area and the Håkjerringdjupet show also a typical thermogenic gas signature, while the natural gas seep close to the Snøhvit field (NAGS) has a thermogenic methane isotope value, but compositional fraction to a higher gas ratio is observed (AKMA3 - Panieri, et al., 2024b).
The goal of the EXTREME25 cruise for its gas program is to deepen the understanding of gas release from the seafloor at both natural seeps and at anthropogenically induced seep sites.
Free gas (gas bubbles) will be sampled by ROV and by using the KYSTDESIGN free standing gas sampler equipped with three sampling bottles. Each sample bottle can be operated separately by a valve. The gas sampler was placed above the bubble stream for sampling. If the bubble stream allowed bubble-flow measurements were performed with the integrated measuring pipe. The measuring pipe has a total capacity of 500 ml, with 25 ml subdivisions. The filling time was stopped at different levels, and a mean bubble-flow rate per minute was calculated. At some locations two bottles were filled, one with gas only, and a second with water and gas to perform quality control for gas compositional and isotope measurements, i. e. gas only versus water with little gas (volume by volume). In addition to free gas, sediment samples will be taken from gravity cores and ROV push and blade cores for head-space gas samples (Isojars). Head-space gas analyses shall also be performed on water samples taken with NISKIN bottles from CTD casts and/or taken by ROV at selected vent sites.

5.3.4 Pore fluid samplings and onboard water measurements

Samples of porewater were obtained from blade cores and from push cores, multicores, and gravity cores at varying intervals based on the expected position of the sulphate-methane transition zone. Before deployment, push core and blade core liners were pre-drilled and sealed with tape. Porewater sampling took place in a cooled room (4 °C) after recovery. The methods used were in line with those detailed in Argentino et al. (2023) and are summarized as follows: 5 cm-long pre-wetted rhizons (0.15 μm mesh) were inserted into the pre-drilled holes (Figure 10), and water samples were obtained by applying suction with 10 mL syringes. The pore water samples were divided into different portions: 1) 2 mL subsamples were transferred into screw cap glass vials for dissolved inorganic carbon (DIC) analysis. We stored DIC samples at 4 °C without any fixative addition, as recent findings have indicated that it could affect the DIC geochemistry of cold seep samples (Argentino et al., 2023). 2) 1 mL was transferred into Eppendorf tubes and stored at -20 °C for sulphate analysis. 3) Samples for trace metals (0.5-1 mL) were treated with 10 μl of ultrapure 65% nitric acid (HNO3) to lower the pH to < 2 and stored at 4 °C.
We measured pH / Conductivity / TDS / Salinity on three water samples collected from ROV-operated Niskin from Frigg, Borealis, and Hurri seep using a Thermo Scientific™ Elite PCTS Pocket Tester.

In blade cores, bulk sediment samples (5 mL) were extracted at 5 cm,10 cm, and 15 cm depths using a cut-off syringe. These samples were then transferred into glass vials containing 5 mL of NaOH (1 M) to halt microbial activity. The vials were sealed with a rubber septum, sealed with aluminium crimp caps, and shaken, after which they were stored upside-down at 4 °C.

Figure 10. Pore water extraction from a blade core.

5.4 Marine Biology

5.4.1 Microbiology

Seawater and sediment samples were collected for molecular analyses, cell counting, microbial enrichments, and geochemical measurements. At each station, seawater was obtained using Niskin bottles and filtered through 3 μm or 0.22 μm membranes, depending on sample type. Sediments were collected directly into 50 mL Falcon tubes using blade corers and push corers. Filters and sediment samples were immediately frozen at -80 °C for DNA and RNA extraction. Seawater filtered at 0.22 μm was transferred into two trace-metal–free 50 mL tubes and stored at 4 °C for geochemical analyses. Subsamples of water and sediment for cell counting were fixed with 2% formaldehyde in cryovials and stored at 4 °C. Additional subsamples were placed in 120 mL vials sealed with butyl rubber stoppers for microbial enrichment experiments and stored at 4 °C until processing. Metadata for each sample, including sampling conditions, environmental observations, and CTD-derived physicochemical parameters, were recorded during collection.

5.4.1.1 Sampling Objectives, Sites, and Context

The sampling aimed to characterise: (i) the microbial diversity hydrothermal and cold-seep systems and sediment characterside by oil seepage at the seafloor, through the collection of chemosynthetic biolfilms, cold-seep oil seepage sediments; (ii) the microbial communities inhabiting the water column above the methane emission flares, captured by sampling water masses across depth layers from the seafloor to mid-water and upper-

water environments; and (iii) the surface-water microbial assemblages, including both prokaryotic and eukaryotic communities.
Sediment layers were collected at the surface and at 3 depths to investigate the microbial community stratification.
Vertical transects along emission flares to assess microbial diversity from deep-sea emissions and the water column.
The horizontal surface transects across the transition from Atlantic to Arctic waters, crossing the polar front. This design will allow us to integrate analysis of benthic, pelagic, and surface microbial processes.
Three main environments guided the sampling design:

- **Seafloor emission areas:** oil seepage sites and cold seep emissions were sampled because of their capacity to sustain localised oases of biodiversity. These systems host nutrient-rich habitats where chemosynthetic microbial communities form the foundations of complex ecosystems extending to higher trophic levels.
- **Water column influenced by emission flares:** vertical transects were performed along emission plumes that may influence microbial diversity over hundreds to thousands of metres. At the Freya site (depth ~3500 m), the emission flare was visible up to approximately 200 m below the surface, providing an ideal system to investigate vertical microbial gradients.
- **Surface waters:** surface sampling characterised microbial communities associated with warm Atlantic waters flowing into the Arctic, a process relevant to rapid ocean warming and Atlantification. The Arctic night provided a rare opportunity to sample phytoplankton under light-limited conditions, for which minimal data exist. It also remains unknown whether deep emissions influence surface microbial assemblages; this sampling allowed exploration of that connection.

5.4.1.2 Sampling Equipment and Procedures

- Sediments and vent/seep fluids were collected using a range of ROV-mounted tools, including push cores, blade cores, and a biosyringe system for targeted sampling of biofilms and fluids. Sediment cores were collected using ROV push cores and blade cores and recovered onboard. Each core was subsampled by slicing discrete layers, which were transferred into 50 mL Falcon tubes. The ROV biosyringe was used to collect biofilms and fluids, which were transferred into dedicated vials and falcon tubes for downstream analyses.
- Water samples from the water column were obtained using Niskin bottles mounted on a CTD rosette, allowing the acquisition of both water samples and high-resolution chemical and physical profiles. Niskin bottles were closed at targeted depths along the vertical transects. Water was filtered onboard through 0.22 µm Sterivex cartridges to capture microbial biomass.

- Surface-water sampling followed the TARA Oceans protocols to ensure comparability with global datasets. Approximately 15 L of seawater was collected and prefiltered through a 200 µm mesh. Size-fractionated filtration was then performed to obtain: (i) a 3 µm fraction, and (ii) a 0.22 µm fraction. These filters were retained for microbial diversity analyses and for comparative studies with existing global datasets.
- Samples used for enrichment (biofilm and sediment) were transferred aseptically into Hungate glass vials, filled with seawater collected from the same sampling spot (fluid vent or water trapped within the sediment collection tools). The glass vials were incubated immediately at 4 °C in the dark.
- Samples used for nucleic acids (DNA and RNA) extraction were aseptically transferred into Falcon tubes and immediately stored at -20°C.
- Water samples were also examined to identify microorganisms that might carry antimicrobial resistance (AMR) genes. The samples were inoculated on Marine Agar (MA) and on MA supplemented with amoxicillin, tetracycline, or meropenem to observe which organisms could grow in the presence of these antibiotics. Microbes that formed colonies under these conditions were considered potential AMR-bearing strains. These candidates will then be suitable for non-destructive genetic analysis to assess whether and what resistance genes are present.

5.4.2 Biomarker analyses

For biomarker analyses, sediment cores (multicorer, bladcore, and pushcore) were subsampled on board at regular depth intervals (either every 0.5 or 1 cm). All subsamples were kept cool at 4 °C for transport and storage until post-cruise laboratory analyses.

Subsamples collected on board will be used post-cruise to investigate recent environmental change in the study area, with a focus on Atlantification and sea-ice retreat over the last centuries. Highly branched isoprenoids (HBis), including the sea-ice proxy IP25, will be measured to reconstruct past seasonal sea-ice conditions. Variations in HBis abundance and distribution will allow us to assess the timing and magnitude of sea-ice decline and to evaluate how closely these changes track the modern northward influence of Atlantic Water.

In parallel, glycerol dialkyl glycerol tetraethers (GDGTs) will be analyzed to characterize archaeal communities involved in anaerobic oxidation of methane (AOM). Downcore changes in AOM-related GDGTs will be used to identify shifts in the sulfate–methane transition zone (SMTZ) and to infer variations in methane flux from the subsurface. These data provide context for environmental changes linked to Atlantification, as both bottom-water warming and changing sedimentation patterns can influence methane cycling and the stability of the SMTZ.

5.4.3 Meiofauna and microfauna diversity (Foraminifera and microeukaryotic)

Samples to study foraminiferal and microeukaryotic biodiversity were collected from various ecosystems, including hydrocarbon seeps and hydrothermal vents. Efforts were made to sample diverse microhabitats such as bacterial mats, tubeworm patches, sponges (on sediment, rock, or carbonate crusts), and reference sites. Community composition across these environments will be analyzed using traditional morphology and eDNA metabarcoding, with mainly sediment samples and water, when sediment was not possible due to the hard ground collected for this purpose. For 2 sites (a microbial mat and a reference site), we decided to compare the preservation methods for soft-shelled foraminifera.

5.4.3.1 Sampling

Sediment samples were recovered using either push cores (with diameters ranging from Ø 8cm) or blade cores (32x25x10cm) deployed with the ROV Aegir. Opportunistic cores were taken using a multicorer in the reference area. The sediment cores were sliced into 5 sediment depth layers (0-1cm, 1-2cm, 2-3cm, 3-4cm, 4-5cm) and fixed in Rose Bengal diluted with ethanol 80% and for a few samples with formaldehyde (4%)/seawater solution.

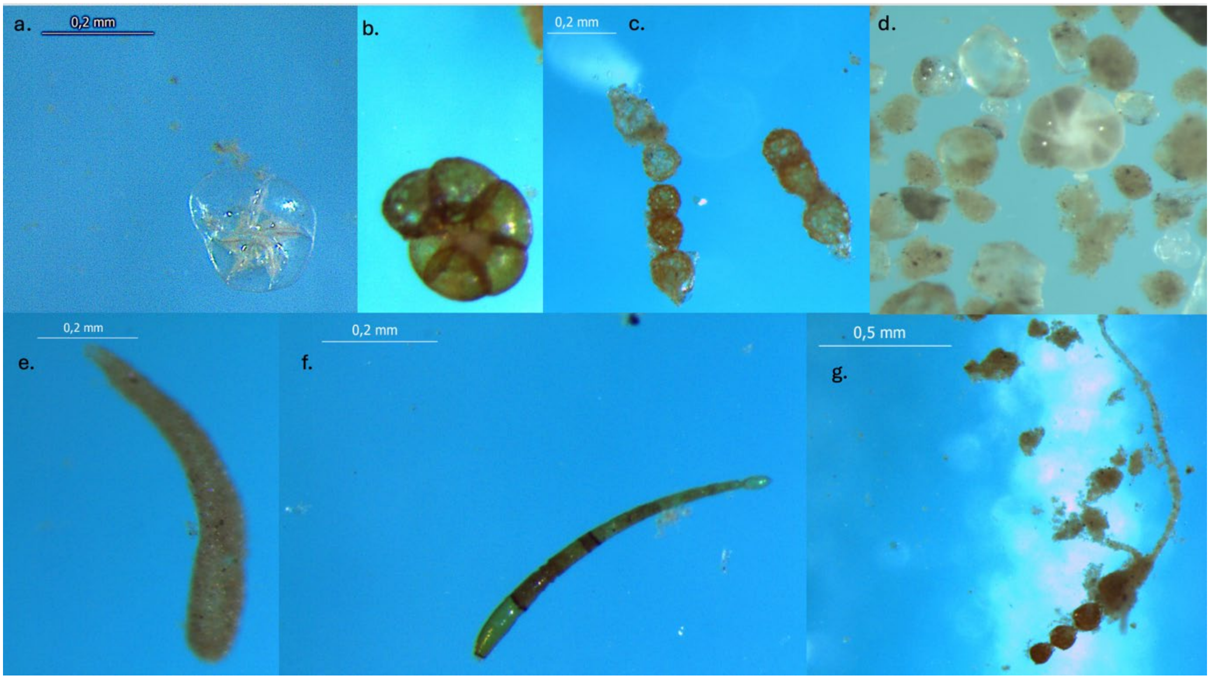

Figure 11. Foraminifera sampled during the EXTREME25 research cruise: Hard-shelled foraminifera (a., b., c., d., g.), soft-shelled foraminifera (e., f.).

Sponges were sampled upon encounter, either directly from the seafloor or attached to substrates (carbonate crusts and rocks). Additional substrates, such as wood and tube worms, were collected when observed. Sponges were dissected into several pieces using scalpels. Those attached to rocks or carbonate crusts were carefully detached with scalpels. Sediments collected via push cores and multicorers were sliced into 1 cm increments to 25 cm depth, when possible. The material was stored in Kautex bottles, packages, glass vials, and small plastic tubes, and mostly preserved in Rose Bengal ethanol solution. Rose Bengal solution (2 g L^{-1}) was prepared by dissolving 2 g of Rose Bengal in 1 L of 96% ethanol. Samples collected during the cruise will be deposited at the University of Vienna for long-term storage and future research.

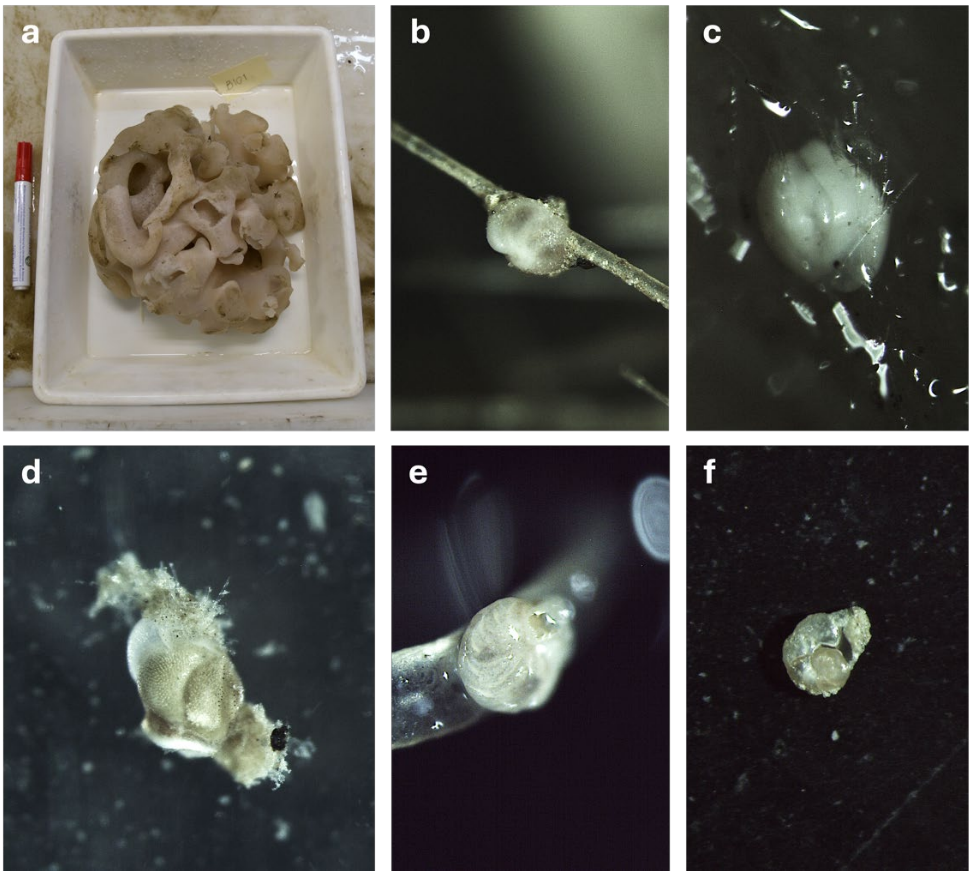

Figure 12. Fauna sampled during the EXTREME25 research cruise: unidentified sponge (a), Cibicides sp. on sponge spicules (b), Quinqueloculina sp. inside sponge tissue (c), Rupertina stabilis detached from a worm tube (d), Lobatula wuellerstorfi attached to a worm tube (e), and Discorbis sp. detached from a worm tube (f). The foraminifera shown in the figure have an approximate size exceeding 150 µm.

Sediment eDNA samples were also collected for molecular analysis. The top sediments were collected using a clean spatula, making sure to avoid the edge of the core, and then kept at -20°C.

Water eDNA samples were collected from a Niskin bottle placed in the ROV drawer. About 500 ml of water was filtered through a Sterivex (0.45µm) filter and kept in -20°C.

5.4.4 Macrofauna

The goal of the macrofauna sampling was to ensure comprehensive coverage of the biodiversity across the different microhabitats at each site. To accomplish this, macrofauna was obtained from samples gathered using ROV-operated Push cores (Ø 8 cm), Blade cores (32*25*10 cm), and Scoop. Additionally, fauna was collected from the surfaces of carbonate rocks. In each cold seep site, we focused on areas with bacterial mats, tubeworm fields, and rocky substrates such as carbonate outcrops to represent the various microhabitats. Pieces of organic material such as wood was also collected by the ROV when encountered.

All macrofauna samples were meticulously sieved using a sieve with mesh sizes 0.5 mm. For rock samples, rocks were washed with seawater to collect loose fauna, and attached fauna was collected with forceps or scalpels. Most of the material was preserved in 96% ethanol, while specific target taxa were separated using a Leica stereomicroscope and then frozen at -80 degrees for genomic studies. Collected samples will be deposited in the Natural History collections of the University Museum of Bergen for secure long-term storage.

Figure 13. Fauna samples from the EXTREME25 research cruise.

5.4.5 Fish sampling

At selected cold seep sites, a baited fish trap was deployed to collect fish for ecological studies, including isotope and gut content analyses. The collected fish were dissected, and organs and tissues were frozen individually at -80 degrees.

5.5 SAGE

5.5.1 ROV Integration

Two SAGE instruments—one configured for methane measurements and the other for carbon dioxide—were mounted on the side of ROV ÆGIR6000 (Figure 14A). Each sensor was fitted with a flow cap over the membrane, which was connected via Tygon tubing routed to the front of the vehicle (Figure 14B). The tubing terminated in a sampling wand housed in the ROV basket and equipped with a sediment filter (Figure 14C). Water drawn through the sampling wand was pumped back to the SAGE sensors. This setup allowed the ROV arm to easily access the sampling wand for targeted measurements. Both SAGE instruments were integrated onto ROV ÆGIR for all dives during EXTREME25 with the exception of dives 1060-2, 1082, and 1083, during which only the methane SAGE was installed.

Figure 14. Mounting location of SAGE on the side of ROV AEGIR600 (A). SAGE instruments on ROV Ægir6000, each equipped with a flow cap and pump (B). SAGE sampling wand fitted with a sediment filter in the arm of the ROV (C).

5.5.2 Ship Underway System Integration

Two SAGE instruments — one configured for methane measurements and the other for carbon dioxide — were integrated into the ship's underway system in the seawater intake laboratory, Level 1. The sensors were installed on the benchtop and connected to the underway seawater line, which continuously supplied seawater from an intake depth of approximately 4m. Underway seawater was turned off in thick sea ice and for occasional cleaning, but otherwise the two SAGE sensors continuously measured methane and carbon dioxide concentrations in the surface waters. Regions of surface methane detection were periodically detected, with underway water samples collected where possible at the same time. Vessel multibeam data from the same location were used when available to assist with identifying the methane source.

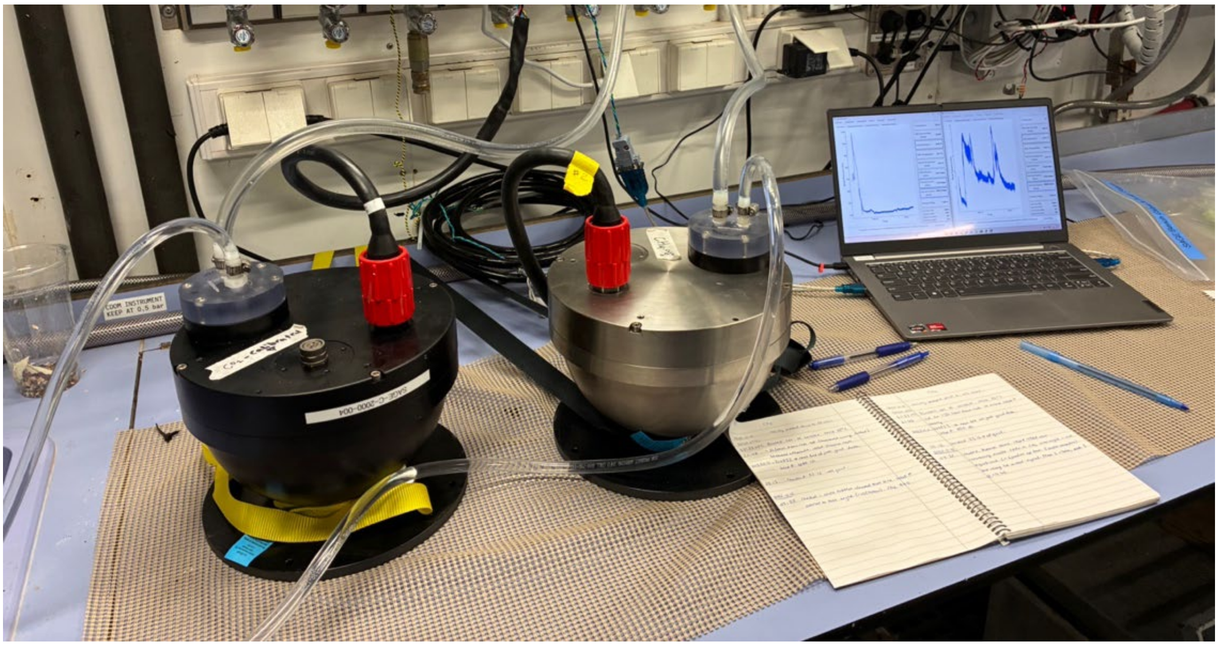

Figure 15. Carbon dioxide (left) and methane (right) SAGE instruments connected to the vessel's underway system for continuous monitoring of dissolved gases at 4m depth.

5.5.3 Discrete water sampling

Discrete water samples were acquired from the CTD rosette, ROV-mounted Niskin bottles, and the vessel's underway system for post-cruise analysis of total dissolved gas concentrations and isotopic composition. 600ml samples of seawater were collected in pre-evacuated, pre-weighed IsoFlasks containing a soluble poison capsule using flushed sampling lines. The goal of these samples was threefold: 1) to validate the concentrations of dissolved gas that were measured in situ by SAGE; 2) to identify the origin of dissolved methane (microbial, thermogenic, etc); 3) to assess the efficacy of this sampling methodology for remote marine fieldwork by comparison against matched samples that were acquired by other cruise participants in glass septum vials.

5.6 Water column data interpretations

Examples of water column data interpretations done on board that guided the ROV dives.

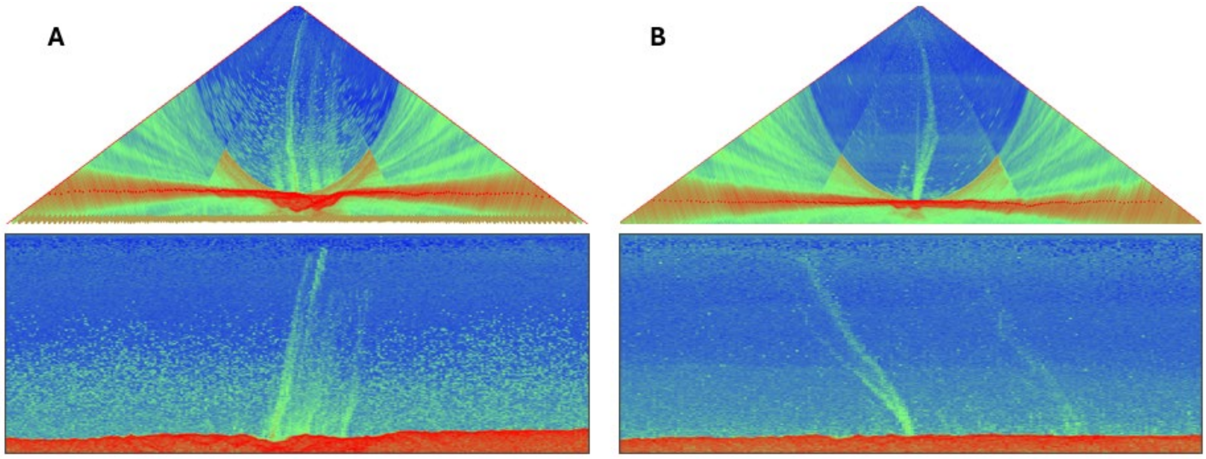

Figure 16. (A) WCD line 0150, fan view, and R-stack. Borealis mud volcano site visited on ROV Dive 1080-1082. Water depth: ~370 m. (B) WCD line 0154, fan view, and R-stack. Tvillingene mud volcano site visited on ROV Dive 1083. Water depth: ~345 m.

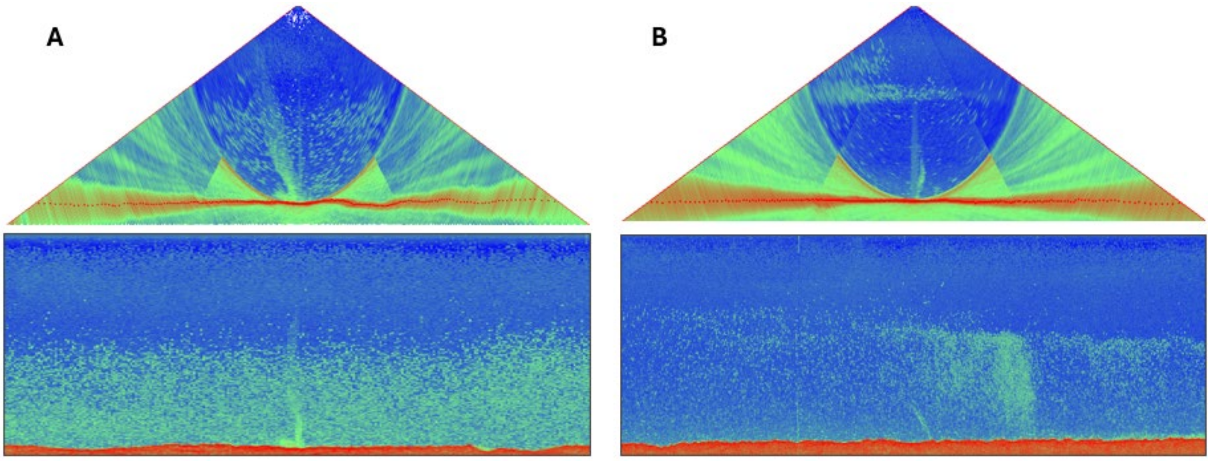

Figure 17. (A) WCD line 0077, fan view and R-stack. Polynya natural seep site visited on ROV Dive 1071. Water depth: ~320 m. (B) WCD line 0179, fan view, and R-stack. Tromsøflaket SW natural seep site visited on ROV Dive 1084. Water depth: ~310 m.

6 Maps of the study sites with activities

6.1 Leg 1

6.1.1 SS01 (Freya Gas Hydrate Mounds) map

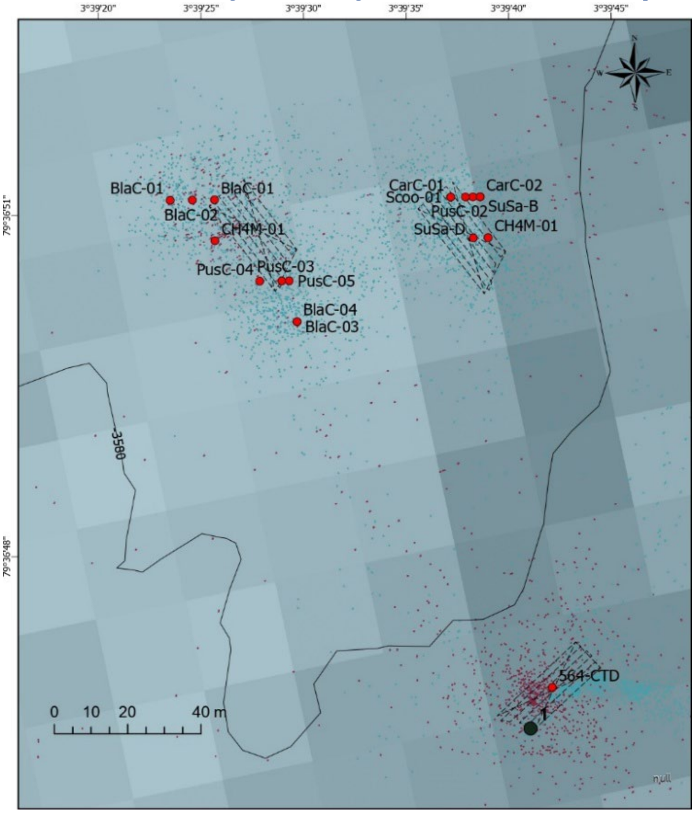

Figure 18. General map of SuperStation 01 illustrating the ROV1060 to ROV1061 survey area.

6.1.2 SS03 (Frigg Vent Field) map

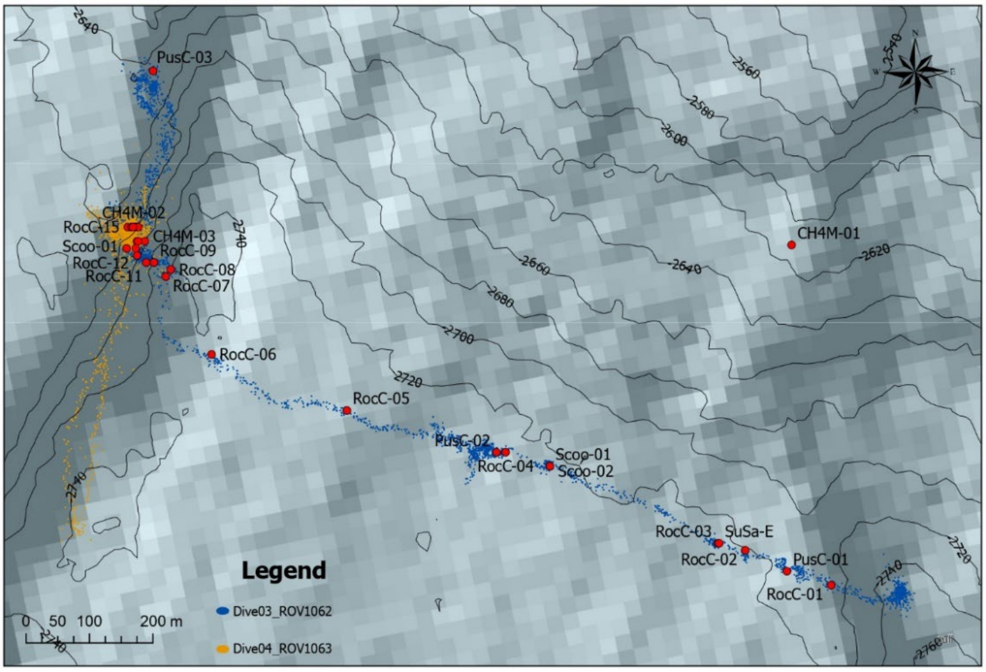

Figure 19. General map of SuperStation03 illustrating the ROV1062 and ROV1063 survey area.

6.1.3 SS05 (Gjalp) map

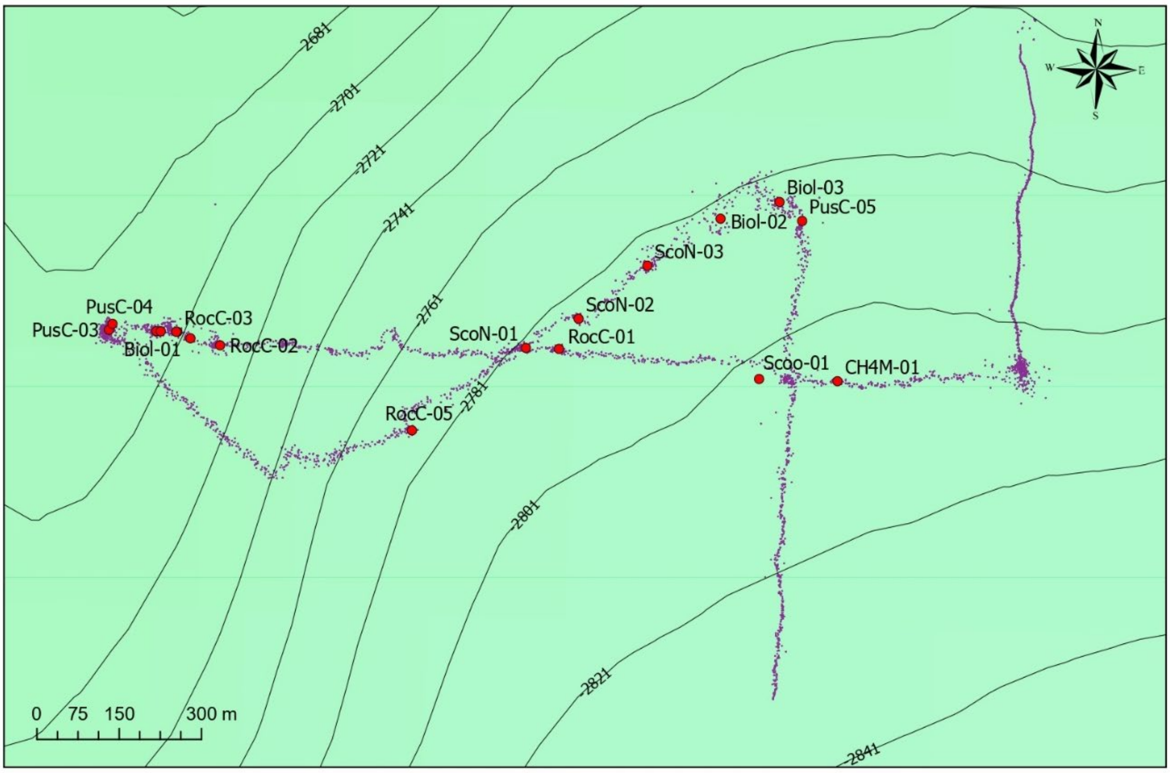

Figure 20. General map of SuperStation05 illustrating the ROV1064 survey area.

6.1.4 SS07 (GFB) map

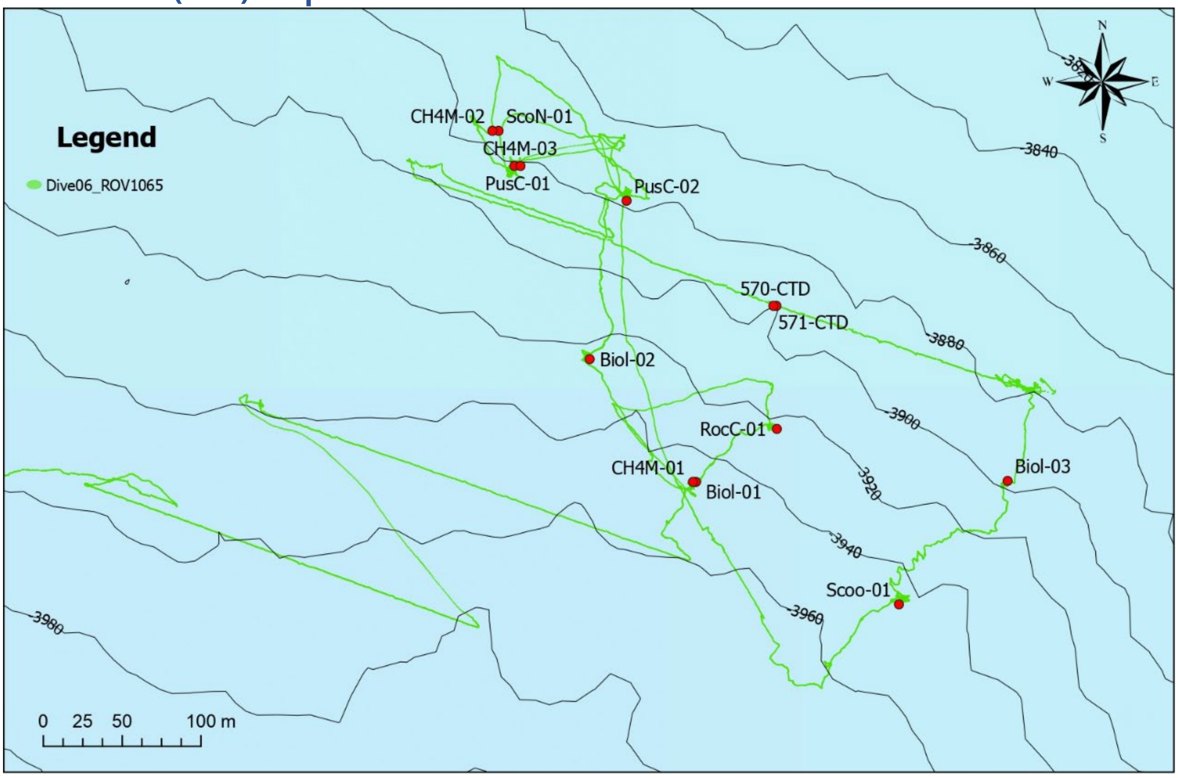

Figure 21. General map of SuperStation07 illustrating the ROV1065 survey area.

6.1.5 SS08 (Prins Karls Forland) map

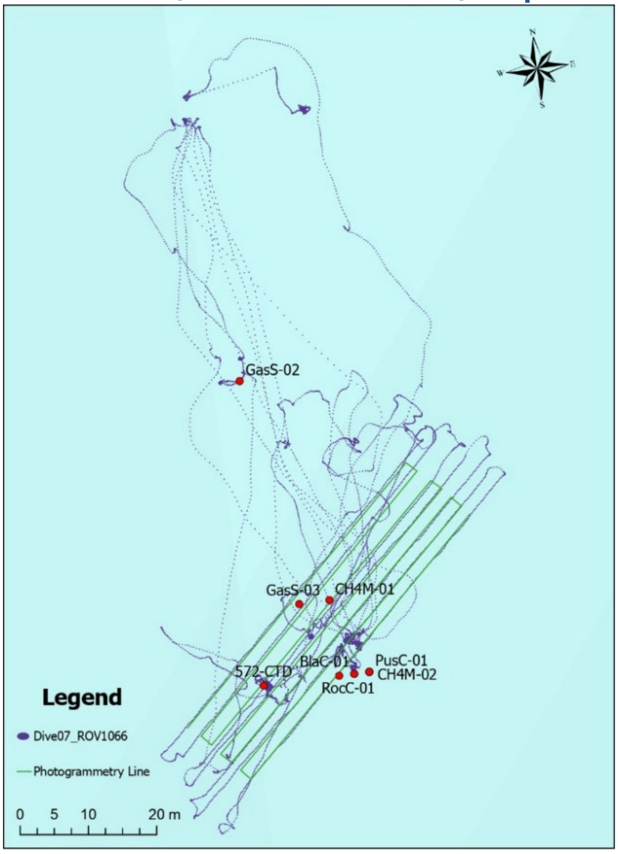

Figure 22. General map of SuperStation08 illustrating the ROV1066 survey area.

6.2 Leg 2

6.2.1 SS09 (Sørkapp Slope) map

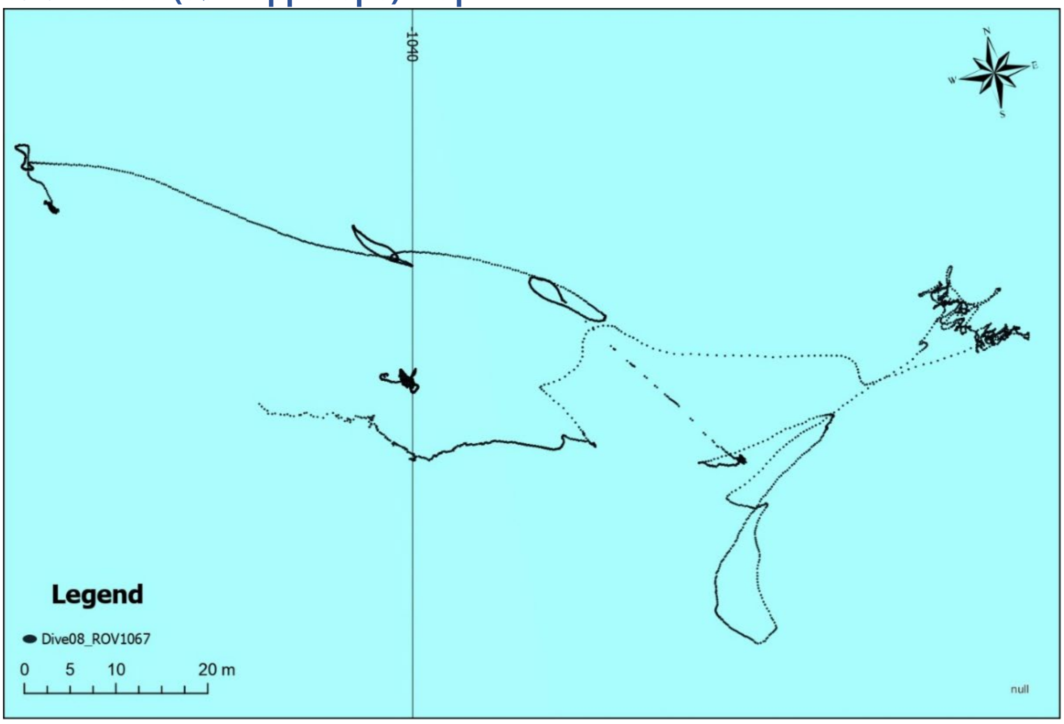

Figure 23. General map of SuperStation09-2 illustrating the ROV1067 survey area.

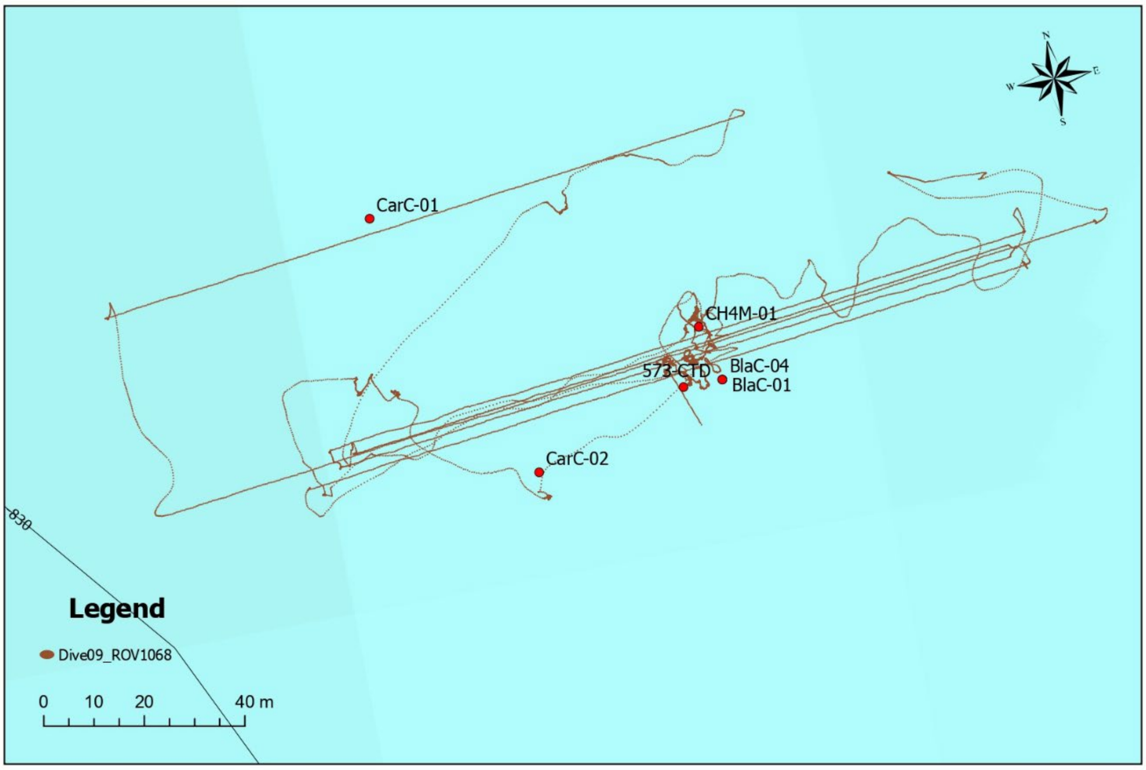

Figure 24. General map of SuperStation09-3 illustrating the ROV1068 survey area.

6.2.2 SS11 (Snøras Seep) map

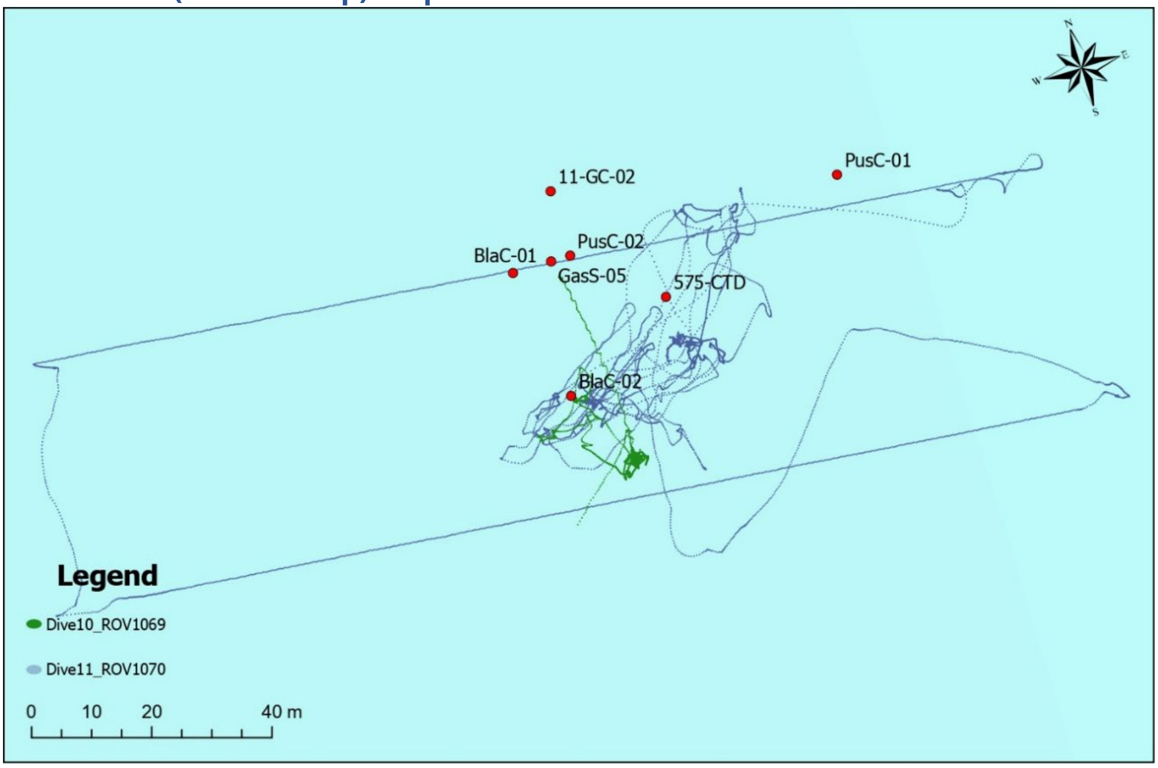

Figure 25. General map of SuperStation11 illustrating the ROV1069 and ROV1070 survey area.

6.2.3 SS12 (Polynya Seep, Kayak, Mist, Hurri, Bask Seep) map

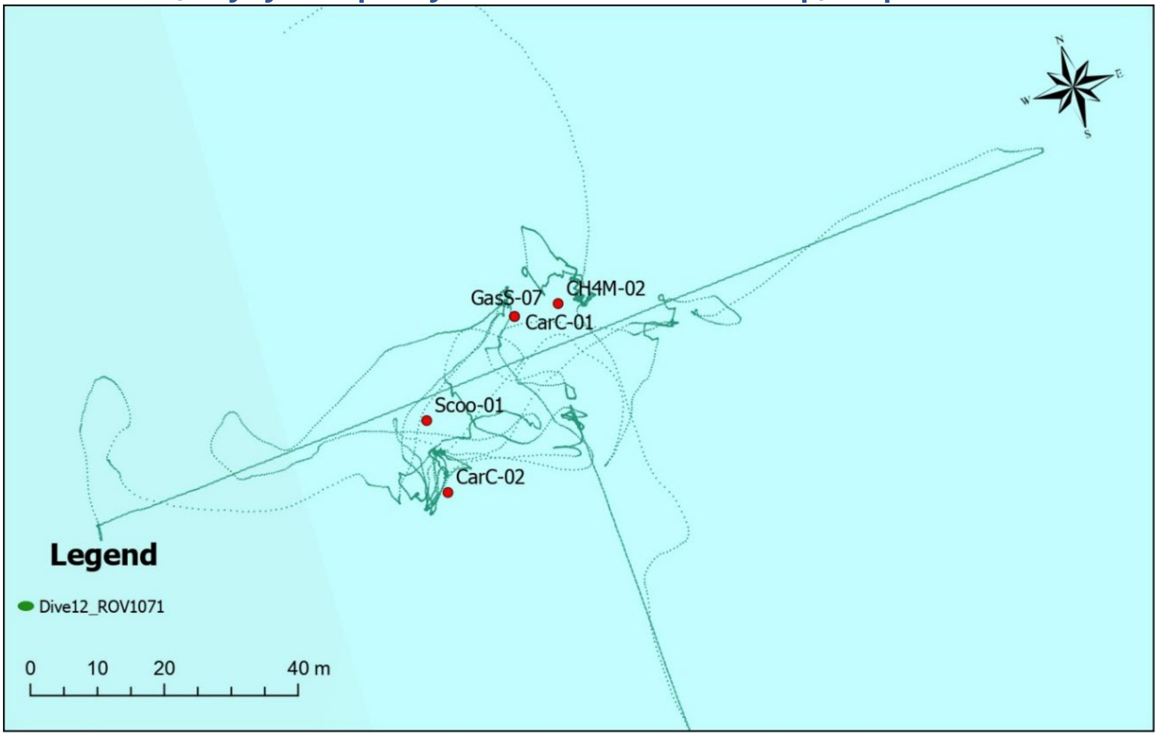

Figure 26. General map of SuperStation12-1 (Polynya Seep) illustrating the ROV1071 survey area.

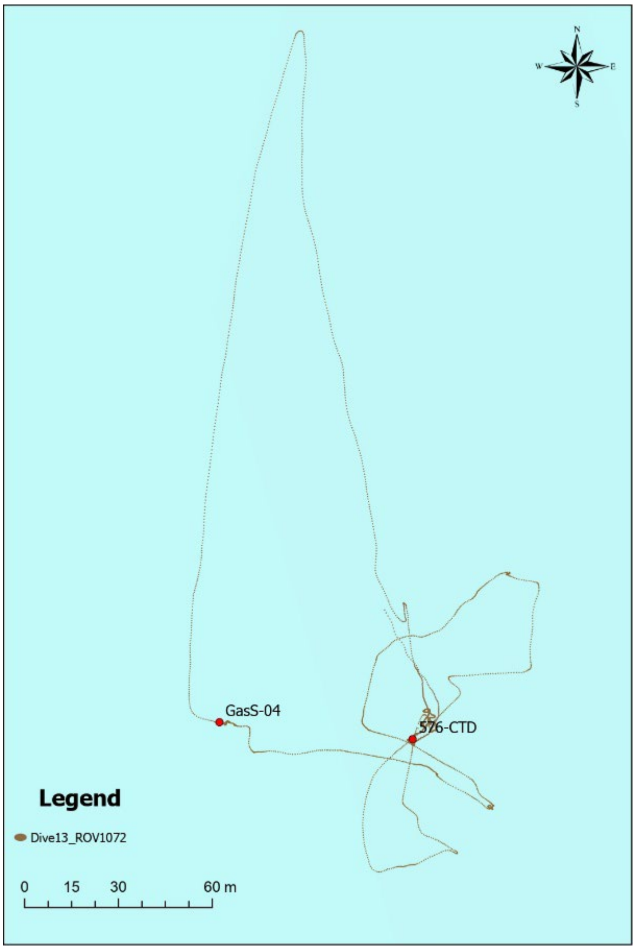

Figure 27. General map of SuperStation12-2 (Kayak) illustrating the ROV1072 survey area.

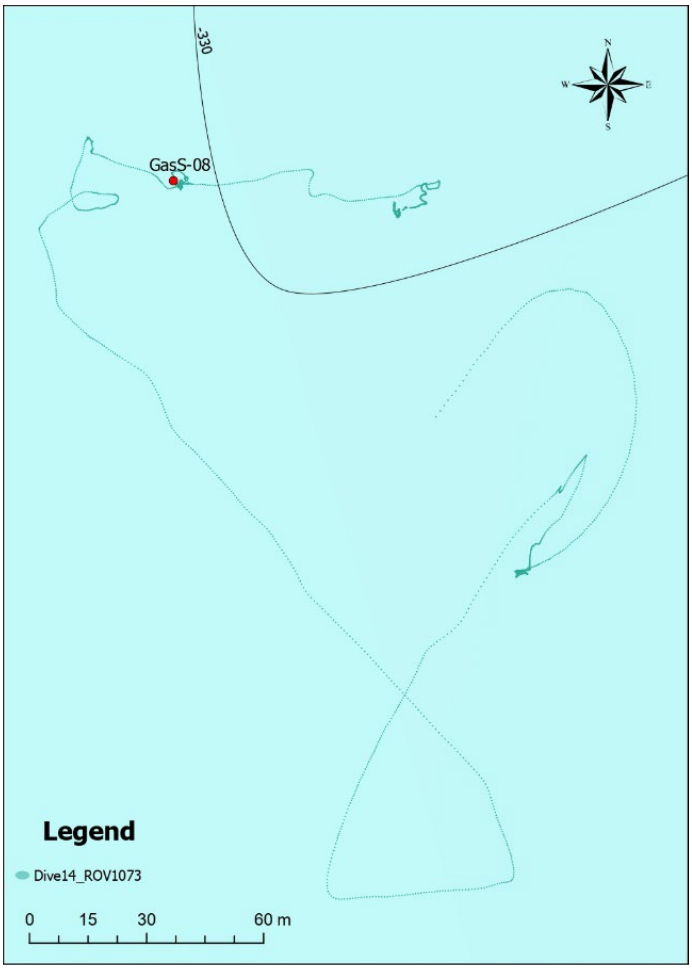

Figure 28. General map of SuperStation12-3 (Mist) illustrating the ROV1073 survey area.

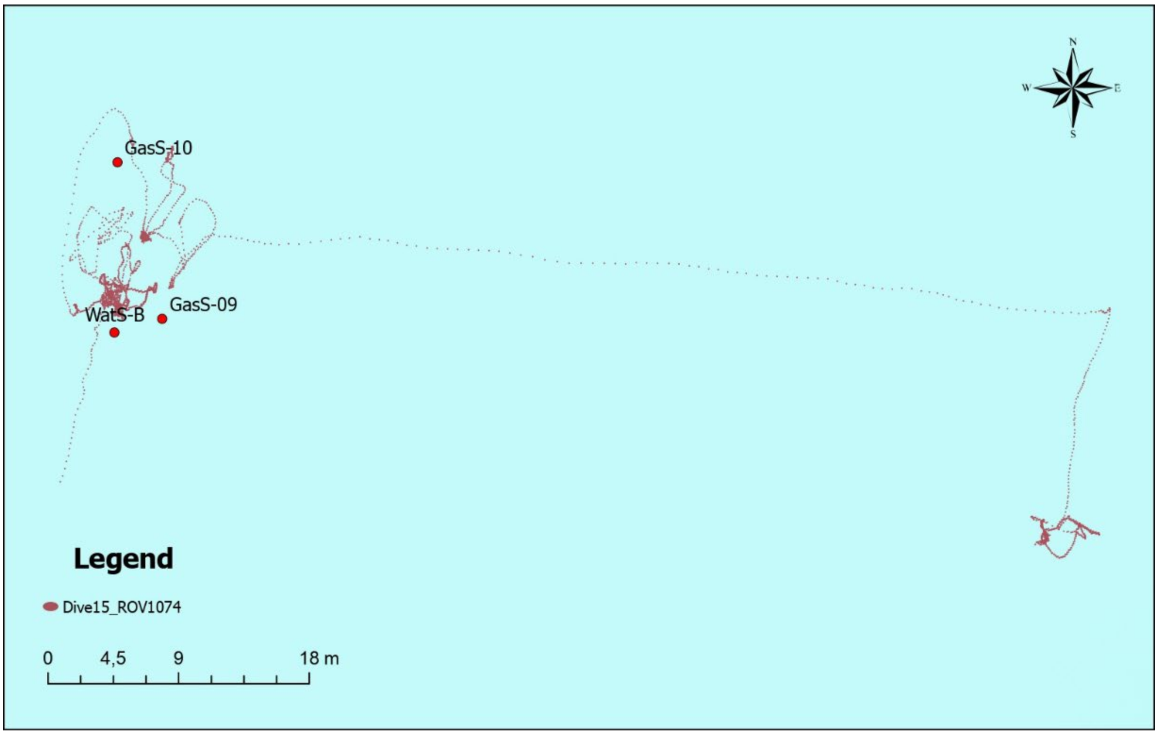

Figure 29. General map of SuperStation12-4 (Hurri) illustrating the ROV1074 survey area.

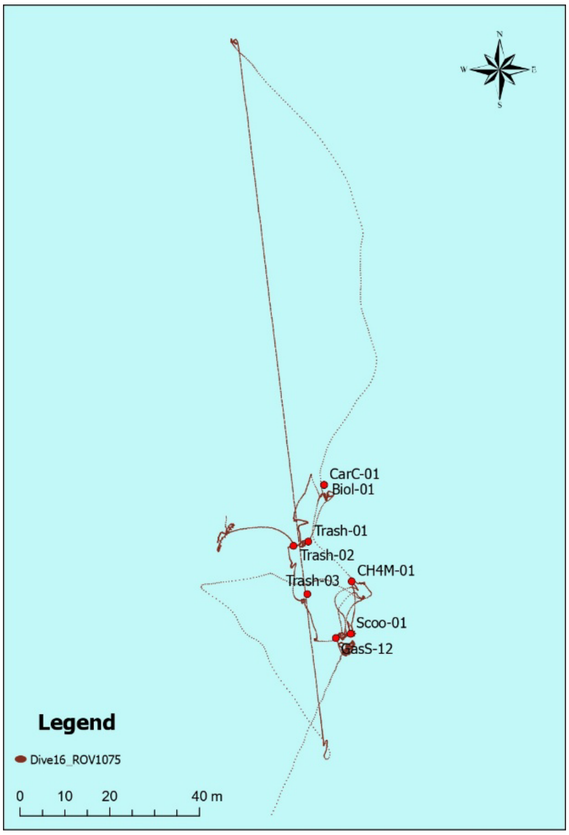

Figure 30. General map of SuperStation12-5 (Bask Seep) illustrating the ROV1075 survey area.

6.2.4 SS13 (Tromsøflaket) map

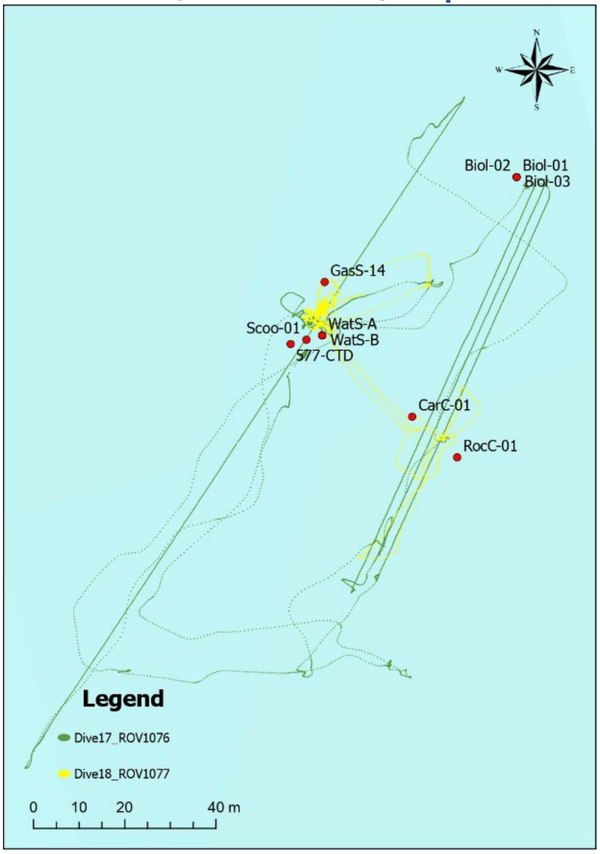

Figure 31. General map of SuperStation13 illustrating the ROV1076 and ROV1077 survey area.

6.2.5 SS14 (7119/9-1) map

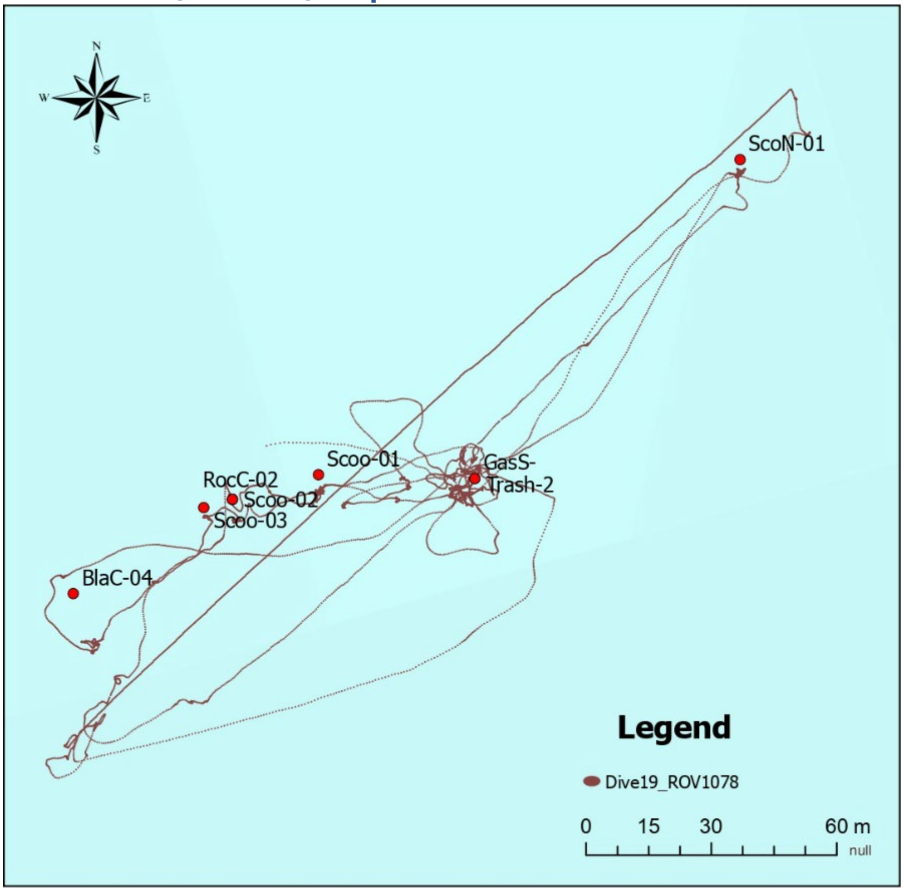

Figure 32. General map of SuperStation14 illustrating the ROV1078 survey area.

6.2.6 SS15 (7119/7-1) map

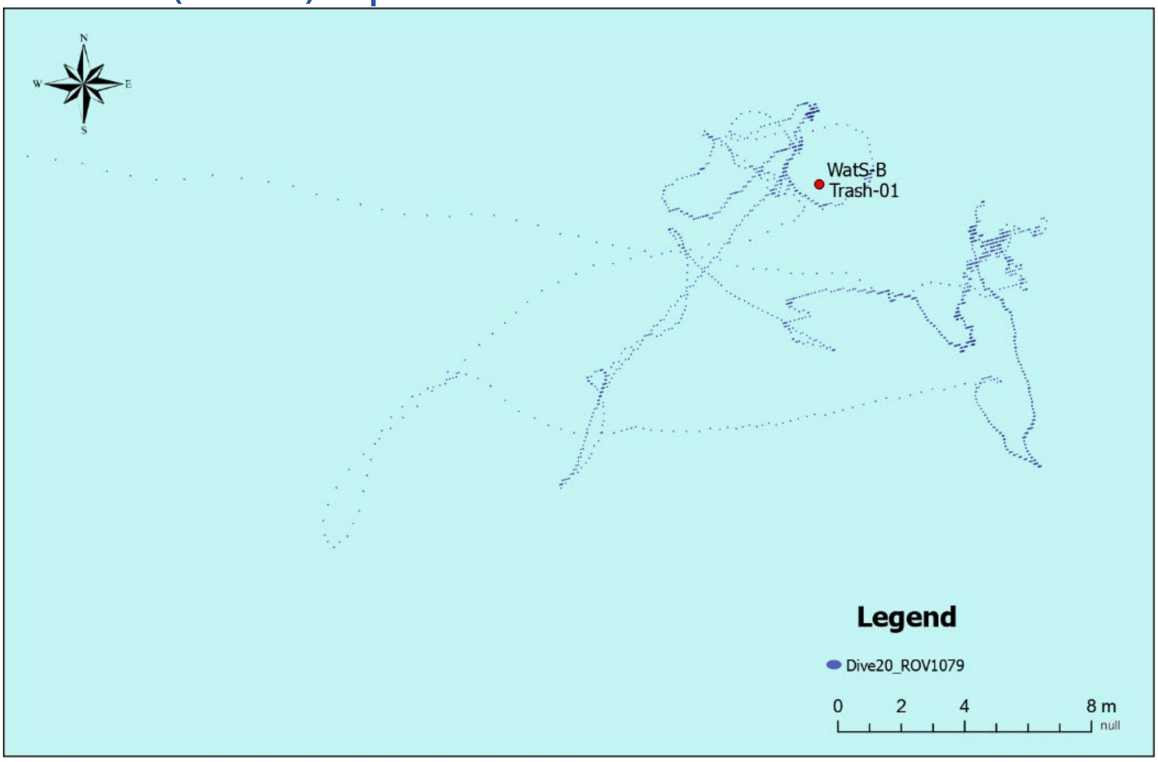

Figure 33. General map of SuperStation15 illustrating the ROV1079 survey area.

6.2.7 SS17 (Outer Bjørnøya) map

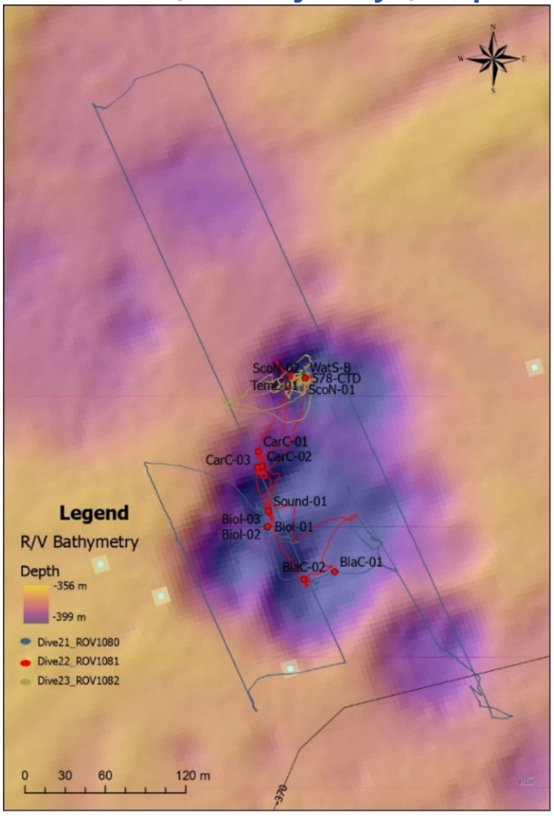

Figure 34. General map of SuperStation17 illustrating the ROV1080, ROV1081, and ROV1082 survey area.

6.2.8 SS18 (Tvillingene) map

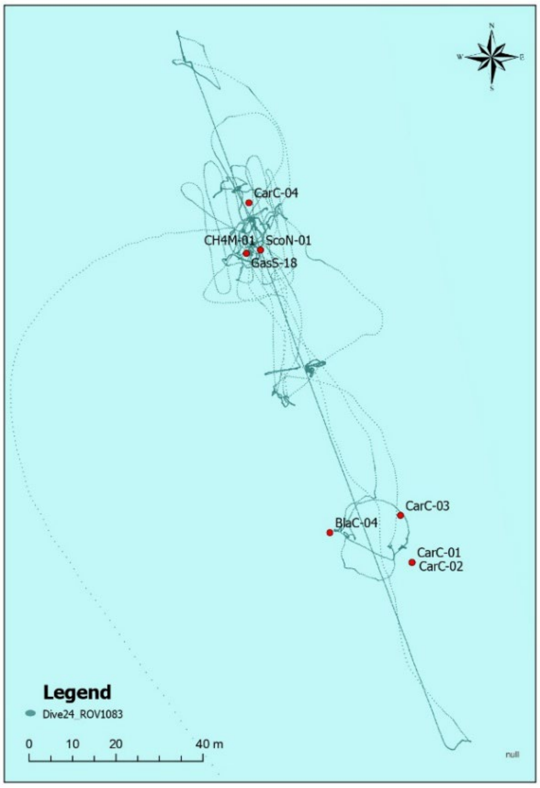

Figure 35. General map of SuperStation18 illustrating the ROV1083 survey area.

6.2.9 SS19 (Tromsøflaket SW) map

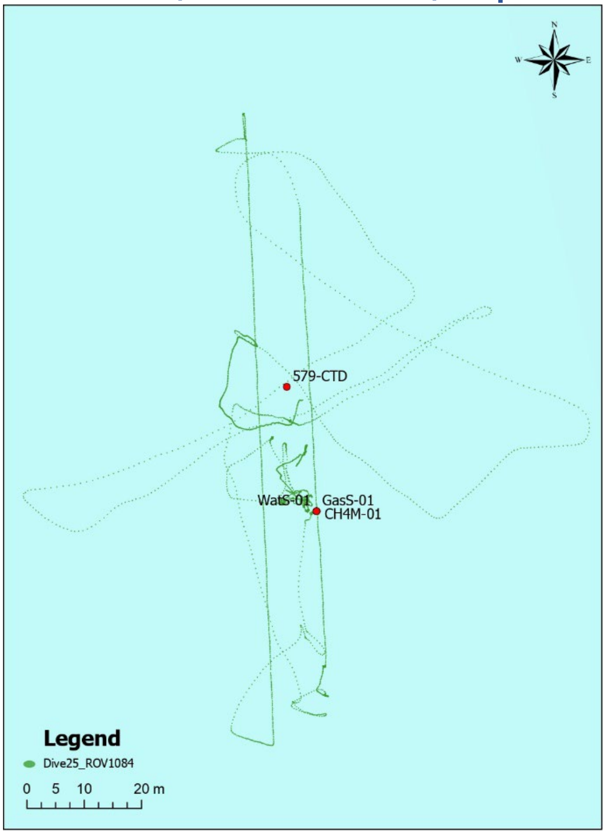

Figure 36. General map of SuperStation19 illustrating the ROV1084 survey area.

6.2.10 SS20 (Fugløybanken) map

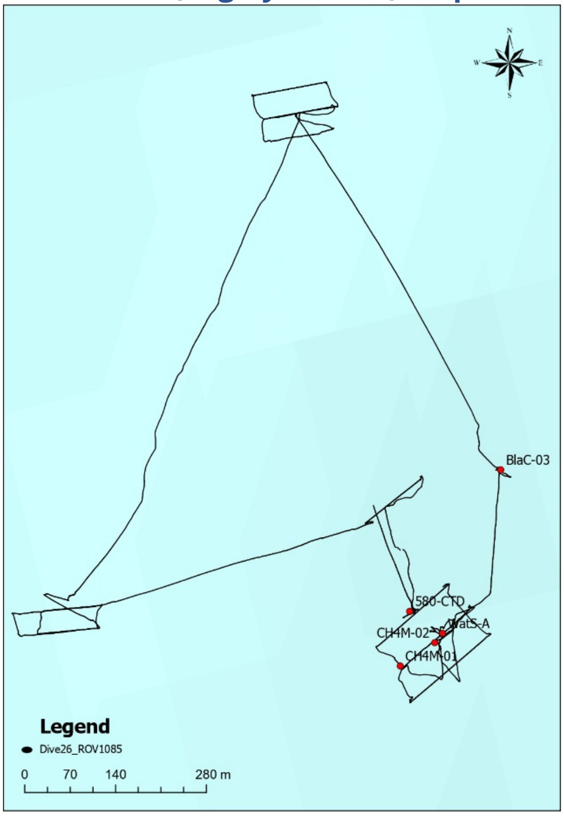

Figure 37. General map of SuperStation20 illustrating the ROV1085 survey area.

7 Media, Outreach, and Dissemination

7.1 Communication and dissemination (by Ann Eileen Lennert and Valentina Lanci)

The aim of the Extreme project is to develop and disseminate a transformative interdisciplinary approach to studying Extreme Environments in the Arctic regions and beyond. Communicating science with a broad range of audiences is a science of its own," and we have embraced this task in an interdisciplinary manner in itself.

Figure 38. The comic developed during the cruise, both telling stories and facts of the research, the people onboard, and the extreme environments we explored together.

The focus of our science communication was on communicating to a broad range of audiences, focusing on the general public but also research communities, informing, educating, raising awareness of science-related topics of the deep-sea world, impacts of climate and environmental change, and nudging people to think, as well as make the right decisions and actions.

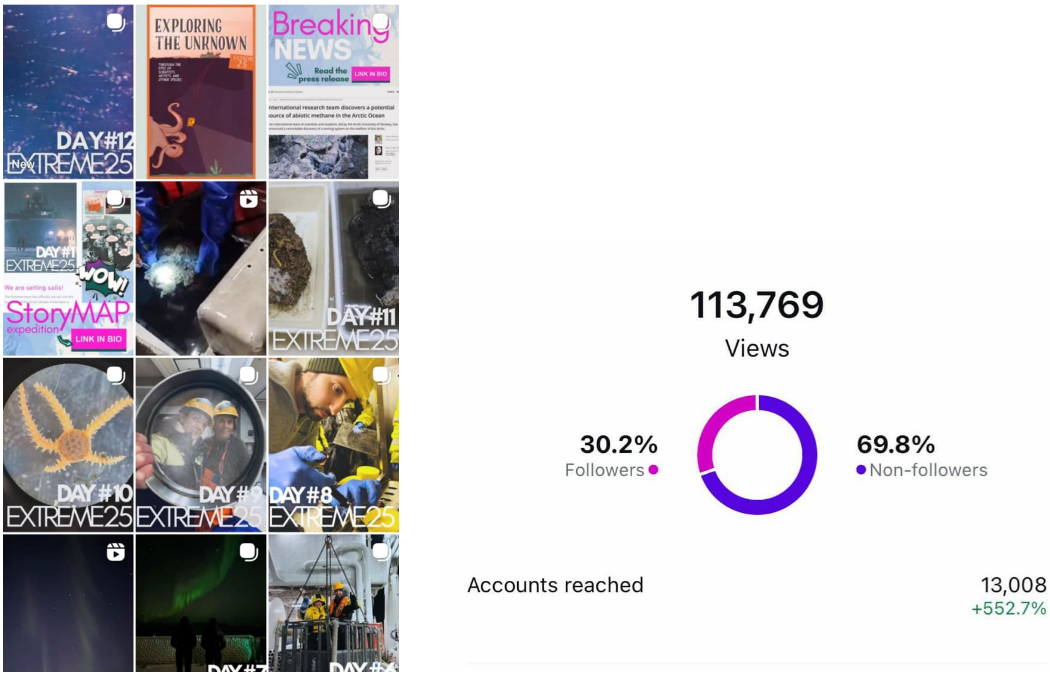

Figure 39. Every day we created new posts, sharing both a diary of the cruise, stories, achievements, and news. We additionally put an effort into resharing stories of the expedition participants. They were, in general, good at posting material on their own channels. This resulted in a larger outreach.

We used visual communication and tools of telling a visual story through social media, a comic series, and a Story map, making it possible to follow the cruise virtually as days passed by. Here, the transmission of information and ideas using symbols, imagery, videos, and maps, combined with text, was a significant tool to simplify the unsimplified, engage and kindle the curiosity of a wide audience, and quickly share throughout media spaces.

Instagram had a large impact due to both the posting and tagging, but also the expedition participants' engagement in making their own stories and sharing across social media spaces. This resulted in our Instagram growing with 344 new followers within the first weeks of preparation for the cruise to the cruise itself. We had, within the cruise period, 113.739 views, where 69.9% were non-followers. All in all, Instagram worked really well as many institutions collaborated in this expedition and helped share the expedition in real time.

The Story map also proved to be a good interface with our Instagram. During the expedition cruise, it has had 500 views. The story map has also been integrated into the Extremes website as the main tool for the dissemination of the cruise in a visual and engaging way.

We published two press releases. The first press release was in connection with the preparation of the expedition, and the second press release was in connection with the scientific discovery of the Frigg vent field. This press release has been covered by several media outlets in Norway and internationally.

7.2 Field Aesthetic

7.2.1 Michael Kjær

During both legs of the cruise, I have been responsible for providing the participating artists with intellectual as well as practical support. As a mediator of visual theory and art history, my role has hence been to develop concepts, best practices, and ways to translate the scientific work on the cruise into critical aesthetic practice. In this role, I have been arranging status and development meetings every day between 09.00 and 10.30. Besides this, I have been doing observation to support my own research project by PASS – The Novo Nordisk Research Center for Practice-based Art Research at the University of Copenhagen: 'Terra Incognito – Field Aesthetics in Extreme Environments'. The main aim of my project is to change our notion of aesthetics as an anthropocentric enterprise into an earth-centered practice. For this reason, I have invited the following four artists to participate in the Extreme25 expedition. They all have highly developed practices, which involve turning environmentally oriented field observation into aesthetic practice. Together, we have been gathering and developing material for the Extremes exhibition in Iceland in October 2026.

During the cruise, Gry Bagøien performed a collaborative performance in the main ROV hangar to create a shared connection to the Fram Strait and foster a heightened reflection on the use of highly advanced technology in deep-sea research. John Grzinich and Thorgerdur Olafsdottir presented examples of their work at a science meeting together with me in a shared performative presentation.

7.2.2 John Grzinich

In committing to the full two legs of the cruise, I am still wondering if I took on more than I expected as an artist. While I took time to educate myself about the science of extreme environments, the in-situ practice of doing the science aboard such a vessel as the Kronprins Haakon took on many new dimensions of experience for me. This was the first time I've been on a research vessel, so I did my best to familiarise myself with the work and get into the daily rhythms of the scientists aboard. I focused on the interface of working with the ROV as it descends into the depths of the Arctic Sea and the procedures that follow its return.

Gathering samples is the main methodology for the scientists to analyze life and geological phenomena in the deep sea, and in my own way, I also was sampling aspects of this process through audio-visual documentation, of which I generated roughly 1 terabyte of data. The ship itself provides a fascinating backdrop for this kind of science to take place, from the high-capacity electrical generation engines that power everything on the ship to the many cleaning rooms and laboratories on board. What unfolds is an intricate daily interplay of navigation, mapping, remote exploration, sampling, and cataloguing. But what truly brought the cruise into focus for me was getting to know the broad scope of disciplines at work in studying extreme environments by the talented scientists assembled. There is a lot to be learned here, and it will take time to process my recordings and develop a new artwork related to the Extremes project. In closing, I want to acknowledge that the invitation by Michael Kjaer on behalf of Giuliana Panieri was very generous, and I greatly appreciate their skill, dedication, and guidance throughout the whole journey.

7.2.3 Hekla Dögg Jonsdottir

After observing and contemplating the interplay between the scientific work in the laboratories of the vessel, the vessel itself, and the Fram Strait in which we were sailing during the 1. Leg, I decided to reflect and expand on what I found to be the core of the multidisciplinary work being carried out between the members of the research team under the leadership of Giuliana Panieri. I sensed that the central driver of this collaborative work is that Giuliana is able to be both precise and result-driven while still saving some 'space', leeway, or freedom for chance to appear, develop, and be noticed. One can also compare this to a kind of magic in a poetic or maybe even childish language of wonder. A leeway for magic occurrences to make their way into science, a leeway for scientific and even artistic curiosity to thrive. With this basic impression, I spent 5 days recording the surface of the Fram Strait, trying to establish a frame for this magic spark to appear. These recordings are to be combined in some not yet defined way with the parallel recordings that the ROV Ægir made on the seabed at the same time. Maybe with the aim of showing in a very direct way our embeddedness in a chunk of water, a section of time, the water column. A kind of linkage of the extreme environments at the aphotic seabed with the dark and at times icy seascapes we were suspended on for these seemingly endless days that still resonate in me.

7.2.4 Gry Bagøien

On the vessel, I recorded songs in the helideck office and in the helicopter hangar, as there the acoustics were better for singing. I set up my equipment in the moon pool and wrote a few songs there, and I recorded underwater in the moon pool, when the prey was down in the depths, where I improvised according to the tones the ship gave through the water in the pool. I meditated in the crow nest where I also wrote lyrics for my last language book/reference work. Every morning, I attended a meeting in the library with the other artists, which was very rewarding for my work. I spent a lot of time staring out of the windows, standing on the deck, and following the underwater work. All these experiences and information I have stored in my body and computer from which I will create one or more works. In addition, we created choir work, which we performed as a united scientific team under and above the water by the moon pool in the main hangar of the vessel.

7.2.5 Thorgerdur Olafsdóttir

During my time on Kronprins Haakon, I have been following the processes of mineral sampling, mostly carbonate rocks collected from the ocean floor.

I'm interested in the transformations they go through; being selected and brought up by a robot, then being carried into the laboratory, where a sort of ritual process starts – with them receiving a label, being washed and rinsed clean of all sediment, then plucked clean of microbes and macro fauna before it's delivered to the geologists where this process continues and the stones are cut and sampled further. Ultimately ending up in storage for further preservation. There are a lot of interesting questions that have come up while I've paid close attention to this scientific process, thoughts concerning care, continuity, responsibility, extraction, heritagization, etc., and the afterlives of the collected samples. I'm very thankful that I've been allowed to observe this process, and it should also be noted that I have an interest in unruly heritage, so waste material has also been part of the collected samples from the ocean floor.
I am developing an idea of a future heritage archive, or a collection, where I want to gather and show a wide range of objects, samples, and representations of natural, cultural, and unruly heritage.

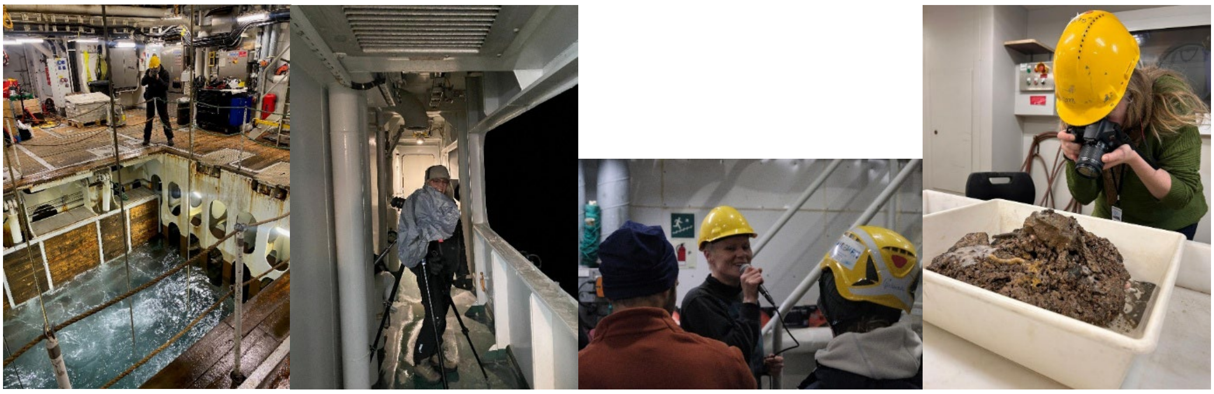

Figure 40. Artists in the field, from left to right: John Grzinich, Hekla Dögg Jonsdottir, Gry Bagøien, and Thorgerdur Olafsdóttir.

7.3 Social Anthropology (by Marta Gentilucci)

My participation as a social anthropologist in the EXTREME25 expedition took place within the EXTREME project, led by Giuliana Panieri, and as part of my EU-funded project OCEAN-MINeD, which aims to build knowledge and unpack "from the inside" the complex networks surrounding deep-sea mining. One of the work packages of my project focuses specifically on life at sea aboard a research vessel, with particular attention to human–machine interactions.
The expedition provided an ideal ethnographic setting for understanding the "behind-the-scenes" of deep-sea science in the Arctic Ocean from the perspectives of natural scientists, engineers, and sea workers. The main methodology I employed was participant observation—a method in which the researcher takes part in daily activities, routines, interactions, and events in order to learn both the explicit and tacit dimensions of a group's practices, as well as their language. This deep immersion in the research life of scientists on board was intended to help me grasp what they experience as meaningful

and important in their efforts to understand extreme environments and ultimately protect the ocean. As Alpa Shah notes, “participant observation is not merely a method of anthropology but a form of knowledge through being and action” (Shah 2017, 48). I documented this work using the anthropological technique of fieldnotes (Sanjek 1990).
Given the intimate nature of the fieldwork and the short duration of the EXTREME expedition (two weeks), I chose not to conduct formal interviews, which can sometimes alter the social and relational dynamics established between the researcher and participants. Because meaningful participant observation requires extended engagement, my fieldwork continues for an additional three weeks on board the same vessel, though with a different scientific crew.
During the expedition, I also took part in morning meetings with the artists and other social scientists involved in the project. These meetings aimed to collaboratively conceptualise the development of an exhibition on the theme of marine extreme environments.
The ethnographic data collected during EXTREME25 will be integrated with other materials—interviews, report analyses, and participant observation at conferences, among others—that I have been gathering since September 2024 as part of my broader research on deep-sea mining. These combined data will be analysed with the aim of producing scientific publications.

7.4 Marine Science and Law (by Violeta S. Radovich)

My aim in the expedition was to advance the use of systematic consultation processes that facilitate research at the crossroads of marine science and law. Moreover, another objective was to advance critical knowledge and understanding of pressing environmental issues comparable to the regulation of renewable energy on the high seas, such as deep-sea mining. My participation in the expedition is planned under my MSCA postdoctoral project HIGH SEAS ENERGY Nr. 101104244, where I study the governance and regulation of the installation of renewable energy platforms on the high seas - marine areas beyond national jurisdiction. The methodology I followed in the expedition was observant participation, and I carried out interviews with marine scientists, industry stakeholders, and artists. I carried out an interdisciplinary and participatory case study to define the environmental risks caused by renewable energy platforms in the sea. I made a short presentation in the expedition regarding my study subject, and I made reference to the rights of nature. It was also truly interesting to participate each morning in a one hour and half hour meeting with the artists and the anthropologist who are in the expedition, analysing the research methods we use while we are in the research vessel.

8 Data management

All the data collected during this expedition and work in progress will be deposited at the UiT Dataverse. Geographical species records of fauna will be deposited in Artskart (https://artskart.artsdatabanken.no) and in GBIF (https://www.gbif.org). DNA barcodes of fauna will be deposited in BOLD Public Data Portal (www.boldsystems.org) and in NCBI GenBank (https://www.ncbi.nlm.nih.gov/genbank/).

9 Acknowledgements

We would like to thank the officers and crew of the RV Kronprins Haakon for their assistance at sea. We are also grateful to all cruise participants for the passion, great professionalism and efficiency demonstrated during the expedition. Norwegian Offshore Directorate and Equinor are acknowledged for their financial support of the expedition. We thank the ROV Ægir6000 team for their competence. At the Department of Geosciences, we thank Bjørn Runar and Carl Ballantine for logistical support prior to the expedition, Fabio Sarti for the data management and post-cruise logistics, all the administrative and laboratory staff for the constant support.

10 Bibliography

Andreassen, K., Hubbard, A., Winsborrow, M., Patton, H., Vadakkepuliyambatta, S., Plaza-Faverola, A., Gudlaugsson, E., Serov, P., Deryabin, A., Mattingsdal, R., Mienert, J., & Bünz, S. (2017). Massive blow-out craters formed by hydrate-controlled methane expulsion from the Arctic seafloor. *Science*, *356*(6341), 948–953. https://doi.org/10.1126/science.aal4500

Argentino, C., Mattingsdal, R., Eidvin, T., Ohm, S. E., & Panieri, G. (2025). A constellation of mud volcanoes originated from a buried Arctic mega-slide, Southwestern Barents Sea. *Scientific Reports*, *15*(1). https://doi.org/10.1038/s41598-025-99578-5

Bernard, B. B. (1979). Methane in marine sediments. *Deep Sea Research Part A. Oceanographic Research Papers*, *26*(4), 429–443. https://doi.org/10.1016/0198-0149(79)90056-6

Chand, S., Knies, J., Geissler, W. H., Plaza-Faverola, A., & Thorsnes, T. (2024). Acoustic evidence of hydrocarbon release associated with the Spitsbergen Transform Fault, north of the Molloy Ridge, Fram Strait. *Frontiers in Earth Science*, *12*. https://doi.org/10.3389/feart.2024.1347252

Chand, S., Thorsnes, T., Rise, L., Brunstad, H., Stoddart, D., Bøe, R., Lågstad, P., & Svolsbru, T. (2012). Multiple episodes of fluid flow in the SW Barents Sea (Loppa High) evidenced by gas flares, pockmarks and gas hydrate accumulation. *Earth and Planetary Science Letters*, *331-332*, 305–314. https://doi.org/10.1016/j.epsl.2012.03.021

Czuba, W., Ritzmann, O., Nishimura, Y., Grad, M., Mjelde, R., Guterch, A., & Jokat, W. (2005). Crustal structure of northern Spitsbergen along the deep seismic transect between the Molloy Deep and Nordaustlandet. *Geophysical Journal International*, *161*(2), 347–364. https://doi.org/10.1111/j.1365-246x.2005.02593.x

Dumais, M. A., Gernigon, L., Olesen, O., Johansen, S. E., & Brönner, M. (2021). New interpretation of the spreading evolution of the Knipovich Ridge derived from aeromagnetic data. *Geophysical Journal International*, *224*(2), 1422–1428. https://doi.org/10.1093/gji/ggaa527

Klenke, M., & Schenke, H. W. (2002). A new bathymetric model for the central Fram Strait. *Marine Geophysical Researches*, *23*(4), 367–378. https://doi.org/10.1023/a:1025764206736

Lein, A., Vogt, P., Crane, K., Egorov, A., & Ivanov, M. (1999). Chemical and isotopic evidence for the nature of the fluid in CH 4 -containing sediments of the Håkon Mosby Mud Volcano. *Geo-*

Marine Letters, *19*(1-2), 76–83. https://doi.org/10.1007/s003670050095

Ligi, M., Cuffaro, M., Muccini, F., & Bonatti, E. (2022). Generation and evolution of the oceanic lithosphere in the North Atlantic. *La Rivista Del Nuovo Cimento*, *45*(9), 587–659. https://doi.org/10.1007/s40766-022-00035-0

MacLeod, C. J., Carlut, J., Escartín, J., Horen, H., & Morris, A. (2011). Quantitative constraint on footwall rotations at the 15°45′N oceanic core complex, Mid-Atlantic Ridge: Implications for oceanic detachment fault processes. *Geochemistry, Geophysics, Geosystems*, *12*(5), n/a-n/a. https://doi.org/10.1029/2011gc003503

Milkov, A. V., & Etiope, G. (2018). Revised genetic diagrams for natural gases based on a global dataset of >20,000 samples. *Organic Geochemistry*, *125*, 109–120. https://doi.org/10.1016/j.orggeochem.2018.09.002

Panieri, G., Argentino, C., Ramalho, S. P., Vulcano, F., Savini, A., Fallati, L., Brekke, T., Galimberti, G., Riva, F., Balsa, J., Eilertsen, M. H., Stokke, R., Steen, I. H., Sahy, D., Kalenitchenko, D., Büenz, S., & Mattingsdal, R. (2024). An Arctic natural oil seep investigated from space to the seafloor. *Science of the Total Environment*, *907*, 167788–167788. https://doi.org/10.1016/j.scitotenv.2023.167788

Panieri, G., Argentino, C., Savini, A., Ferré, B., Hemmateenejad, F., Eilertsen, M. H., Mattingsdal, R., Ramalho, S. P., Eidvin, T., Youngs, S., Colson, B. C., Pauline, A., Kapit, J. A., Swanborn, D., Rogers, A. D., Angeles, I. B., Polteau, S., Kalenitchenko, D., Buenz, S., & Mazzini, A. (2025). Sanctuary for vulnerable Arctic species at the Borealis Mud Volcano. *Nature Communications*, *16*(1). https://doi.org/10.1038/s41467-024-55712-x

Panieri, G., Bünz, S., Fornari, D. J., Escartín, J., Serov, P., Jansson, P., Torres, M. E., Johnson, J. T., Hong, W.-L., Sauer, S., Garcia, R. G., & Gracias, N. (2017). An integrated view of the methane system in the pockmarks at Vestnesa Ridge, 79°N. *Marine Geology*, *390*, 282–300. https://doi.org/10.1016/j.margeo.2017.06.006

Panieri, G., Bünz, S., Savini, A., Rogers, A. D., Colson, B., Argentino, C., Dausse, D., Swanborn, D., Goetz, E., Ernsten, E., Hemmateenejad, F., Barrenechea Angeles, I., Viola, I., Hayden-Nygren, J., Andersen, K., Rolley, L., Eilertsen, M. H., Cosserat, O., Vågenes, P., & Andersen, R. (2024).

AKMA3 Cruise Report. *Septentrio Reports*, *1*. https://doi.org/10.7557/7.7745

Sanfilippo, A., Stracke, A., Genske, F., Scarani, S., Cuffaro, M., Basch, V., Borghini, G., Brunelli, D., Ferrando, C., Peyve, A. A., & Ligi, M. (2024). Upwelling of melt-depleted mantle under Iceland. *Nature Geoscience*, *17*(10), 1046–1052. https://doi.org/10.1038/s41561-024-01532-z

Serov, P., Vadakkepuliyambatta, S., Mienert, J., Patton, H., Portnov, A., Silyakova, A., Panieri, G., Carroll, M. L., Carroll, J., Andreassen, K., & Hubbard, A. (2017). Postglacial response of Arctic Ocean gas hydrates to climatic amelioration. *Proceedings of the National Academy of Sciences*, *114*(24), 6215–6220. https://doi.org/10.1073/pnas.1619288114

Shah, A. (2017). Ethnography? Participant observation, a potentially revolutionary praxis. *HAU: Journal of Ethnographic Theory*, *7*(1), 45–59. https://doi.org/10.14318/hau7.1.008

Smith, D. K., Escartín, J., Schouten, H., & Cann, J. R. (2008). Fault rotation and core complex formation: Significant processes in seafloor formation at slow-spreading mid-ocean ridges (Mid-Atlantic Ridge, 13°-15°N). *Geochemistry, Geophysics, Geosystems*, *9*(3), n/a-n/a. https://doi.org/10.1029/2007gc001699

Talwani, M., & Eldholm, O. (1977). Evolution of the Norwegian-Greenland Sea. *Geological Society of America Bulletin*, *88*(7), 969. https://doi.org/10.1130/0016-7606(1977)88%3C969:eotns%3E2.0.co;2

Tucholke, B. E., Lin, J., & Kleinrock, M. C. (1998). Megamullions and mullion structure defining oceanic metamorphic core complexes on the Mid-Atlantic Ridge. *Journal of Geophysical Research: Solid Earth*, *103*(B5), 9857–9866. https://doi.org/10.1029/98jb00167

Vadakkepuliyambatta, S., Bünz, S., Mienert, J., & Chand, S. (2013). Distribution of subsurface fluid-flow systems in the SW Barents Sea. *Marine and Petroleum Geology*, *43*, 208–221. https://doi.org/10.1016/j.marpetgeo.2013.02.007

Vogt, P. R., Cherkashev, G. A., Ginsburg, G. D., Ivanov, G. I., Milkov, A. V., Crane, K., Sundvor, A., Пименов, Н. В., & Егоров, А. А. (1997). Haakon Mosby Mud Volcano provides unusual example of venting. *Eos, Transactions American Geophysical Union*, *78*(48), 549–557. https://doi.org/10.1029/97eo00326

Whiticar, M. J. (1999). Carbon and hydrogen isotope systematics of bacterial formation and oxidation of methane. *Chemical Geology*, *161*(1-3), 291–314. https://doi.org/10.1016/s0009-2541(99)00092-3

11 Appendix

11.1 Table I. Leg 1 and Leg 2 ROV sampling log

Super Station	Latitude	Longitude	Date	ROV dive	Sample ID	Depth (m)	Environment
SS1 Freya mounds	79.6130	3.6620	12.11.2025	ROV1060	IG25-9-KH-01-ROV1060-BlaC-01	3572	Edge of the mound with tubeworms
					IG25-9-KH-01-ROV1060-CH4M-01	3573	SAGE measurement on the mound crater
			13.11.2025	ROV1061	IG25-9-KH-01-ROV1061-CarC-01	3571	Area 2 of photomosaic - At the edge of mound
					IG25-9-KH-01-ROV1061-Scoo-01	3571	Frankenstein Scoop - Area 2 of photomosaic - on mound with tubeworms
					IG25-9-KH-01-ROV1061-CarC-02	3573	Area 2 of photomosaic - on mound with mix of rocks, carbonate, white things
					IG25-9-KH-01-ROV1061-CH4M-01	3573	SAGE measurement around same mound where we collect Scoo-01
					IG25-9-KH-01-ROV1061-PusC-01	3573	On top of the mound, mostly muddy
					IG25-9-KH-01-ROV1061-PusC-02	3572	Within the depression of the same mound of PusC-01
					IG25-9-KH-01-ROV1061-SuSa-D	3572	On the mound area 2 - on tubeworm forest
					IG25-9-KH-01-ROV1061-SuSa-B	3572	On the same mound of SuSa-D, area 2 - around carbonate
					IG25-9-KH-01-ROV1061-PusC-03	3572	In area 1 with zonation - on tubeworm forest with microbial mat
					IG25-9-KH-01-ROV1061-PusC-04	3572	In area 1 with zonation - on tubeworm forest with microbial mat
					IG25-9-KH-01-ROV1061-PusC-05	3572	In area 1 with zonation - on the second zone without tubeworm forest and microbial mat (some big worms on mud)

					IG25-9-KH-01-ROV1061-BlaC-04	3572	In area 1 with zonation - on third zone with amphipods, anemone, etc., on tubeworms
					IG25-9-KH-01-ROV1061-BlaC-03	3572	In area 1 with zonation - outer zone with amphipods, tubeworm, etc. - honeycomb area
					IG25-9-KH-01-ROV1061-BlaC-02	3573	Just close to the gas hydrate crater - area 1
					IG25-9-KH-01-ROV1061-BlaC-01	3571	Gas hydrates
SS03 Frigg vent field	79.4297	3.2758	14.11.2025	ROV1062	IG25-9-KH-03-ROV1062-RocC-01	2711	A rock with a lot of fauna attached (anemones, sponges, etc.) on muddy seafloor
					IG25-9-KH-03-ROV1062-PusC-01	2709	On a totally muddy seafloor
					IG25-9-KH-03-ROV1062-RocC-02	2716	Rock from muddy seafloor
					IG25-9-KH-03-ROV1062-RocC-03	2720	Big redish rock with attached fauna
					IG25-9-KH-03-ROV1062-SuSa-E	2721	Suction sampling on a community on muddy seafloor
					IG25-9-KH-03-ROV1062-Scoo-01	2719	On the rock collection
					IG25-9-KH-03-ROV1062-Scoo-02	2719	On the rock collection
					IG25-9-KH-03-ROV1062-RockC-04	2725	Black rock on the outcrop
					IG25-9-KH-03-ROV1062-PusC-02	2731	On the patch of shells and unknown materials
					IG25-9-KH-03-ROV1062-RocC-05	2724	Rock on muddy seafloor
					IG25-9-KH-03-ROV1062-RocC-06	2732	Rock on muddy seafloor
					IG25-9-KH-03-ROV1062-RocC-07	2725	Rock on base of slope
					IG25-9-KH-03-ROV1062-RocC-08	2728	Rock on base of slope
					IG25-9-KH-03-ROV1062-RocC-09	2721	Rock from a rock debris at the base of scarp
					IG25-9-KH-03-ROV1062-RocC-10	2721	Rock from a rock debris at the base of scarp
					IG25-9-KH-03-ROV1062-RocC-11	2700	Rock on the slope scarp
					IG25-9-KH-03-ROV1062-RocC-12	2694	Scraping of the rocks in the ridge, collecting debris (white inside)
					IG25-9-KH-03-ROV1062-CH4M-01	2686	SAGE measurement close to area with minerals along the scarp
					IG25-9-KH-03-ROV1062-RocC-13	2677	Rock on the scarp

					IG25-9-KH-03-ROV1062-RocC-14	2676	Rock on the scarp
					IG25-9-KH-03-ROV1062-CH4M-02	2669	SAGE measurement close to the microbial mat
					IG25-9-KH-03-ROV1062-RocC-15	2661	Rock on scarp after microbial mat
					IG25-9-KH-03-ROV1062-CH4M-03	2673	Around the outcrop
					IG25-9-KH-03-ROV1062-SuSa-C	2668	Suction sampling on microbial mat observed before
					IG25-9-KH-03-ROV1062-SuSa-G	2668	Suction sampling on microbial mat observed before and sediment around, suction of a fish, laying close to mat
					IG25-9-KH-03-ROV1062-RocC-16	2669	From whitish loose rocks covered by microbial mat
					IG25-9-KH-03-ROV1062-RocC-17	2669	Rock on the top of the scarp
					IG25-9-KH-03-ROV1062-CH4M-04	2665	Around the outcrop
					IG25-9-KH-03-ROV1062-PusC-03	2636	Muddy seafloor
			15.11.2025	ROV1063	IG25-9-KH-03-ROV1063-WatS-01	2669	Water sample top of microbial mat with shimmering water
					IG25-9-KH-03-ROV1063-WatS-02	2669	Same as Niskin 01 but there were holes on bottle - Failed
					IG25-9-KH-03-ROV1063-CH4M-01	2669	SAGE measurement on microbial mat and shimmering water
					IG25-9-KH-03-ROV1063-TemL-01	2669	While SAGE measuring, Temperature Probe measuring at the same location
					IG25-9-KH-03-ROV1063-BioSyr-01	2669	SAGE and Tprobe still measuring, taking microbial films and samples around the same hole and around
					IG25-9-KH-03-ROV1063-RocC-01	2669	Rock at the same location with microbe, orange/brownish part with limpets on it
					IG25-9-KH-03-ROV1063-PusC-04	2665	On muddy seafloor on slope
					IG25-9-KH-03-ROV1063-BlaC-02	2668	Patch of red tubeworm forest but without microbial mat (very dark sediment underneath)

					IG25-9-KH-03-ROV1063-BlaC-01	2669	Adjacent area to BlaC-02 with spare tubeworms on muddy slope (Sclerolinum) and some shells around (less dark sediment underneath)
					IG25-9-KH-03-ROV1063-Scoo-01	2671	Many dead mussel shells on the slope at the edge of rocky area covered by mud
					IG25-9-KH-03-ROV1063-Scoo-02	2671	Many dead mussel shells on the slope at the edge of rocky area covered by mud
					IG25-9-KH-03-ROV1063-SuSa-F	2669	Around shimmering water
					IG25-9-KH-03-ROV1063-SuSa-A	2669	Side of shimmering water
SS05 Gjalp	79.6167	1.3902	16.11.2025	ROV1064	IG25-9-KH-05-ROV1064-CH4M-01	2805	Start measuring with SAGE
					IG25-9-KH-05-ROV1064-Scoo-01	2803	Red rock with fauna attached and radiolarian around
					IG25-9-KH-05-ROV1064-RocC-01	2777	Rock with attached fauna
					IG25-9-KH-05-ROV1064-RocC-02	2677	Rock with sponge, tunicate, shrimp, anemone and wood
					IG25-9-KH-05-ROV1064-Bio-01	2673	A sponge on muddy seafloor
					IG25-9-KH-05-ROV1064-RocC-03	2676	A small rock with sponge
					IG25-9-KH-05-ROV1064-RocC-04	2677	A rock with sponge and anemone
					IG25-9-KH-05-ROV1064-PusC-01	2679	On muddy seafloor
					IG25-9-KH-05-ROV1064-PusC-02	2874	Close to a rock with sponge on it in muddy seafloor
					IG25-9-KH-05-ROV1064-PusC-03	2687	Muddy seafloor
					IG25-9-KH-05-ROV1064-PusC-04	2886	Muddy seafloor
					IG25-9-KH-05-ROV1064-RocC-05	2716	A rock with sponge
					IG25-9-KH-05-ROV1064-ScooN-01	2766	Mud sample around a rock
					IG25-9-KH-05-ROV1064-ScooN-02	2782	A piece of wood on seafloor
					IG25-9-KH-05-ROV1064-ScooN-03	2786	Unknown green bio like seaweed close to a rock
					IG25-9-KH-05-ROV1064-Bio-02	2782	Wood close to rock
					IG25-9-KH-05-ROV1064-Bio-03	2780	Hydrozoa that was attached to rock

					IG25-9-KH-05-ROV1064-PusC-05	2703	Reference core
SS07 GFB	79.7951	3.1792	17.11.2025	ROV1065	IG25-9-KH-07-ROV1065-Bio-01	3947	Glass sponge on muddy-coarse seafloor
					IG25-9-KH-07-ROV1065-CH4M-01	3941	Start measuring SAGE
					IG25-9-KH-07-ROV1065-RocC-01	3928	Rock (white carbonate?) with stock of sponge
					IG25-9-KH-07-ROV1065-Bio-02	3924	Glass sponge on muddy-coarse seafloor
					IG25-9-KH-07-ROV1065-Scoo-01	3949	From an area with disturbed sediments
					IG25-9-KH-07-ROV1065-Bio-03	3896	Piece of wood
					IG25-9-KH-07-ROV1065-ScooN-01	3870	A vein of white material on muddy seafloor (loose)
					IG25-9-KH-07-ROV1065-CH4M-02	3868	Measuring SAGE top of ScooN-01 area
					IG25-9-KH-07-ROV1065-CH4M-03	3877	SAGE measurement on microbial mat
					IG25-9-KH-07-ROV1065-PusC-01	3877	On microbial mat
					IG25-9-KH-07-ROV1065-PusC-02	3872	On tubeworms and amphipods nearby honeycomb area
SS08 Prins Karls Forland	78.4934	10.5237	18.11.2025	ROV1066	IG25-9-KH-08-ROV1066-CH4M-01	110	SAGE measurement on bubbles and microbial mat
					IG25-9-KH-08-ROV1066-RocC-01	112	Rock with microbial mat on a big patch of microbial mat
					IG25-9-KH-08-ROV1066-PusC-01	112	Close to microbial mat
					IG25-9-KH-08-ROV1066-BlaC-01	112	At the edge of microbial mat
					IG25-9-KH-08-ROV1066-BlaC-04	112	Middle of microbial mat with oil
					IG25-9-KH-08-ROV1066-ScooN-01	112	Sediments close to mat but full of oil underneath
					IG25-9-KH-08-ROV1066-CH4M-02	112	Taking a rock with snail on it, top of the mat
					IG25-9-KH-08-ROV1066-Scoo-01	112	Middle of mat, rock with filamentous microbe
					IG25-9-KH-08-ROV1066-Gas-02	110	On mat with gas and oil bubbles
					IG25-9-KH-08-ROV1066-Gas-03	111	On mat with gas bubbles
					IG25-9-KH-08-ROV1066-CH4M-03	112	SAGE profile way up
SS09-2 Sørkapp Slope	76.4394	13.9462	20.11.2025	ROV1067	Nan		Mooring observation

SS09-3 Sørkapp Slope	76.4482	14.2506	20.11.2025	ROV1068	IG25-9-KH09-3-ROV1068-CH4M-01	824	SAGE measurement on top of microbial mat
					IG25-9-KH09-3-ROV1068-BlaC-04	825	On microbial mat, whitish/dark sediment
					IG25-9-KH09-3-ROV1068-BlaC-01	827	At the edge of microbial mat with tubeworms
					IG25-9-KH09-3-ROV1068-CarC-01	827	A piece of carbonate from a bigger carbonate with many fauna (three pieces)
					IG25-9-KH09-3-ROV1068-CarC-02	827	A piece of carbonate from a bigger carbonate with much fauna attached
SS11 Snøras Seep	72.7954	20.6254	21.11.2025	ROV1069	IG25-9-KH11-ROV1069-PusC-01	425	On microbial mat and tubeworms
					IG25-9-KH11-ROV1069-PusC-02	425	On microbial mat and tubeworms
					IG25-9-KH11-ROV1069-GasS-05	425	On microbial mat and tubeworms
					IG25-9-KH11-ROV1069-BlaC-01	424	On tubeworm forest with a small patch of microbial mat
				ROV1070	IG25-9-KH11-ROV1070-BlaC-02	424	Ghost tubeworm on muddy seafloor
SS12-1 Polynya Seep	72.3541	20.2159	22.11.2025	ROV1071	IG25-9-KH12-1-ROV1071-GasS-07	333	Top of carbonate crust, full of red fish and bubbles
					IG25-9-KH12-1-ROV1071-CarC-01	333	At the same location GasS-07 was collected, top layer of carbonate
					IG25-9-KH12-1-ROV1071-Scoo-01	334	Microbial mat with ghost tubeworms, bubbles, and hard substrate
					IG25-9-KH12-1-ROV1071-CarC-02	334	Bubbling carbonate with ghost tubeworms
					IG25-9-KH12-1-ROV1071-CH4M-02	332	SAGE transect way up
SS12-2 Kayak	72.3289	19.9111	22.11.2025	ROV1072	IG25-9-KH12-2-ROV1072-GasS-04	332	Around the well and inside it
SS12-3 Mist	72.2897	19.9989	22.11.2025	ROV1073	IG25-9-KH12-3-ROV1073-GasS-08	324	Gas sampler inside well, microbial mat around the edge
SS12-4 Hurri	72.2008	19.7173	22.11.2025	ROV1074	IG25-9-KH12-4-ROV1074-GasS-10	311	Gas sampler on well with bubbles
					IG25-9-KH12-4-ROV1074-GasS-09	311	Gas sampler on well with bubbles
					IG25-9-KH12-4-ROV1074-WatS-B	311	Water samples on top of the well with bubbles

SS12-5 Bask Seep	72.1580	19.7269	22.11.2025	ROV1075	IG25-9-KH12-5-ROV1075-CarC-01	317	Very small carbonate close to a microbial mat with bubbles
					IG25-9-KH12-5-ROV1075-Bio-01	317	Round sponge close to microbial mat
					IG25-9-KH12-5-ROV1075-Trash-01	317	Trash on carbonate crust
					IG25-9-KH12-5-ROV1075-Trash-02	318	A push core within carbonate (not from us)
					IG25-9-KH12-5-ROV1075-Trash-03	318	A buoy under carbonate
					IG25-9-KH12-5-ROV1075-Scoo-01	318	Microbial mat bubbling on coarse seafloor, just the top layer, very hard seafloor
					IG25-9-KH12-5-ROV1075-CH4M-01	317	Start measuring SAGE in this location
					IG25-9-KH12-5-ROV1075-GasS-12	318	Gas sample on microbial mat bubbling on coarse seafloor
SS13 Tromsøflaket	71.3107	18.9960	23.11.2025	ROV1076	IG25-9-KH13-ROV1076-Bio-01	227	A sponge that was attached to rock
					IG25-9-KH13-ROV1076-Bio-02	227	A yellowish encrusting big sponge
					IG25-9-KH13-ROV1076-Bio-03	227	A blue encrusting sponge
				ROV1077	IG25-9-KH13-ROV1077-CH4M-01	225	SAGE measurement on microbial mat with bubbles
					IG25-9-KH13-ROV1077-GasS-14	227	Gas sampler was placed on the top of bubbling microbial mat
					IG25-9-KH13-ROV1077-WatS-01	226	On a bubbling mat, quite close to the gas sampler
					IG25-9-KH13-ROV1077-WatS-02	226	On a bubbling mat, quite close to the gas sampler
					IG25-9-KH13-ROV1077-Scoo-01	228	Scoop on microbial mat with snails, lots of bubbles come out
					IG25-9-KH13-ROV1077-ScooN-01	228	Scoop on another microbial mat in the area
					IG25-9-KH13-ROV1077-CarC-01	228	Carbonate with small sponges
					IG25-9-KH13-ROV1077-RocC-01	229	Rock covered with biofilm
SS14 7119/9-1	71.4148	19.8281	23.11.2025	ROV1078	IG25-9-KH-14-ROV1078-ScooN-01	198	On microbial mat with tubeworms and bubbles
					IG25-9-KH-14-ROV1078-RocC-01	196	Rock on microbial mat also covered by biofilm
					IG25-9-KH-14-ROV1078-Trash-01	197	A buoy on seafloor
					IG25-9-KH-14-ROV1078-GasS-	197	

					IG25-9-KH-14-ROV1078-Scoo-01	198	Bubbling microbial mat with tubeworms, on rock or carbonate?
					IG25-9-KH-14-ROV1078-RocC-01	198	A piece of unusual rock/carbonate/cement? Environment: grey and white "soft" layer around with structure similar to a little cave
					IG25-9-KH-14-ROV1078-CH4M-01	198	On top of this structure that RocC-01 was collected
					IG25-9-KH-14-ROV1078-Scoo-02	198	Scoop from this structure that RocC-01 was collected, different layer with different color
					IG25-9-KH-14-ROV1078-Scoo-03	198	Scoop from this structure that RocC-01 was collected, different layer with different color
					IG25-9-KH-14-ROV1078-Scoo-04	199	Nearby area with same structure, microbial mat with bubbling
					IG25-9-KH-14-ROV1078-CH4M-02	199	Same area as Scoo-04
					IG25-9-KH-14-ROV1078-BlaC-02	199	Same area as Scoo-05
					IG25-9-KH-14-ROV1078-RocC-03	199	Crust thing on this area
					IG25-9-KH-14-ROV1078-BlaC-04	198	Reference core
					IG25-9-KH-14-ROV1078-GasS-	197	
					IG25-9-KH-14-ROV1078-Trash-02	195	Buoy on the seafloor
SS15 7119/7-1	71.3953	19.2536	23.11.2025	ROV1079	IG25-9-KH-15-ROV1079-GasS-06	235	Inside the well, bubbling with microbial mat and tubeworms
					IG25-9-KH-15-ROV1079-GasS-15	235	Inside the well, bubbling with microbial mat and tubeworms
					IG25-9-KH-15-ROV1079-WatS-	233	Same location as GasS-06 and GasS-15
					IG25-9-KH-15-ROV1079-Trash-01	236	A bucket around well
SS17 Outer Bjørnøya	72.4390	17.6777	24.11.2025	ROV1080	IG25-9-KH17-ROV1080-Fish cage	382	Placing fish cage between carbonate with microbial mat, red fish and coral
				ROV1081	IG25-9-KH17-ROV1081-BlaC-01	394	On big mat with many faunas, tubeworms, sea spiders, snails, hermit crab
					IG25-9-KH17-ROV1081-BlaC-02	396	Inside a fresh mat on rim of gryphons

					IG25-9-KH17-ROV1081-CarC-01	381	Small piece of carbonate around bigger crust
					IG25-9-KH17-ROV1081-CarC-02	389	Big piece of carbonate
					IG25-9-KH17-ROV1081-CarC-03	385	Medium piece
					IG25-9-KH17-ROV1081-Bio-01	396	Dead fish at gryphon crater
				ROV1082	IG25-9-KH-17-ROV1082-TemL-01	397	At the center of gryphon with shimmering water
					IG25-9-KH-17-ROV1082-CarC-01	397	Carbonate crust just at the edge of gryphon with microbial mat and dark sediment on top
					IG25-9-KH-17-ROV1082-ScooN-01	397	All the sediment with silver fish, snails, and.. close to tiny crater near main gryphon
					IG25-9-KH-17-ROV1082-ScooN-02	397	All the sediment with silver fish, snails, and.. close to tiny crater near main gryphon
					IG25-9-KH-17-ROV1082-CTD	394	On top of gryphon
					IG25-9-KH-17-ROV1082-CH4M-01	384	SAGE profile way up, starting from gryphon
SS18 Tvillingene	72.5846	17.4011	24.11.2025	ROV1083	IG25-9-KH-18-ROV1083-GasS-18	363	Carbonate, bubbles and fish near the gryphon
					IG25-9-KH-18-ROV1083-BlaC-04	362	Edge of microbial mat with tubeworms
					IG25-9-KH-18-ROV1083-CarC-01	360	Small piece of carbonate on top of a big carbonate crust
					IG25-9-KH-18-ROV1083-CarC-02	360	Small piece from middle layer of big crust (same as CarC-01)
					IG25-9-KH-18-ROV1083-CarC-03	360	From another side of this crust (same as CarC-01)
					IG25-9-KH-18-ROV1083-CarC-04	362	A big carbonate on the seafloor underneath a big crust
					IG25-9-KH-18-ROV1083-ScooN-01	363	Ghost tubeworms
					IG25-9-KH-18-ROV1083-CH4M-01	363	SAGE profile starting from the top of ghost tubeworms
SS19 Tromsøflaket SW	71.0222	17.1675	25.11.2025	ROV1084	IG25-9-KH-19-ROV1084-GasS-17	316	On small mat with bubbles
					IG25-9-KH-19-ROV1084-WatS-01	317	On same location as GasS-17
					IG25-9-KH-19-ROV1084-CH4M-01	317	On the way up

SS20 Fugløybanken	70.3856	17.4500	25.11.2025	ROV1085	IG25-9-KH-20-ROV1085-BlaC-03	146	Microbial mat bubbling on sandy seafloor
					IG25-9-KH-20-ROV1085-CH4M-01	139	Microbial mat between rocks
					IG25-9-KH-20-ROV1085-CH4M-02	142	Top of microbial mat, rocky seafloor

11.2 Table II. Complete station's log

Location	Station Id	Date	Time (UTC)	Lat.[N] Long. [E]	Water Depth [m]
Freya gas hydrate mounds	IG25-9-KH-01-ROV-1060	12/11	14:49	79°36.774' 03°39.678'	3576
Freya gas hydrate mounds	IG25-9-KH-01_ROV1060-BlaC-01	12/11	17:25	79°36.852' 03°39.426'	3573
Freya gas hydrate mounds	IG25-9-KH-01_ROV1060-CH4M-01	12/11	17:30	79°36.846' 03°39.426'	3573
Freya gas hydrate mounds	IG25-9-KH-564-CTD	12/11	21:25	79°36.780' 03°39.696'	3563
Freya gas hydrate mounds	IG25-9-KH-01-ROV-1061	13/11	07:50	79°36.780' 03°39.720'	3577
Freya gas hydrate mounds	IG25-9-KH-01_ROV1061-VMap-01	13/11	10:00	79°36.846' 03°39.486'	3577

Freya gas hydrate mounds	IG25-9-KH-01_ROV1061-VMap-02	13/11	10:46	79°36.834' 03°39.636'	3597
Freya gas hydrate mounds	IG25-9-KH-01_ROV1061-CarC-01	13/11	11:44	79°36.852' 03°39.618'	3571
Freya gas hydrate mounds	IG25-9-KH-01_ROV1061-Scoo-01	13/11	11:48	79°36.852' 03°39.618'	3571
Freya gas hydrate mounds	IG25-9-KH-01_ROV1061-CarC-02	13/11	11:58	79°36.852' 03°39.642'	3573
Freya gas hydrate mounds	IG25-9-KH-01_ROV1061-CH4M-01	13/11	12:06	79°36.846' 03°39.648'	3573
Freya gas hydrate mounds	IG25-9-KH-01_ROV1061-PusC-01	13/11	12:23	79°36.852' 03°39.636'	3569
Freya gas hydrate mounds	IG25-9-KH-01_ROV1061-PusC-02	13/11	12:31	79°36.852' 03°39.630'	3572
Freya gas hydrate mounds	IG25-9-KH-01_ROV1061-SuSa-D	13/11	12:51	79°36.846' 03°39.636'	3572

Freya gas hydrate mounds	IG25-9-KH-01_ROV1061-SuSa-B	13/11	12:55	79°36.852' 03°39.642'	3572
Freya gas hydrate mounds	IG25-9-KH-01_ROV1061-VMap-03	13/11	13:10	79°36.774' 03°39.672'	3570
Freya gas hydrate mounds	IG25-9-KH-01_ROV1061-VMap-04	13/11	14:08	79°36.834' 03°39.468'	3577
Freya gas hydrate mounds	IG25-9-KH-01_ROV1061-PusC-03	13/11	14:32	79°36.840' 03°39.480'	3572
Freya gas hydrate mounds	IG25-9-KH-01_ROV1061-PusC-04	13/11	14:49	79°36.840' 03°39.462'	3572
Freya gas hydrate mounds	IG25-9-KH-01_ROV1061-PusC-05	13/11	14:56	79°36.840' 03°39.486'	3572
Freya gas hydrate mounds	IG25-9-KH-01_ROV1061-BlaC-04	13/11	15:10	79°36.834' 03°39.492'	3572
Freya gas hydrate mounds	IG25-9-KH-01_ROV1061-BlaC-03	13/11	15:22	79°36.834' 03°39.492'	3572

Freya gas hydrate mounds	IG25-9-KH-01_ROV1061-BlaC-02	13/11	15:48	79°36.852' 03°39.408'	3573
Freya gas hydrate mounds	IG25-9-KH-01_ROV1061-BlaC-01	13/11	16:20	79°36.852' 03°39.390'	3572
Molloy Deep	IG25-9-KH-02-GC-01	14/11	01:50	79°09.678' 02°52.650'	5550
Molloy Deep	IG25-9-KH-02-GC-01_#01_0-95	14/11	01:50	79°09.678' 02°52.650'	5550
Molloy Deep	IG25-9-KH-02-GC-01_#02_95-195	14/11	01:50	79°09.678' 02°52.650'	5550
Molloy Deep	IG25-9-KH-02-GC-01_#03_195-295	14/11	01:50	79°09.678' 02°52.650'	5550
Molloy Deep	IG25-9-KH-02-GC-01_CoreCatcher	14/11	01:50	79°09.678' 02°52.650'	5550
Molloy Deep	IG25-9-KH-565-CTD	14/11	04:18	79°09.678' 02°52.650'	5550

Molloy Deep	IG25-9-KH-566-CTD	14/11	04:45	79°09.678' 02°52.650'	5550
Frigg Vent Field	IG25-9-KH-03-ROV-1062	14/11	07:36	79°25.476' 03°20.100'	
Frigg Vent Field	IG25-9-KH-03_ROV1062-RocC-01	14/11	09:03	79°25.482' 03°19.776'	2711
Frigg Vent Field	IG25-9-KH-03_ROV1062-PusC-01	14/11	09:16	79°25.494' 03°19.572'	2709
Frigg Vent Field	IG25-9-KH-03_ROV1062-RocC-02	14/11	09:25	79°25.512' 03°19.380'	2716
Frigg Vent Field	IG25-9-KH-03_ROV1062-RocC-03	14/11	09:31	79°25.518' 03°19.254'	2720
Frigg Vent Field	IG25-9-KH-03_ROV1062-SuSa-E	14/11	09:34	79°25.518' 03°19.260'	2721
Frigg Vent Field	IG25-9-KH-03_ROV1062-Scoo-01	14/11	09:57	79°25.584' 03°18.480'	2719

Frigg Vent Field	IG25-9-KH-03_ROV1062-Scoo-02	14/11	10:01	79°25.584' 03°18.480'	2719
Frigg Vent Field	IG25-9-KH-03_ROV1062-RocC-04	14/11	10:07	79°25.596' 03°18.276'	2725
Frigg Vent Field	IG25-9-KH-03_ROV1062-PusC-02	14/11	10:53	79°25.596' 03°18.234'	2731
Frigg Vent Field	IG25-9-KH-03_ROV1062-RocC-05	14/11	11:17	79°25.632' 03°17.544'	2724
Frigg Vent Field	IG25-9-KH-03_ROV1062-RocC-06	14/11	11:35	79°25.680' 03°16.920'	2732
Frigg Vent Field	IG25-9-KH-03_ROV1062-RocC-07	14/11	11:43	79°25.746' 03°16.710'	2725
Frigg Vent Field	IG25-9-KH-03_ROV1062-RocC-08	14/11	11:46	79°25.752' 03°16.734'	2728
Frigg Vent Field	IG25-9-KH-03_ROV1062-RocC-09	14/11	11:55	79°25.758' 03°16.656'	2721

Frigg Vent Field	IG25-9-KH-03_ROV1062-RocC-10	14/11	11:56	79°25.758' 03°16.656'	2721
Frigg Vent Field	IG25-9-KH-03_ROV1062-RocC-11	14/11	12:10	79°25.758' 03°16.620'	2700
Frigg Vent Field	IG25-9-KH-03_ROV1062-RocC-12	14/11	12:15	79°25.764' 03°16.578'	2694
Frigg Vent Field	IG25-9-KH-03_ROV1062-CH4M-01	14/11	12:24	79°25.770' 03°19.602'	2686
Frigg Vent Field	IG25-9-KH-03_ROV1062-RocC-13	14/11	12:39	79°25.776' 03°16.578'	2677
Frigg Vent Field	IG25-9-KH-03_ROV1062-RocC-14	14/11	12:43	79°25.770' 03°16.572'	2676
Frigg Vent Field	IG25-9-KH-03_ROV1062-CH4M-02	14/11	12:50	79°25.788' 03°16.560'	2669
Frigg Vent Field	IG25-9-KH-03_ROV1062-RocC-17	14/11	12:52	79°25.788' 03°16.560'	2669

Frigg Vent Field	IG25-9-KH-03_ROV1062-RocC-15	14/11	13:20	79°25.788' 03°16.536'	2661
Frigg Vent Field	IG25-9-KH-03_ROV1062-VMap-01	14/11	13:37	79°25.782' 03°16.548'	2660
Frigg Vent Field	IG25-9-KH-03_ROV1062-CH4M-03	14/11	14:17	79°25.776' 03°16.614'	2673
Frigg Vent Field	IG25-9-KH-03_ROV1062-SuSa-C	14/11	14:20	79°25.788' 03°16.578'	2668
Frigg Vent Field	IG25-9-KH-03_ROV1062-SuSa-G	14/11	14:32	79°25.788' 03°16.578'	2668
Frigg Vent Field	IG25-9-KH-03_ROV1062-RocC-16	14/11	14:38	79°25.788' 03°16.566'	2669
Frigg Vent Field	IG25-9-KH-03_ROV1062-CH4M-04	14/11	14:53	79°25.788' 03°16.572'	2665
Frigg Vent Field	IG25-9-KH-03_ROV1062-PusC-03	14/11	15:51	79°25.920' 03°16.656'	2636

Southern Yermak Plateau	IG25-9-KH-04-MC-01_005_0-50	14/11	23:50	79°49.014' 06°15.180'	962
Southern Yermak Plateau	IG25-9-KH-04-MC-02_001_0-48	15/11	00:47	79°49.014' 06°15.174'	963
Southern Yermak Plateau	IG25-9-KH-04-MC-02_002_0-18	15/11	00:47	79°49.014' 06°15.174'	963
Southern Yermak Plateau	IG25-9-KH-04-MC-02_004_0-23	15/11	00:47	79°49.014' 06°15.174'	963
Southern Yermak Plateau	IG25-9-KH-04-MC-02_005_0-36	15/11	00:47	79°49.014' 06°15.174'	963
Southern Yermak Plateau	IG25-9-KH-04-MC-02_006_0-50	15/11	00:47	79°49.014' 06°15.174'	963
Southern Yermak Plateau	IG25-9-KH-567-CTD	15/11	01:30	79°49.014' 06°31.800'	963
Frigg Vent Field	IG25-9-KH-03-ROV-1063	15/11	10:54	79°25.782' 03°16.548'	2700

Frigg Vent Field	IG25-9-KH-03_ROV1063-VMap-01	15/11	12:23	79°25.770' 03°16.584'	2674
Frigg Vent Field	IG25-9-KH-03_ROV1063-WatS-01	15/11	13:30	79°25.788' 03°16.566'	2669
Frigg Vent Field	IG25-9-KH-03_ROV1063-WatS-02	15/11	13:42	79°25.788' 03°16.560'	2669
Frigg Vent Field	IG25-9-KH-03_ROV1063-CH4M-01	15/11	14:40	79°25.788' 03°16.554'	2669
Frigg Vent Field	IG25-9-KH-03_ROV1063-TemL-01	15/11	14:49	79°25.788' 03°16.554'	2669
Frigg Vent Field	IG25-9-KH-03_ROV1063-Bsyr-01	15/11	14:58	79°25.788' 03°16.554'	2669
Frigg Vent Field	IG25-9-KH-03_ROV1063-RocC-01	15/11	15:13	79°25.788' 03°16.554'	2669
Frigg Vent Field	IG25-9-KH-03_ROV1063-PusC-04	15/11	15:43	79°25.776' 03°16.584'	2669

Frigg Vent Field	IG25-9-KH-03_ROV1063-BlaC-02	15/11	16:02	79°25.788' 03°16.566'	2669
Frigg Vent Field	IG25-9-KH-03_ROV1063-BlaC-01	15/11	16:10	79°25.788' 03°16.584'	2669
Frigg Vent Field	IG25-9-KH-03_ROV1063-Scoo-01	15/11	16:25	79°25.770' 03°16.530'	2672
Frigg Vent Field	IG25-9-KH-03_ROV1063-Scoo-02	15/11	16:27	79°25.770' 03°16.530'	2672
Frigg Vent Field	IG25-9-KH-03_ROV1063-SuSa-F	15/11	16:34	79°25.788' 03°16.560'	2669
Frigg Vent Field	IG25-9-KH-03_ROV1063-SuSa-A	15/11	16:40	79°25.788' 03°16.560'	2669
Gjalp	IG25-9-KH-568-CTD	16/11	08:28	79°38.334' 01°21.048'	2597
Gjalp	IG25-9-KH-05-ROV-1064	16/11	08:52	79°37.002' 01°23.412'	

Gjalp	IG25-9-KH-05_ROV1064-CH4M-01	16/11	10:21	79°36.990' 01°22.440'	2805
Gjalp	IG25-9-KH-05_ROV1064-Scoo-01	16/11	10:30	79°36.990' 01°22.014'	2803
Gjalp	IG25-9-KH-05_ROV1064-RocC-01	16/11	10:57	79°37.014' 01°20.922'	2777
	IG25-9-KH-05_ROV1064-RocC-02	16/11	11:37	79°37.008' 01°19.080'	2677
Gjalp	IG25-9-KH-05_ROV1064-Biol-01	16/11	11:43	79°37.014' 01°18.918'	2673
Gjalp	IG25-9-KH-05_ROV1064-RocC-03	16/11	11:46	79°37.020' 01°18.846'	2676
Gjalp	IG25-9-KH-05_ROV1064-RocC-04	16/11	11:51	79°37.020' 01°18.732'	2677
Gjalp	IG25-9-KH-05_ROV1064-PusC-01	16/11	11:58	79°37.020' 01°18.756'	2679

Gjalp	IG25-9-KH-05_ROV1064-PusC-02	16/11	12:07	79°37.020' 01°18.840'	2674
Gjalp	IG25-9-KH-05_ROV1064-PusC-03	16/11	12:17	79°37.020' 01°18.474'	2687
Gjalp	IG25-9-KH-05_ROV1064-PusC-04	16/11	12:23	79°37.026' 01°18.492'	2686
Gjalp	IG25-9-KH-05_ROV1064-RocC-05	16/11	13:17	79°36.930' 01°20.136'	2716
Gjalp	IG25-9-KH-05_ROV1064-ScoN-01	16/11	13:36	79°37.014' 01°20.742'	2766
Gjalp	IG25-9-KH-05_ROV1064-ScoN-02	16/11	13:44	79°37.044' 01°21.024'	2782
Gjalp	IG25-9-KH-05_ROV1064-ScoN-03	16/11	13:55	79°37.098' 01°21.390'	2786
Gjalp	IG25-9-KH-05_ROV1064-Biol-02	16/11	14:05	79°37.146' 01°21.780'	2782

Gjalp	IG25-9-KH-05_ROV1064-Biol-03	16/11	14:16	79°37.164' 01°22.098'	2780
Gjalp	IG25-9-KH-05_ROV1064-PusC-05	16/11	14:25	79°37.146' 01°22.224'	2783
Ice Station	IG25-9-KH-06-IS-01	16/11	18:30	79°40.542' 00°39.240'	
Ice Station	IG25-9-KH-06-IS-02	16/11	18:30	79°40.542' 00°39.240'	
GFB	IG25-9-KH-07-ROV-1065	17/11	09:10	79°47.706' 03°10.752'	4000
GFB	IG25-9-KH-07_ROV1065-Biol-01	17/11	12:31	79°47.718' 03°10.800'	3947
GFB	IG25-9-KH-07_ROV1065-CH4M-01	17/11	12:36	79°47.718' 03°10.794'	3941
GFB	IG25-9-KH-07_ROV1065-RocC-01	17/11	12:46	79°47.736' 03°10.956'	3928

GFB	IG25-9-KH-07_ROV1065-Biol-02	17/11	13:09	79°47.760' 03°10.596'	3924
GFB	IG25-9-KH-07_ROV1065-Scoo-01	17/11	13:57	79°47.676' 03°11.190'	3949
GFB	IG25-9-KH-07_ROV1065-Biol-03	17/11	14:18	79°47.718' 03°11.400'	3896
GFB	IG25-9-KH-07_ROV1065-MBat-01	17/11	14:34	79°47.748' 03°11.442'	3769
GFB	IG25-9-KH-07_ROV1065-ScoN-01	17/11	15:48	79°47.838' 03°10.422'	3870
GFB	IG25-9-KH-07_ROV1065-CH4M-02	17/11	15:52	79°47.838' 03°10.410'	3868
GFB	IG25-9-KH-07_ROV1065-CH4M-03	17/11	16:00	79°47.826' 03°10.452'	3877
GFB	IG25-9-KH-07_ROV1065-PusC-01	17/11	16:25	79°47.826' 03°10.464'	3877

GFB	IG25-9-KH-07_ROV1065-PusC-02	17/11	16:33	79°47.814' 03°10.668'	3872
GFB	IG25-9-KH-569-CTD	17/11	19:00	79°47.556' 03°06.672'	4158
GFB	IG25-9-KH-570-CTD	17/11	20:14	79°47.778' 03°10.956'	3874
GFB	IG25-9-KH-571-CTD	17/11	21:22	79°47.778' 03°10.950'	3863
Prins Karls Foreland	IG25-9-KH-08-ROV-1066	18/11	13:20	78°29.604' 10°31.422'	115
Prins Karls Foreland	IG25-9-KH-08_ROV1066-CH4M-01	18/11	13:38	78°29.568' 10°31.410'	110
Prins Karls Foreland	IG25-9-KH-08_ROV1066-VMap-02	18/11	13:41	78°29.538' 10°31.458'	110
Prins Karls Foreland	IG25-9-KH-08_ROV1066-RocC-01	18/11	14:43	78°29.562' 10°31.416'	112

Prins Karls Foreland	IG25-9-KH-08_ROV1066-PusC-01	18/11	14:55	78°29.562' 10°31.422'	112
Prins Karls Foreland	IG25-9-KH-08_ROV1066-BlaC-01	18/11	15:11	78°29.562' 10°31.416'	112
Prins Karls Foreland	IG25-9-KH-08_ROV1066-BlaC-04	18/11	15:18	78°29.562' 10°31.422'	112
Prins Karls Foreland	IG25-9-KH-08_ROV1066-ScoN-01	18/11	15:25	78°29.562' 10°31.422'	112
Prins Karls Foreland	IG25-9-KH-08_ROV1066-CH4M-02	18/11	15:30	78°29.562' 10°31.422'	112
Prins Karls Foreland	IG25-9-KH-08_ROV1066-Scoo-01	18/11	15:38	78°29.562' 10°31.422'	112
Prins Karls Foreland	IG25-9-KH-08_ROV1066-GasS-02	18/11	15:55	78°29.586' 10°31.386'	110
Prins Karls Foreland	IG25-9-KH-08_ROV1066-GasS-03	18/11	16:31	78°29.568' 10°31.398'	111

Prins Karls Foreland	IG25-9-KH-08_ROV1066-CH4M-03	18/11	17:22	78°29.562' 10°31.410'	112
Prins Karls Foreland	IG25-9-KH-572-CTD	18/11	17:44	78°29.562' 10°31.380'	112
Sørkapp Slope	IG25-9-KH-09_01-MC-03_001_0-45	20/11	04:20	76°33.318' 12°55.860'	1482
Sørkapp Slope	IG25-9-KH-09_01-MC-03_002_0-37	20/11	04:20	76°33.318' 12°55.860'	1482
Sørkapp Slope	IG25-9-KH-09_01-MC-03_003_0-48	20/11	04:20	76°33.318' 12°55.860'	1482
Sørkapp Slope	IG25-9-KH-09_01-MC-03_004_0-44	20/11	04:20	76°33.318' 12°55.860'	1482
Sørkapp Slope	IG25-9-KH-09_01-MC-03_005_0-38	20/11	04:20	76°33.318' 12°55.860'	1482
Sørkapp Slope	IG25-9-KH-09_01-MC-03_006_0-45	20/11	04:20	76°33.318' 12°55.860'	1482

Sørkapp Slope	IG25-9-KH-09_02-ROV-1067	20/11	07:06	76°26.364' 13°56.772'	1031
Sørkapp Slope	IG25-9-KH-09_03-ROV-1068	20/11	08:56	76°26.892' 14°15.036'	830
Sørkapp Slope	IG25-9-KH-09_03_ROV1068-CH4M-01	20/11	09:26	76°26.898' 14°15.054'	824
Sørkapp Slope	IG25-9-KH-573-CTD	20/11	09:50	76°26.892' 14°15.042'	810
Sørkapp Slope	IG25-9-KH-09_03_ROV1068-MBat-01	20/11	09:50	76°26.910' 14°15.156'	792
Sørkapp Slope	IG25-9-KH-09_03_ROV1068-VMap-01	20/11	10:50	76°26.898' 14°15.204'	813
Sørkapp Slope	IG25-9-KH-09_03_ROV1068-BlaC-04	20/11	11:39	76°26.892' 14°15.060'	826

Sørkapp Slope	IG25-9-KH-09_03_ROV1068-BlaC-01	20/11	11:58	76°26.892' 14°15.060'	827
Sørkapp Slope	IG25-9-KH-09_03_ROV1068-CarC-01	20/11	12:09	76°26.916' 14°14.916'	827
Sørkapp Slope	IG25-9-KH-09_03_ROV1068-CarC-02	20/11	12:18	76°26.886' 14°14.970'	826
Bjørnøya	IG25-9-KH-574-CTD	20/11	19:30	75°33.612' 16°30.522'	256
Snøras Seep	IG25-9-KH-11-ROV-1069	21/11	14:19	72°47.730' 20°37.548'	430
Snøras Seep	IG25-9-KH-11_ROV1069-MBat-01	21/11	14:46	72°47.742' 20°37.608'	397
Snøras Seep	IG25-9-KH-575-CTD	21/11	15:32	72°47.736' 20°37.548'	428
Snøras Seep	IG25-9-KH-11_ROV1069-PusC-01	21/11	15:49	72°47.742' 20°37.608'	425

Snøras Seep	IG25-9-KH-11_ROV1069-PusC-02	21/11	15:53	72°47.742' 20°37.524'	425
Snøras Seep	IG25-9-KH-11_ROV1069-GasS-05	21/11	16:10	72°47.742' 20°37.518'	425
Snøras Seep	IG25-9-KH-11_ROV1069-BlaC-01	21/11	16:24	72°47.742' 20°37.506'	424
Snøras Seep	IG25-9-KH-11-ROV-1070	21/11	17:52	72°47.724' 20°37.524'	427
Snøras Seep	IG25-9-KH-11_ROV1070-BlaC-02	21/11	18:14	72°47.730' 20°37.512'	424
Snøras Seep	IG25-9-KH-11-GC-02	21/11	19:28	72°47.748' 20°37.524'	429
Snøras Seep	IG25-9-KH-11-GC-02_#1_0-63	21/11	19:28	72°47.748' 20°37.524'	429
Snøras Seep	IG25-9-KH-11-GC-02_#2_63-163	21/11	19:28	72°47.748' 20°37.524'	429

Snøras Seep	IG25-9-KH-11-GC-02_CoreCatcher	21/11	19:28	72°47.748' 20°37.524'	429
Snøras Seep	IG25-9-KH-11-MC-04	21/11	21:14	72°47.754' 20°37.542'	
Polynya Seep	IG25-9-KH-12_1-ROV-1071	22/11	07:07	72°21.246' 20°12.954'	335
Polynya Seep	IG25-9-KH-12_1_ROV1071-GasS-07	22/11	07:41	72°21.258' 20°12.942'	333
Polynya Seep	IG25-9-KH-12_1_ROV1071-CarC-01	22/11	08:21	72°21.258' 20°12.942'	333
Polynya Seep	IG25-9-KH-12_1_ROV1071-MBat-01	22/11	08:33	72°21.246' 20°12.816'	292
Polynya Seep	IG25-9-KH-12_1_ROV1071-Scoo-01	22/11	09:10	72°21.252' 20°12.912'	334
Polynya Seep	IG25-9-KH-12_1_ROV1071-CarC-02	22/11	09:18	72°21.246' 20°12.912'	334

Polynya Seep	IG25-9-KH-12_1_ROV1071-CH4M-02	22/11	09:35	72°21.258' 20°12.954'	332
Kayak	IG25-9-KH-12_2-ROV-1072	22/11	10:45	72°19.734' 19°54.666'	335
Kayak	IG25-9-KH-12_2_ROV1072-GasS-04	22/11	11:22	72°19.746' 19°54.564'	332
Kayak	IG25-9-KH-576-CTD	22/11	11:27	72°19.734' 19°54.666'	331
Mist	IG25-9-KH-12_3-ROV-1073	22/11	12:59	72°17.382' 19°59.934'	330
Mist	IG25-9-KH-12_3_ROV1073-GasS-08	22/11	13:19	72°17.394' 19°59.844'	324
Hurri	IG25-9-KH-12_4-ROV-1074	22/11	15:11	72°12.048' 19°43.038'	315
Hurri	IG25-9-KH-12_4_ROV1074-GasS-10	22/11	15:27	72°12.072' 19°42.942'	311

Hurri	IG25-9-KH-12_4_ROV1074-GasS-09	22/11	15:47	72°12.066' 19°42.942'	311
Hurri	IG25-9-KH-12_4_ROV1074-WatS-B	22/11	15:53	72°12.066' 19°42.936'	311
Bask Seep	IG25-9-KH-12_5-ROV-1075	22/11	16:44	72°09.480' 19°43.614'	320
Bask Seep	IG25-9-KH-12_5_ROV1075-MBat-01	22/11	17:01	72°09.444' 19°43.626'	283
Bask Seep	IG25-9-KH-12_5_ROV1075-CarC-01	22/11	17:22	72°09.480' 19°43.656'	317
Bask Seep	IG25-9-KH-12_5_ROV1075-Biol-01	22/11	17:24	72°09.480' 19°43.656'	317
Bask Seep	IG25-9-KH-12_5_ROV1075-Ctra-01	22/11	17:28	72°09.474' 19°43.644'	317
Bask Seep	IG25-9-KH-12_5_ROV1075-Ctra-02	22/11	17:30	72°09.474' 19°43.638'	318

Bask Seep	IG25-9-KH-12_5_ROV1075-Ctra-03	22/11	17:33	72°09.468' 19°43.638'	318
Bask Seep	IG25-9-KH-12_5_ROV1075-Scoo-01	22/11	17:44	72°09.462' 19°43.650'	318
Bask Seep	IG25-9-KH-12_5_ROV1075-CH4M-01	22/11	17:50	72°09.468' 19°43.656'	317
Bask Seep	IG25-9-KH-12_5_ROV1075-GasS-12	22/11	17:52	72°09.462' 19°43.644'	318
Snøras Seep	IG25-9-KH-11-MC-04b	22/11	21:14	72°47.754' 20°37.542'	
Tromsøflaket	IG25-9-KH-577-CTD	23/11	06:55	71°18.636' 18°59.748'	227
Tromsøflaket	IG25-9-KH-13-ROV-1076	23/11	07:14	71°18.636' 18°59.748'	230
Tromsøflaket	IG25-9-KH-13_ROV1076-MBat-01	23/11	07:48	71°18.618' 18°59.706'	209

Tromsøflaket	IG25-9-KH-13_ROV1076-VMap-01	23/11	08:13	71°18.606' 18°59.754'	217
Tromsøflaket	IG25-9-KH-13_ROV1076-Biol-01	23/11	08:43	71°18.648' 18°59.844'	227
Tromsøflaket	IG25-9-KH-13_ROV1076-Biol-02	23/11	08:44	71°18.648' 18°59.844'	227
Tromsøflaket	IG25-9-KH-13_ROV1076-Biol-03	23/11	08:45	71°18.648' 18°59.844'	227
Tromsøflaket	IG25-9-KH-13-ROV-1077	23/11	09:36	71°18.642' 18°59.760'	230
Tromsøflaket	IG25-9-KH-13_ROV1077-CH4M-01	23/11	09:48	71°18.636' 18°59.766'	225
Tromsøflaket	IG25-9-KH-13_ROV1077-GasS-14	23/11	09:49	71°18.642' 18°59.766'	227
Tromsøflaket	IG25-9-KH-13_ROV1077-WatS-A	23/11	10:06	71°18.636' 18°59.760'	226

Tromsøflaket	IG25-9-KH-13_ROV1077-WatS-A	23/11	10:06	71°18.636' 18°59.760'	226
Tromsøflaket	IG25-9-KH-13_ROV1077-Scoo-01	23/11	10:17	71°18.636' 18°59.754'	228
Tromsøflaket	IG25-9-KH-13_ROV1077-ScoN-01	23/11	10:22	71°18.636' 18°59.760'	228
Tromsøflaket	IG25-9-KH-13_ROV1077-CarC-01	23/11	10:26	71°18.624' 18°59.784'	228
Tromsøflaket	IG25-9-KH-13_ROV1077-RocC-01	23/11	10:28	71°18.618' 18°59.796'	229
01.09.7119	IG25-9-KH-14-ROV-1078	23/11	13:18	71°24.888' 19°49.686'	200
01.09.7119	IG25-9-KH-14_ROV1078-ScoN-01	23/11	13:40	71°24.918' 19°49.836'	198

01.09.7119	IG25-9-KH-14_ROV1078-RocC-01	23/11	13:56	71°25.068' 19°49.674'	196
01.09.7119	IG25-9-KH-14_ROV1078-Ctra-01	23/11	13:59	71°25.068' 19°49.644'	197
01.09.7119	IG25-9-KH-14_ROV1078-Scoo-01	23/11	15:05	71°24.894' 19°49.638'	198
01.09.7119	IG25-9-KH-14_ROV1078-RocC-02	23/11	15:18	71°24.894' 19°49.602'	198
01.09.7119	IG25-9-KH-14_ROV1078-CH4M-01	23/11	15:23	71°24.894' 19°49.602'	198
01.09.7119	IG25-9-KH-14_ROV1078-Scoo-02	23/11	15:34	71°24.894' 19°49.602'	198
01.09.7119	IG25-9-KH-14_ROV1078-Scoo-03	23/11	15:39	71°24.894' 19°49.590'	198

01.09.7119	IG25-9-KH-14_ROV1078-Scoo-04	23/11	15:48	71°42.882' 19°49.530'	199
01.09.7119	IG25-9-KH-14_ROV1078-CH4M-02	23/11	15:49	71°42.882' 19°49.530'	199
01.09.7119	IG25-9-KH-14_ROV1078-BlaC-02	23/11	15:57	71°42.882' 19°49.530'	199
01.09.7119	IG25-9-KH-14_ROV1078-RocC-03	23/11	16:04	71°42.882' 19°49.530'	199
01.09.7119	IG25-9-KH-14_ROV1078-BlaC-04	23/11	16:08	71°24.888' 19°49.530'	198
01.09.7119	IG25-9-KH-14_ROV1078-GasS-	23/11	16:19	71°24.888' 19°49.698'	197
01.09.7119	IG25-9-KH-14_ROV1078-Ctra-02	23/11	16:23	71°24.888' 19°49.698'	195

01.07.7119	IG25-9-KH-15-ROV-1079	23/11	17:59	71°23.718' 19°15.216'	238
01.07.7119	IG25-9-KH-15_ROV1079-GasS-06	23/11	18:10	71°23.718' 19°15.204'	235
01.07.7119	IG25-9-KH-15_ROV1079-GasS-06	23/11	18:10	71°23.718' 19°15.204'	235
01.07.7119	IG25-9-KH-15_ROV1079-WatS-B	23/11	18:30	71°23.718' 19°15.204'	233
01.07.7119	IG25-9-KH-15_ROV1079-Ctra-	23/11	18:31	71°23.718' 19°15.204'	236
Multicore Station	IG25-9-KH-16-MC-05_001_0-47	23/11	21:22	71°26.952' 18°50.706'	272
Multicore Station	IG25-9-KH-16-MC-05_001_0-47	23/11	21:22	71°26.952' 18°50.706'	272
Multicore Station	IG25-9-KH-16-MC-05_001_0-47	23/11	21:22	71°26.952' 18°50.706'	272

Multicore Station	IG25-9-KH-16-MC-05_001_0-47	23/11	21:22	71°26.952' 18°50.706'	272
Multicore Station	IG25-9-KH-16-MC-05_001_0-47	23/11	21:22	71°26.952' 18°50.706'	272
Outer Bjørnøya	IG25-9-KH-17-ROV-1080	24/11	07:12	72°26.268' 17°40.668'	400
Outer Bjørnøya	IG25-9-KH-17_ROV1080-Biol-01	24/11	07:39	72°26.286' 17°40.584'	382
Outer Bjørnøya	IG25-9-KH-17_ROV1080-Biol-01	24/11	07:39	72°26.286' 17°40.584'	382
Outer Bjørnøya	IG25-9-KH-17_ROV1080-Biol-01	24/11	07:39	72°26.286' 17°40.584'	382
Outer Bjørnøya	IG25-9-KH-17_ROV1080-MBat-01	24/11	07:44	72°26.280' 17°40.608'	355
Outer Bjørnøya	IG25-9-KH-17-ROV-1081	24/11	10:14	72°26.286' 17°40.590'	400

Outer Bjørnøya	IG25-9-KH-17_ROV1081-BlaC-01	24/11	10:44	72°26.262' 17°40.656'	394
Outer Bjørnøya	IG25-9-KH-17_ROV1081-BlaC-02	24/11	10:54	72°26.262' 17°40.614'	396
Outer Bjørnøya	IG25-9-KH-17_ROV1081-CarC-01	24/11	11:08	72°26.316' 17°40.596'	381
Outer Bjørnøya	IG25-9-KH-17_ROV1081-CarC-02	24/11	11:16	72°26.310' 17°40.596'	389
Outer Bjørnøya	IG25-9-KH-17_ROV1081-CarC-03	24/11	11:19	72°26.310' 17°40.590'	385
Outer Bjørnøya	IG25-9-KH-17-SR-01	24/11	11:20	72°26.292' 17°40.590'	
Outer Bjørnøya	IG25-9-KH-17_ROV1081-Biol-01	24/11	11:49	72°26.340' 17°40.680'	

Outer Bjørnøya	IG25-9-KH-17-ROV-1082	24/11	12:42	72°26.340' 17°40.662'	400
Outer Bjørnøya	IG25-9-KH-17_ROV1082-WatS-B	24/11	13:05	72°26.340' 17°40.680'	396
Outer Bjørnøya	IG25-9-KH-17_ROV1082-TemL-01	24/11	13:09	72°26.340' 17°40.680'	397
Outer Bjørnøya	IG25-9-KH-17_ROV1082-CarC-01	24/11	13:12	72°26.340' 17°40.680'	397
Outer Bjørnøya	IG25-9-KH-17_ROV1082-ScoN-01	24/11	13:16	72°26.340' 17°40.680'	397
Outer Bjørnøya	IG25-9-KH-17_ROV1082-ScoN-02	24/11	13:19	72°26.340' 17°40.680'	397
Outer Bjørnøya	IG25-9-KH-578-CTD	24/11	14:01	72°26.340' 17°40.680'	394

Outer Bjørnøya	IG25-9-KH-17_ROV1082-CH4M-01	24/11	14:13	72°26.340' 17°40.680'	384
Tvillingene	IG25-9-KH-18-ROV-1083	24/11	16:15	72°35.076' 17°24.066'	360
Tvillingene	IG25-9-KH-18_ROV1083-CH4M-01	24/11	16:38	72°35.094' 17°24.054'	336
Tvillingene	IG25-9-KH-18_ROV1083-MBat-01	24/11	16:39	72°35.124' 17°24.042'	310
Tvillingene	IG25-9-KH-18_ROV1083-GasS-18	24/11	17:12	72°35.094' 17°24.048'	363
Tvillingene	IG25-9-KH-18_ROV1083-BlaC-04	24/11	17:38	72°35.058' 17°24.054'	362
Tvillingene	IG25-9-KH-18_ROV1083-CarC-01	24/11	17:44	72°35.052' 17°24.084'	360

Tvillingene	IG25-9-KH-18_ROV1083-CarC-02	24/11	17:46	72°35.052' 17°24.084'	360
Tvillingene	IG25-9-KH-18_ROV1083-CarC-03	24/11	17:47	72°35.058' 17°24.084'	360
Tvillingene	IG25-9-KH-18_ROV1083-CarC-04	24/11	17:59	72°35.100' 17°24.054'	362
Tvillingene	IG25-9-KH-18_ROV1083-ScoN-01	24/11	18:08	72°35.094' 17°24.054'	363
Tromsøflaket SW	IG25-9-KH-579-CTD	25/11	07:09	71°01.332' 17°10.038'	322
Tromsøflaket SW	IG25-9-KH-19-ROV-1084	25/11	07:15	71°01.332' 17°10.050'	315
Tromsøflaket SW	IG25-9-KH-19_ROV1084-MBat-01	25/11	07:38	71°01.320' 17°10.020'	288

Tromsøflaket SW	IG25-9-KH-19_ROV1084-GasS-01	25/11	08:03	71°01.320' 17°10.038'	316
Tromsøflaket SW	IG25-9-KH-19_ROV1084-WatS-01	25/11	08:18	71°01.320' 17°10.038'	317
Tromsøflaket SW	IG25-9-KH-19_ROV1084-CH4M-01	25/11	08:22	71°01.320' 17°10.038'	317
Fugløybanken	IG25-9-KH-20-ROV-1085	25/11	13:10	70°23.136' 17°27.000'	145
Fugløybanken	IG25-9-KH-580-CTD	25/11	13:23	70°23.136' 17°26.994'	145
Fugløybanken	IG25-9-KH-20_ROV1085-MBat-01	25/11	13:31	70°23.226' 17°27.096'	112
Fugløybanken	IG25-9-KH-20_ROV1085-MBat-02	25/11	14:00	70°23.202' 17°26.250'	109

Fugløybanken	IG25-9-KH-20_ROV1085-MBat-03	25/11	15:00	70°23.556' 17°27.102'	
Fugløybanken	IG25-9-KH-20_ROV1085-BlaC-03	25/11	16:02	70°23.232' 17°27.294'	146
Fugløybanken	IG25-9-KH-20_ROV1085-MBat-04	25/11	16:27	70°23.130' 17°27.144'	
Fugløybanken	IG25-9-KH-20_ROV1085-CH4M-01	25/11	17:12	70°23.094' 17°26.940'	139
Fugløybanken	IG25-9-KH-20_ROV1085-WatS-A	25/11	17:28	70°23.112' 17°27.060'	142
Fugløybanken	IG25-9-KH-20_ROV1085-CH4M-02	25/11	17:29	70°23.106' 17°27.036'	142